Evaluation of Hybrid-Electric Propulsion Systems for Unmanned Aerial Vehicles

by

Jay Michael Todd Matlock
B.Eng., University of Victoria, 2016

A Thesis Submitted in Partial Fulfillment of the
Requirements for the Degree of

MASTER OF APPLIED SCIENCE

in the Department of Mechanical Engineering

Evaluation of Hybrid-Electric Propulsion Systems for Unmanned Aerial Vehicles

by

Jay Michael Todd Matlock
B.Eng., University of Victoria, 2016

Supervisory Committee

Dr. Afzal Suleman, Supervisor
Department of Mechanical Engineering

Dr. Curran Crawford, Departmental Member
Department of Mechanical Engineering

Abstract

The future of aviation technology is transitioning to cleaner, more efficient and higher endurance aircraft solutions. As fully electric propulsion systems still fall short of the operational requirements of modern day aircraft, there is increasing pressure and demand for the aviation industry to explore alternatives to fossil fuel driven propulsion systems. The primary focus of this research is to experimentally evaluate hybrid electric propulsion systems (HEPS) for Unmanned Aerial Vehicles (UAV) which combine multiple power sources to improve performance. HEPS offer several potential benefits over more conventional propulsion systems such as a smaller environmental impact, lower fuel consumption, higher endurance and novel configurations through distributed propulsion. Advanced operating modes are also possible with HEPS, increasing the vehicle's versatility and redundancy in case of power source failure.

The primary objective of the research is to combine all of the components of a small-scale HEPS together in a modular test bench for evaluation. The test bench uses components sized for a small-scale UAV including a $2.34kW$ two-stroke $35cc$ engine and a $1.65kW$ brushless DC motor together with an ESC capable of regenerative braking. Individual components were first tested to characterize performance, and then all components were assembled together in a parallel configuration to observe system-level performance. The parallel HEPS is capable of functioning in the four required operating modes: EM Only, ICE Only, Dash Mode (combined EM and ICE power) as well as Regenerative Mode where the onboard batteries get recharged. Further, the test bench was implemented with a supervisory controller to optimize system performance and run each component in the most efficient region to achieve torque requirements programmed into mission profiles. The logic based controller operates with the ideal operating line (IOL) concept and is implemented with a custom LabView GUI.

The system is able to run on electric power or ICE power interchangeably without making any modifications to the transmission as the one-way bearing assembly engages for whichever power source is rotating at the highest speed. The most impressive of these sets of tests is the Dash mode testing where the output torque of the propeller is supplied from both the EM and ICE. Working in tandem, it was proved that the EM was drawing $19.9A$ of current which corresponds to an estimated $0.57Nm$ additional torque to the propeller for a degree of hybridization of 49.91%. Finally, the regenerative braking mode was proven to be operational, capable of recharging the battery systems at $13A$. All of these operating modes attest to the flexibility and convenience of having a hybrid-electric propulsion system.

The results collected from the test bench were validated against the models created in the aircraft simulation framework. This framework was created in MATLAB to simulate the performance of a small UAV and compare the performance by swapping in various propulsion systems. The purpose of the framework is to make direct comparisons of HEPS performance for parallel and series architectures against conventional electric and gasoline configuration UAVs, and explore the trade-offs. Each aircraft variable in the framework was modelled parametrically so that parameter sweeps could be run to observe the impact on the aircraft's performance. Finally, rather than comparing propulsion systems in steady-state, complex mission profiles were created that simulate real life applications for UAVs. With these experiments, it was possible to observe which propulsion configurations were best suited for each

mission type, and provide engineers with information about the trade-offs or advantages of integrating hybrid-electric propulsion into UAV design.

In the Pipeline Inspection mission, the exact payload capacities of each aircraft configuration could be observed in the fuel burn versus $C_{L,cruise}$ parameter sweep exercise. It was observed that the parallel HEPS configuration has an average of $3.52kg$ lower payload capacity for the $35kg$ aircraft (17.6%), but has a fuel consumption reduction of up to 26.1% compared to the gasoline aircraft configuration. In the LIDAR Data collection mission, the electric configuration could be suitable for collection ranges below $100km$ but suffers low LIDAR collection times. However, at $100km$ LIDAR collection range, the series HEPS has an endurance of $16hr$ and the parallel configuration has an endurance of $19hr$. In the Interceptor mission, at $32kg$ TOW, the parallel HEPS configuration has an endurance/TOW of $1.3[hr/kg]$ compared to $1.15[hr/kg]$ for the gasoline aircraft. This result yields a 13% increase in endurance from $36.8hr$ for gasoline to $41.6hr$ for the parallel HEPS. Finally, in the Communications Relay mission, the gasoline configuration is recommended for all TOW above $28kg$ as it has the highest loiter endurance.

Keywords: hybrid propulsion, series and parallel architecture; unmanned aerial vehicles;

Contents

List of Tables

List of Figures

Acknowledgments

I would first like to thank Professor Afzal Suleman for the opportunity to work on this project for my Master's of Applied Science Degree. I am thankful that I was given the opportunity to explore a research area that I am passionate in, and given the support and tools to succeed. This research project provided me with extreme challenges to test my mechanical engineering aptitude, as well as forced me to learn new and exciting skills in electrical and software engineering. This multidisciplinary project expanded my knowledge of many areas and will hopefully influence my future aircraft design to explore advanced and efficient propulsion systems.

This project would not have been possible without the support and resources of the University of Victoria Center for Aerospace Research, UVIC CfAR. Not only did UVIC CfAR provide facilities for the experimentation to take place, but invaluable guidance from the extremely talented staff made this project a reality. The entire group at CfAR works hard to ensure success on all their projects, and I am very gracious for the support and patience given to me during my Masters degree. In the early stages of conceptual design and theoretical analysis, the contributions of Dr. Jenner Richards, Stephen Warwick and Dr. Jose Vale, with the MATLAB framework were instrumental in laying the foundation for the project. During the prototyping and manufacturing stages of the parallel hybrid test bench, Dr. Maxym Rukosuyev applied his vast mechanical and machining knowledge to make improvements to our design. The experimentation stage of the project was split into several stages of complexity, each with their own issues and problems which could not have been overcome without the hands-on expertise of John Rafaelli. In the CfAR electrical department, the advice and troubleshooting efforts from Kieran, Pablo, Peter, Ali, Grant and Babak ensured the successful operation and data collection of the test bench, and ensured reliability for future experimentation. Along the way, I would like to thank the contributions and experimentation from the undergraduate students Cameron Pettit, Ali Hamood and Phillip Carvalho from both the University of Victoria and Universidade de Lisboa Instituto Superior Tecnico. I am confident that the parallel hybrid project will continue to be successful thanks to the current work and insightful experiments from Roy Ledwosinski as well as undergraduate students at UVIC. I would like to extend a special thank-you to Leonardo Machado for his contributions to all aspects of the project, and incredibly positive attitude! Leonardo's keen eye for detail, steadfast work ethic and impressive problem solving skills ensured success of the hybrid project.

Finally, I would like to extend a personal thank you to all my friends and family who supported me throughout this project. The love and encouragement given to me during the most difficult portions of the project made all the difference in allowing me to persevere and achieve my goals. My wonderful girlfriend Jess has been incredibly patient and provided unwavering love through the late hours and stress of the project. My beloved Mom and Dad, sister Jill and brother Scott have been with me every step of my undergraduate and graduate degree and have given me the confidence needed to succeed! All of my friends and family have been intrigued by the progress and design of my hybrid-electric aircraft, and I could not have done it without you.

Nomenclature

Greek symbols

Ω	Resistance.
ω	Rotational Speed.
ρ	Density.
τ	Torque.

Roman symbols

$BSFC$	Brake Specific Fuel Consumption.
C_L	Coefficient of lift.
EM	Electric Motor.
GUI	Graphical User Interface.
$HEPS$	Hybrid Electric Propulsion System.
I	Current.
ICE	Internal Combustion Engine.
IOL	Ideal Operating Line.
kV	Motor speed constant.
TOW	Take Off Weight.
UAV	Unmanned Aerial Vehicle.
V	Voltage.

Subscripts

∞	Free-stream condition.
bat	Battery.
EM	Electric Motor.
$prop$	Propeller.

Chapter 1

Introduction

The transition to cleaner and more efficient aircraft technology is at the forefront of modern aerospace research. With increasing social pressure for companies to involve energy efficient and renewable technologies with their products, the aviation industry is exploring options into 'green energy' propulsion systems. As part of this effort, the University of Victoria Center for Aerospace Research (UVIC CfAR) is exploring the viability of small scale aircraft utilizing a hybrid-electric propulsion system (HEPS). This exploration includes the theoretical research into the performance of hybrid-electric systems, as well as experimentation and validation at the component and system level.

Modern unmanned aerial vehicles (UAV) are mainly comprised of either internal combustion engines or electric motor propulsion systems. For small UAVs, these systems are cost-effective and simple to implement, but each have inherent disadvantages. On small scale UAV platforms energy density is an important consideration as a large portion of take-off weight is dedicated to fuel systems. Even exceeding the allowable mass and volume for fuel systems by a small amount can have drastic impacts on the payload capability and performance of the UAV. Electric aircraft are endurance-limited because of the low energy density of modern batteries, but offer high-torque capability throughout their operating range. Internal combustion engines on UAVs typically need to be oversized for cruise requirements because of the large power requirement of the take-off segment of the mission. This means that they are typically larger and heavier than needed for the majority of flight in order to satisfy the climb-out requirements. If these propulsion systems can be effectively combined, a hybrid system could benefit from the endurance of an ICE, but with the high-power output capabilities of the EM.

In the UAV market, there are many different projects and companies looking into incorporating HEPS into their vehicle designs. The scale of these UAVs vary drastically, from small-scale below $10kg$ up to full-sized commercial transport aircraft. Further, these UAVs are designed to perform missions and tasks across an extremely wide range of applications, from package delivery, short-run passenger transport as well as large-scale cargo transport. With the magnitude of variance between different projects and designs in the aerospace HEPS market, it is difficult for engineers to draw useful conclusions for which designs are superior.

It is clear that it would be advantageous to develop a framework in order to evaluate HEPS UAV per-

formance and assist design engineers. To form a fair and unbiased comparison, a MATLAB framework was created that evaluates aircraft performance independently from propulsion system performance. This way, the propulsion system of the aircraft can be swapped out for various technologies and compared against each other to observe trade-offs and advantages of each propulsion architecture. By only manipulating the variables of the propulsion system of the aircraft, trade studies can be conducted to explore the impacts on the design.

In order to validate the findings of the MATLAB framework, and explore the performance of a HEPS for a UAV, the objective was to design and implement a hybrid-electric system for bench testing. By exploring the main challenges of designing and implementing a HEPS system on a bench, useful lessons would be learned for future implementation of the system into an airframe. Further, the test bench would provide an experimental environment for HEPS exploration of various components, configurations, and controllers to fully analyze the design space.

Intermediate steps of 'proof-of-concept' testing were critical in the development of the HEPS as many of the components and use cases for the components were non-typical. For instance, typical UAVs that use electric propulsion systems have electronic speed controllers to control the electric motors, but this test bench also had to test regenerative braking where the motor acted as a generator. Special considerations had to be made in the specifications of HEPS components and required component-level testing and validation before implementing into the system. Further, development of outside experimental test rigs, such as the development of a EM thrust test rig, were required to fully characterize component performance.

Not only is an experimental apparatus required for analysis of a UAV HEPS, but also a test environment to accurately collect data on the system performance. LabView was used with a National Instruments data acquisition (DAQ) unit in order to control the hybrid test bench, as well as collect critical performance data. This testing environment allowed for the implementation of a supervisory controller for test-engineers to interact with the hybrid. As improvements were made to the controller, their performance difference could be directly measured on the test bench. In fact, the LabView test environment also allows for operators to run a 'simulated' test where the logic and function of the controller can be evaluated without starting the HEPS.

The results and findings from this research will allow for the detailed analysis of hybrid-electric propulsion systems for UAVs, and influence future aircraft designs. Implementation of HEPS can not only improve the performance of UAVs, but also open up the operational envelope with complex and advanced configurations that are not feasible on conventional aircraft propulsion architectures.

1.1 University of Victoria Center for Aerospace Research

This project is done in collaboration with the University of Victoria Center for Aerospace Research, UVIC CfAR. Working at the leading edge of the emerging aerospace industry research, UVIC specializes in unmanned aerial systems, or UAS. UAS encompass everything including the ground station communications, on-board payloads and autopilot systems, as well as the unmanned aerial vehicle, (UAV) itself.

Unmanned aircraft technology is the fastest growing sector in the aerospace industry in Canada. Partnering with large companies from around the world such as Boeing, Bombardier, Embraer, Defense Research and Development Canada (DRDC) and the Canadian Department of Defense, UVIC CfAR designs, builds and tests fully autonomous unmanned aerial vehicles. CfAR is involved in a wide range of research activities including initial conceptualization and prototyping, detailed design and manufacturing, as well as conducting extensive testing at Transport Canada approved flight test ranges across Canada.

From conventional sail-plane architectures, to more advanced joined-wing and blended wing body aircraft, UVIC CfAR is committed to pushing the limits of capability for small aircraft. These UAS are used for a multitude of applications spanning several sectors, including aerial mapping for precision agriculture, wildlife monitoring, search and rescue or civil disaster response, telecommunications, and mining exploration. Platforms have not been limited to fixed-wing aircraft architectures; CfAR also conducts testing with a wide range of multi-rotors from custom made hexcopters, first-person view quadcopters, and more conventional videography drones for observation and mapping. With the increasing demand of green UAV technology, UVIC CfAR is pursuing this research area and is a leading institution exploring the detailed design and optimization for HEPS.

UVIC CfAR specializes in projects of unconventional or unique aircraft vindication, but also offers several sail-plane UAV platforms in which to test conceptual designs. The sail plane architecture considered as the main platform for this research is the QT1, an optimized design to maximize payload mass and volume. As this aircraft was developed to be modular, it can be used in a wide range of applications and configurations for various UAV missions. With the available payload mass and volume of the aircraft maximized, the design space for developing a HEPS is open for several configuration and sizing options.

Figure 1.1: UVIC CfAR QT1 Aircraft on display at the University of Victoria, and render on the pneumatic launch system.

The efforts in this research are the beginning of explorations into hybrid-electric technologies for UAVs at UVIC CfAR. The developments and findings of this research will be extremely influential towards future aircraft designs and will provide useful tools to correctly analyze HEPS performance. Following the large interest of the aviation sector to explore efficient and novel propulsion architectures, UVIC CfAR is pursuing future projects and design work with hybrid architectures.

1.2 Motivation

The motivation of this research is to explore the viability of hybrid-electric propulsion systems on small-scale aircraft called 'Unmanned Aerial Vehicles' in order to prove this technology's capability. Once this technology can be proved at a smaller scale, the findings can be scaled up for use in larger applications such as commercial aircraft. Typically, aircraft technologies are first explored at a scaled and smaller level to prove that the airframe or technology is viable.

Applications in civil and military aviation could potentially benefit from hybrid-electric propulsion technologies, including extended and more efficient flight, quieter operations and advanced configurations. One such configuration which is made possible with hybrid-electric propulsion technologies is 'vertical take-off and landing' (VTOL) where the aircraft is capable of taking off and landing vertically like a helicopter, but is still efficient in horizontal flight for cruise. A hybrid configuration would be able to supply vertical lift with ancillary electric motors, and use a combustion engine or hybrid system as the main power plant.

The emergence of hybrid-electric propulsion systems into the aviation sector is still in its infancy, and requires substantial development before hybrid systems will be widely seen. As is the trend for the majority of new aviation technologies, the concepts are tested on smaller and simpler aircraft at first in order to validate performance, and mitigate risks and costs of failure. UAVs are *soaring* in popularity in commercial and military applications; for instance, the US Military had only 50 UAVs in 2008, but that number grew to over 6,000 UAVs in 2011. [1] The proliferation of aircraft in commercial markets applies not only to small-scale UAVs but to large scale commercial transport aircraft as well. Based on the cutting-edge research of UAVs around the world, hybrid propulsion systems are becoming realistic for full-scale aviation projects. In 'Conceptual Design of Hybrid-Electric Transport Aircraft', Pornet and Isikveren state "The introduction of hybrid-electric technology has dramatically expanded the design space and the full-potential of these technologies will be drawn through synergetic, tightly-coupled morphological and systems integration emphasizing propulsion." [2]

During the combustion process the most critical green-house-gas emissions are carbon dioxide (CO_2), nitrogen oxides (NO_X) as well as wasted unburned hydrocarbons. In the year 2000 677 megatons of CO_2 were emitted from the aviation sector, which accounts for about $2-3\%$ of human's total contribution, and is expected to climb to 2437 megatons by 2050 (2.437 trillion kilograms). [3] At the surface of the earth, NO_X is a catalyst in the production of ozone O_3 and as such is considered a large contributor to global warming. However, an important factor to consider is that the reactive properties of NO_X generating ozone are more efficient at the cruise altitudes of typical aircraft. [4]

Large scale aviation industry is not only motivated by environmental savings that can come from more efficient propulsion technologies. From an economics standpoint, fuel costs for commercial airlines account for roughly 30% of all expenses! [5] Based on estimates collected from the ICAO environmental report in 2013, the number of commercial airline flights are expected to triple between 2010 and 2040 to over 94.3 million operations annually. Airlines will need to purchase over $40,000$ new aircraft in the next 20 years to satisfy this demand. [4] Reports collected by FlightRadar24 estimate that there are

over $10,000$ aircraft in the air at any given time. [6] With no foreseeable decline in air-traffic or ridership, it is clear that a reduction of fuel consumption would be an attractive financial incentive for commercial airlines that would also have positive environmental impacts.

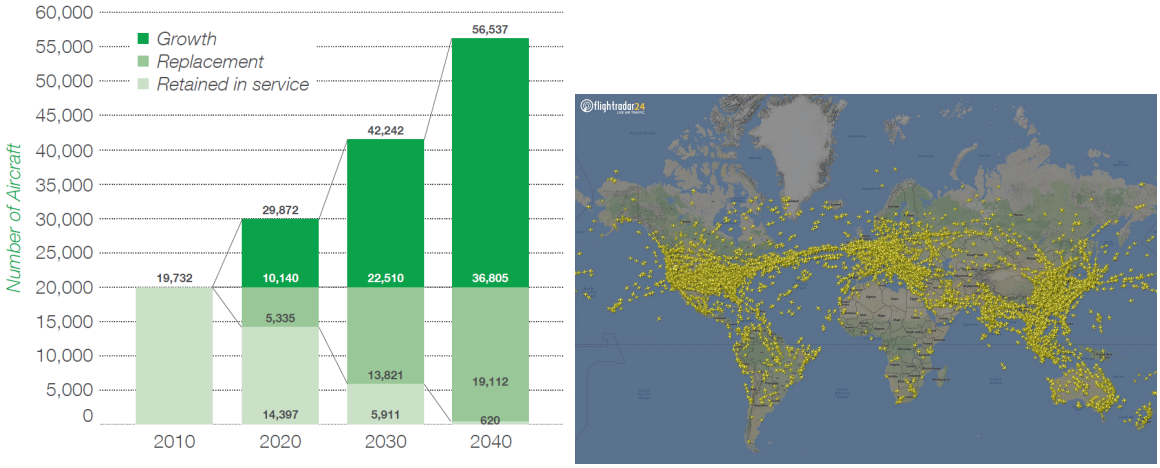

Figure 1.2: Passenger aircraft fleet evolution estimates from ICAO 2013. [4] FlightRadar24 illustration of a typical day of global air traffic. [6]

To achieve the ambitious goals set out in “Flightpath 2050” by the European Commission and the Strategic Research and Innovation Agenda (SRIA), drastic changes and improvements need to be made to the aviation industry. These goals include a 75% decrease in the CO_2 emissions per passenger kilometer, 90% reduction in NO_X emissions, 65% reduction in perceived noise, and emission free taxiing. [7] Similar and consistently aggressive targets are also formulated in Vision 2020, AGAPE 2020 and in NASA Environmentally Responsible Aviation N+, summarized by Pornet and Isikveren. [2] Exciting new concepts and designs are being worked on by teams around the world, and are explored in detail in the State of The Art that could drastically reduce emissions in aviation propulsion systems. To reach the goals of the Flightpath 2050 or AGAPE 2020 plans, substantial research of hybrid propulsion UAVs must first be explored.

1.3 Problem Description

Traditional forms of propulsion systems for unmanned aerial vehicles face draw-backs that could be potentially solved with a hybrid-electric propulsion system. In order to properly evaluate the performance of a hybrid electric UAV, it must first be compared against a baseline aircraft which utilizes more conventional electric motors or combustion engines. Generating theoretical results of a hybrid electric aircraft allows for the qualitative analysis of the system, but require validation before definitive conclusions can be drawn. The efforts in this research not only provide a strong framework to conduct theoretical work, but also a robust and modular test bench in order to collect experimental data. It is with these tools that the performance evaluation of a hybrid-electric aircraft can be conducted.

1.4 State of the Art

Hybrid electric architectures have existed across multiple industries for years, most prevalent in the automotive industry. Early designs of a Hybrid Electric Vehicle (HEV) date back to 1899 when two hybrid vehicles were presented at the Paris Salon [8]. However, it was not until 1997 that HEVs became widely available to the general public with the release of the Toyota Prius in 1999. Now, HEVs comprise a substantial portion of modern vehicles on the road. Both these automobiles demonstrated hybrid vehicle capability and operate more efficiently than gasoline counterparts. These results sparked an interest in pursuing the same approach in different industries, including public city transport buses, trucks, trains and marine vessels. [9] [10] [11]

Implementation of HEPS into the aviation industry is still in its infancy and development stages of experimentation. Parallel hybrid architectures couple the ICE and EM directly with a form of mechanical coupling so that the power demand can be met by the combustion engine, or the electric machine directly. Since the EM and ICE work together to meet power demand, each of the components are reduced in size. In addition, since a separate generator is not required as in a series architecture, there are potential mass savings of 8% by using a parallel architecture as shown in a study by Harmon, Frank and Joshi on a small UAV. [12] In a parallel application, the ICE may not always be operating within its most efficient zone which makes an impact on energy efficiency. To counteract this, the literature suggests the application of a continuously variable transmission (CVT) to optimize gearing of the ICE and the output shaft of the aircraft. [13] Further, an electronic engine control unit coupled with the CVT is suggested by Brace et al. in order to determine the ideal engine torque and speed to most efficiently deliver the power demand. [14]

The most popular hybrid architecture system in large scale automotive, locomotive systems and marine vessels are series configurations. The flexibility and scalability of the series hybrids is appealing to many applications, as well as the physical decoupling of the power generation system and the propulsor outputs. This means that, for example, in a large marine vessel application a large diesel generator can be located in the center of the ship in a large area accessible to maintenance crews and operators, while the electric motor propulsors can be distributed throughout the vessel in less accessible locations, or even submerged. The same concept is true for the aviation industry, where the aircraft can have a power plant located in the main fuselage of the aircraft, and small electric motors placed throughout the wing surfaces. With the mechanical decoupling, the combustion engine is able to operate in its most efficient range to minimize fuel consumption, and this allows for precise system sizing. In a series hybrid configuration, larger and heavier electrical machines are required to accommodate peak power demands, as well as an alternator is required in addition to the electric motor propulsor. Not only are the additional components required, but series hybrid architectures present large energy conversion losses. The chemical energy in the fuel source is converted to mechanical energy in combustion, then converted to electrical energy in the generator. As this energy is transmitted to the electric motor propulsor there are transmission losses, and then the energy is converted from electrical energy back to mechanical energy in the electric motor to the propeller or output blades. In an early study conducted by Harmats

and Weihs from Technion – Israel Institute of Technology, series HEPS for UAVs were not recommended due to these conversion losses. [15]

1.4.1 Hybrid-Electric UAVs

One of the first groups to successfully implement a parallel HEPS for a small-scale UAV is 'Project Condor' with the Air Force Institute of Technology in 2010. [16] This project explored the complexities of various control algorithms, and implementation designs for ground and flight testing. Figure 1.3 shows the hybrid system on a dynamometer, as well as assembled on an airframe.

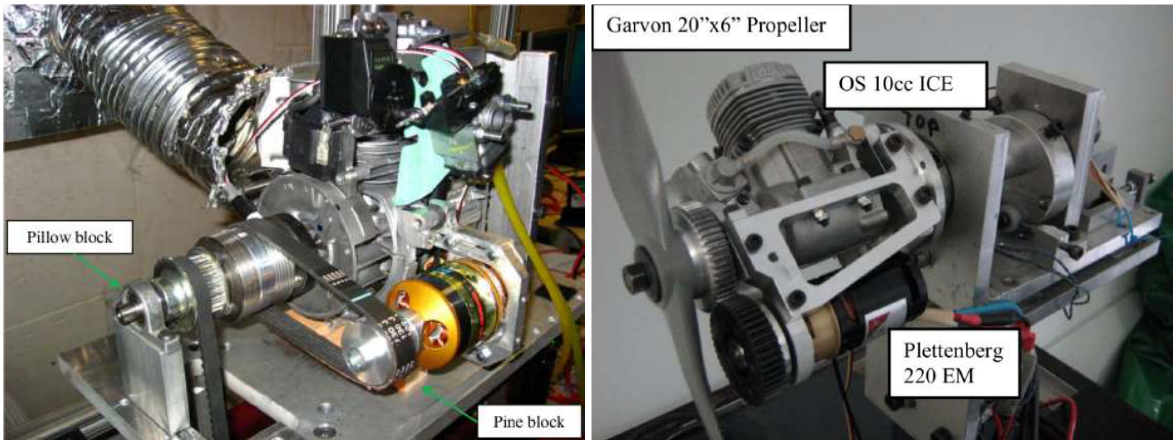

Figure 1.3: Air Force Institute of Technology's Project Condor parallel HEPS on dynamometer (left) and Queensland University parallel HEPS test bench prototype. (right) [16] [17]

In 2011 the University of Colorado published findings of the research they're conducting with their project in the design and implementation of a parallel HEPS of similar size. [18] Through the testing, compared to a gasoline UAV baseline design, the parallel HEPS was projected to achieve a 15% increase in fuel efficiency. Glassock et al at the Queensland University continued to contribute to this research area in 2012 with their experimentation of a small-scale parallel HEPS design that uses a $10cc$ methanol two-stroke combustion engine with a $600W$ BLDC. [17] In this research, dynamometer and wind-tunnel testing of the parallel HEPS yielded an overall propulsive efficiency of 17% above the baseline non-hybrid powerplant.

Launchpoint Technologies in the United States is developing designs for complex power flow designs referred to as 'propulsion-by-wire' that can adapt to flight conditions and vary propulsive power sources and magnitude, making it a good candidate for hybrid designs. The ability to replace typical mechanical systems of pistons, pneumatics and shafts with high-powered electronics allow for flexibility and large variance in power based on demand. Launchpoint Technologies is underway in the development of their VTOL tilt-wing aircraft concept, and are developing a 2-stroke combustion engine with alternator system that is able to output $6kW$ continuously, running at $7500RPM$, and only weighs $4.12kg$. [19] Systems such as this one could assist in the development of many vehicles in this size class.

For research projects using UAVs and sensitive measurement equipment, it is of interest to minimize onboard vibration, lower acoustic signatures as well as lower exhaust thermal signatures. Making use of HEPS can also unlock the use of UAVs in enhanced flight environments including increase altitude

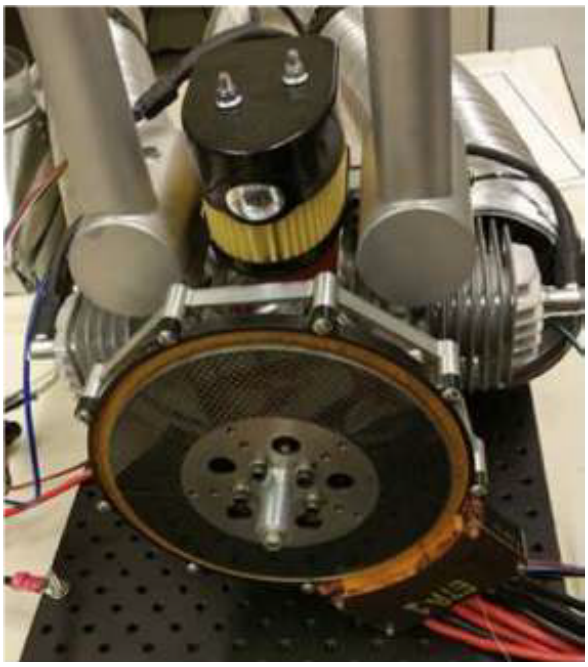

Figure 1.4: Launchpoint Technologies 6kW 2-stroke ICE and Alternator design. [19]

operations. In a case study by Isikeveren and Yezeguelian of Safran, a Eulair Twin2 Drone (MTOW 900kg) was explored for various hybrid architectures to increase the flight endurance by 20% while also implementing a de-icing system for high altitude operation. [20] The final candidate design was an organic-rankine cycle (ORC) parallel HEPS that had an increase of 16% endurance with no de-icing system, and a 4% endurance increase with the de-icing system.

Researchers at the US Army Combat Capabilities Development Command (CCDC) Army Research Laboratory are investigating VTOL UAS platforms for package delivery applications. [21] The CRC-20 and CRC-3 shown in the following figure are the $20lb$ and $2.5lb$ respective quad-rotor biplane tailsitter UAS vehicles are being evaluated for both series and parallel HEPS, specifically for vehicle performance and mass predictions.

Figure 1.5: Army Research Lab's CRC-20 (top) and CRC-3 (bottom) quad-rotor biplane tailsitter UAVs.[21]

Maximizing efficiency of a HEPS system is a critical aspect of the research area for all types of propulsors. Exciting progress is being made by Exonetik Turbo Inc in Sherbrooke, Canada with their high-efficiency recuperated inside-out ceramic turbogenerator. [22] The Inside-Out Ceramic Turbine (ICT)

is heavier than conventional simple-cycle turbogenerators, but the efficiency gain of ICT-recuperated system reduces required fuel-weight which provided a 200% payload improvement in a case study of a 4-passenger eVTOL aircraft. Further, this series-hybrid design provided an operational range 8-times larger than the battery only energy source.

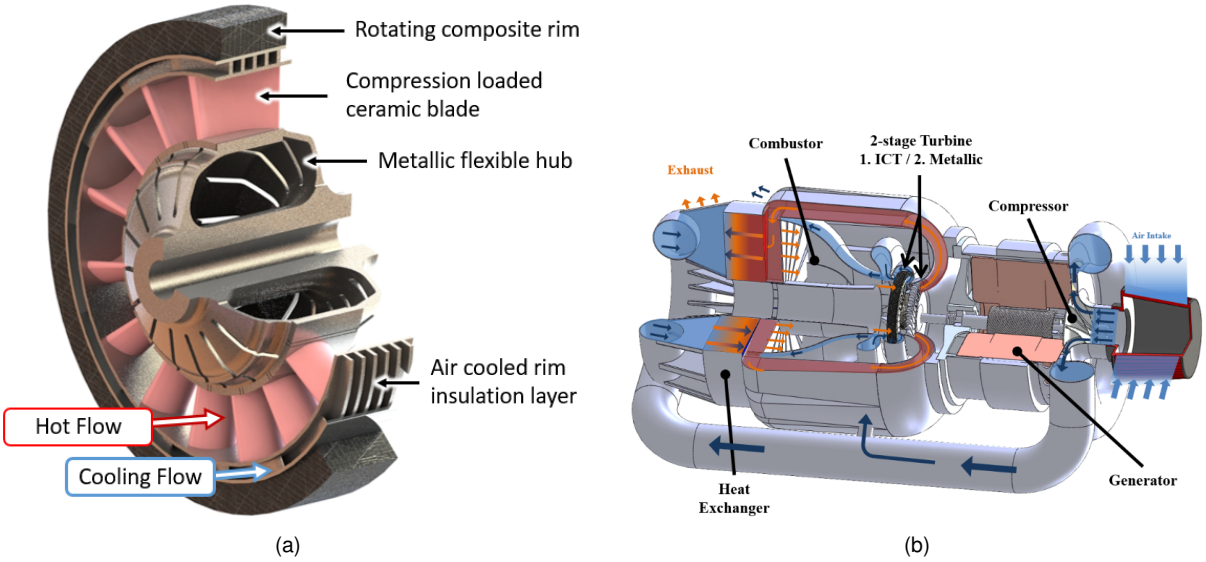

(a) (b)

Figure 1.6: Exonetik demonstrated Inside-out Ceramic Turbine prototype (left) and turbogenerator conceptual architecture (right). [22]

To effectively combine two or more power sources, and optimize their efficiencies based on complex power paths, a supervisory controller is required for the HEPS. The role of the controller is to determine the power and torque command for the engine, motor, and regenerative braking to maximize the entire system's efficiency. The simplest control strategy to implement in the supervisory controller is a rule-based strategy that establishes criteria for switching between operating modes. The controller aims to maintain each of the components in their most efficient regions of operation, although these regions often do not coincide. Therefore, the ideal operating line (IOL) concept introduced by Hung and Gonzalez is a suitable solution for this type of controller. [13] The IOL represents operating points for each combination of torque and speed for the engine where the brake specific fuel consumption (BSFC) is minimized. This point represents the operating point where the engine consumes the least amount of fuel for the desired output power. Simulation conducted in this research calculated a 6.5% fuel savings over the engine only configuration. Further simulation work by Harmon showed that for a rule based controller using the IOL concept on a $13.4kg$ UAV had an energy reduction of 54% and 22% for a one hour and three hour ISR mission respectively compared to a 4-stroke engine baseline. [23] Research is not only being conducted on small scale UAVs, but on large transport aircraft as well. Findings in the research of smaller scale projects can be used to drive engineering design decisions on larger scale aircraft.

1.4.2 Large Scale Aircraft

A prominent example of a large scale HEPS system designs on aircraft is the E-Fan X Project between Airbus, Siemens and Rolls-Royce Electric. [24] This impressive project for large scale aviation hybrid-

electric technical demonstrator should begin flight testing in 2020.

(a) Airbus E-Fan X.

(b) Boeing SUGAR Freeze.

(c) Airbus E Thrust.

(d) Bauhaus Luftfahrt CENTERLINE.

Figure 1.7: (a) “Airbus’ E-Fan X is a complex hybrid demonstrator that will validate technologies expected to generate double-digit percentage in aircraft fuel savings.” [24] (b) Boeing SUGAR Freeze Aircraft concept. [25] (c) Airbus E Thrust Conceptual Design using aircraft wake boundary-layer ingesting electric fans. [26] (d) Bauhaus Luftfahrt design of the CENTRELINE aircraft that uses aft-fuselage propulsor to re-energise fuselage wake. [27]

Further, additional joint projects with Siemens AG and Diamond Aircraft in 2018 have been announced for first flight of a jointly developed multi-engine aircraft. [28] Research conducted in a partnership between NASA and Boeing in the United States called Subsonic Ultra Green Aircraft Research (SUGAR) has been exploring hybrid electric concepts for achieving the following goals in the 2030-2040 time frame:

- 71 decibel reduction in noise
- Greater than 75% reduction on nitrogen oxide emissions (CAEP/6)
- Greater than 70% reduction in fuel burn

The project is divided into several sub-projects which include a high-span / high aspect ratio trussed wing design ‘SUGAR-High’, a hybrid electric commercial airliner ‘SUGAR-Volt’ and a futuristic hybrid ‘SUGAR-Freeze’ that uses liquefied natural gas, batteries, cryogenically cooled electric motors as well as fuel cells. [25] On the SUGAR-High, unswept high aspect ratio wings are possible with the struts beneath each wing, which also reduce the thickness to chord ratio. Simulations in this project estimate that the SUGAR-High is able to achieve a 39% reduction in fuel consumption for a 900 nautical mile mission, with possible improvements of up to 58%. [29]

At Airbus, a concept for narrow body design is being explored that would accommodate 100 passengers, a $1000Wh/kg$ battery system used in a series HEPS, and 6 electrically driven fans positioned to ingest aircraft boundary layer wake, or recharge batteries during descent using fan wind milling. [30] The technologies that will enable this design, including the high capacity battery system and the high temperature super-conductive machines are still out of reach, and this project is expected for completion in 2050.

Bauhaus Luftfahrt project CENTRELINE "Concept validation study for fuselage wake-filling propulsion integration" demonstrates the proof of concept for a propulsive-airframe concept. This design uses a turbo-electrically driven device at the aft of the fuselage that entrains and re-energizes the fuselage boundary layer flow to compensate viscous drag effects of the fuselage wake field. The project aims to reduce CO_2 and NO_X emissions by 11% over conventional reference aircraft by 2035. [27]

In commercial aviation, hybrid-electric propulsion systems are a promising technology when exploring challenging goals set in programs such as 2050 EU Flightpath/SRIA, NASA ARMD Strategic Implementation Plan, and the US Air Force ATTAM program. HEPS have potential benefits in maximizing fuel efficiency, reducing working emissions, as well as reducing operational noise. [31] With proliferation of aircraft and small UAV use in urban areas, noise reduction is an important area of research to minimize noise pollution. Further applications for HEPS technologies can be used for significant improvements to operation envelopes with unique configurations such as distributed propulsion and VTOL, which will enable unorthodox mission capabilities.

In 2018, a group at NASA Ames Research Center completed extensive research into conceptual vehicle design for VTOL Air Taxi Operations, presented with AHS Aeromechanics Design for Transformative Vertical Lift. Their research, part of the NASA Revolutionary Vertical Lift Technology (RVLT) Project, explores single, six, and fifteen passenger vehicle designs with 50, 200 and 400 nautical mile range capabilities, and includes concepts for using distributed propulsion with a series turbo-electric propulsion system. [32]

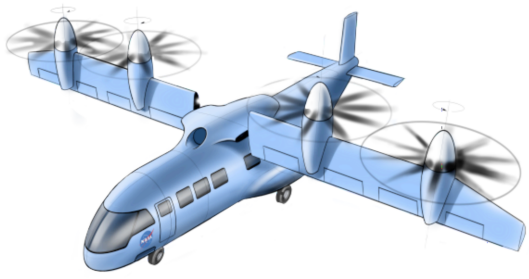

Figure 1.8: NASA Ames Research Center concept vehicle for VTOL air taxis, 15 PAX tiltwing with turboelectric propulsion. [32]

It is clear that large companies have high levels of interest in the various advantages hybrid technologies can offer to commercial transport aircraft.

1.4.3 HEPS in Urban Air Mobility (UAM)

Recently, following on the technological breakthroughs and unmanned multirotor configurations using distributed propulsion, a large influx of hybrid-electric and fully electric VTOL designs has been explored in the Urban Air Mobility (UAM) sector. These designs have large variance in size, style, and operational range, but most follow concepts of operation that can benefit from hybrid electric architectures. Urban Air Mobility is the most dynamic area in electric and HEPS aircraft at the moment, with new companies and groups contributing to the research every day. The groups are comprised of new ventures, as well as large established companies from around the world. In fact, in a study by Bauhaus Luftfahrt in 2019, there are 114 projects spanning 25 countries. [33]

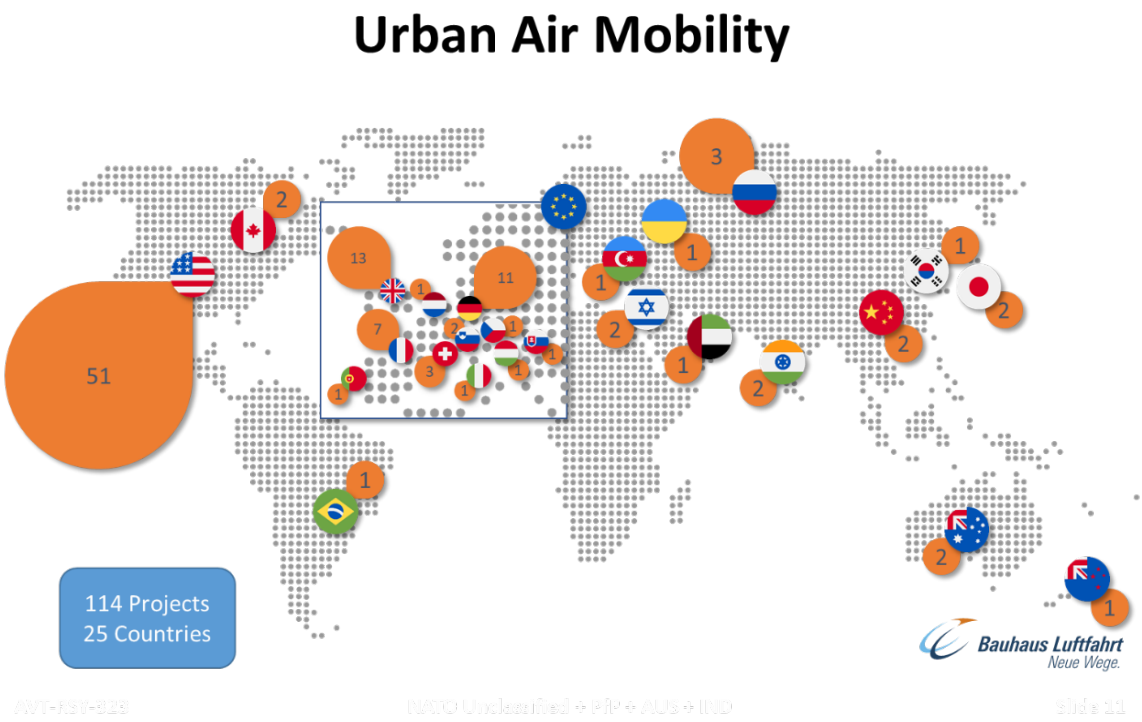

Figure 1.9: Map of worldwide Urban Air Mobility Projects as of October 2019. [33]

Some of the most prominent players in the UAM market include Pipistrel from Slovenia with their 801 eVTOL Aircraft unveiled in June 2019 that has 8 lift fans and a tractor propeller. [34] Also of note is Volocopter with their 'VoloCity' design capable of carrying 2 passengers with the 18 on board rotors. [35] A3 by Airbus is also exploring vehicles in the UAM market with their single passenger 'Vahana' model, as well as their 4-passenger CityAirbus multirotor design. [36]

1.4.4 HEPS Simulation Frameworks

Simulation frameworks are critical in the design process for these hybrid aircraft and are enabling research groups to push the bounds of the technology. In conjunction with the experimental analysis being conducted, there are some large efforts being made in the theoretical design space of HEPS aircraft as well. Indeed, several groups are working on design and optimization frameworks including NASA Glenn,

Figure 1.10: Pipistrel 801 eVTOL (top left) and Volocopter 'Volocity' (top right) and CityAirbus by Airbus A3 (bottom) UAM concepts. [34][35][36]

NASA Langley, Georgia Tech, ESAero, Bauhaus Luftfahrt, University of Illinois, HyPSim, and Stanford University. NASA Glenn is creating the Dymos Model 2 environment with their X-57 project novel electrified aircraft concepts in 2017. [37] NASA Langley has developed LEAPS (Layered and Extensible Aircraft Performance System) to explore aircraft design as well as mission analysis, including HEPS as published in 2018. [38] At Georgia Tech, GT-HEAT is being used to model distributed propulsion systems that take advantage of series hybrid architectures. [39] Hybrid Aircraft Propulsion System Synthesis (HAPSS) developed by ESAero in 2012 is used to design, size and explore performance of aircraft propulsion systems. [40] Bauhaus Luftfahrt is currently using methodologies developed by Pornet et al. in the exploration of hybrid technologies for large commercial aircraft to be developed for 2035. [41] At the University of Illinois, mission and emission analysis is taking place (starting in 2018) using their simulation framework for commercial transport aircraft. [42] A group from the University of Pisa developed a tool to simulate hybrid aircraft performance called HyPSim. [43] Finally, Stanford University SUAVE is an open-source environment for multi-fidelity conceptual vehicle design. In 2019, published work explores the SUAVE framework for eVTOL and hybrid aircraft design and analysis. [44] All of these models can be used to explore design trade-offs between architectures, make predictions for system performance, as well as provide insight for aircraft component sizing and optimization.

1.4.5 Challenges in Electrification of Aircraft

Results found in experimental research for UAVs using HEPS will be influential in the design of aircraft systems, but massive amounts of detailed simulation are also required for design optimization. The Institut Supérieur de l'Aéronautique et de l'Espace (ISAE-SUPAERO), Université de Toulouse in France, is working on a generalised methodology for sizing of air vehicles with HEPS. [45] The tool being developed

will provide guidance to groups designing and developing HEPS, notably presenting a modified Breguet range equation for fuel/battery weight calculations. The group at ISAE-SUPAERO also conducted a case study with a Pilatus PC-12 that showed the series and parallel architectures far outperforming the electric architecture. The tool can explore operational range for a various considerations in battery specific energy, as shown in Figure 1.11.

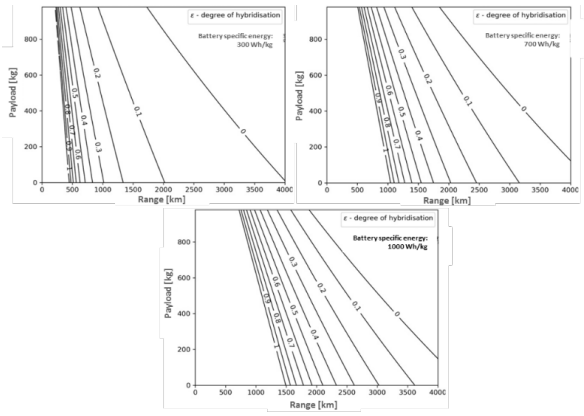

Figure 1.11: Payload-Range analysis for a hypothetical PC-12 equivalent with series hybrid propulsion, for three values of battery specific energy. [45]

Most of the hybrid architectures considered for aviation includes battery systems to supplement power of the aircraft. In fact, many architectures would not be able to function without large on-board battery storage systems. However, the main difficulty with large battery storage in aircraft is the severe weight penalty compared to hydrocarbon fuels such as JetA, Gasoline or Diesel. The following figure from Costello at Embry-Riddle Aeronautical University explores this difficulty when exploring NASA's centennial challenge. It can be seen that Lithium-Ion battery technology drastically falls behind other fuel types for specific energy and energy density. [46]

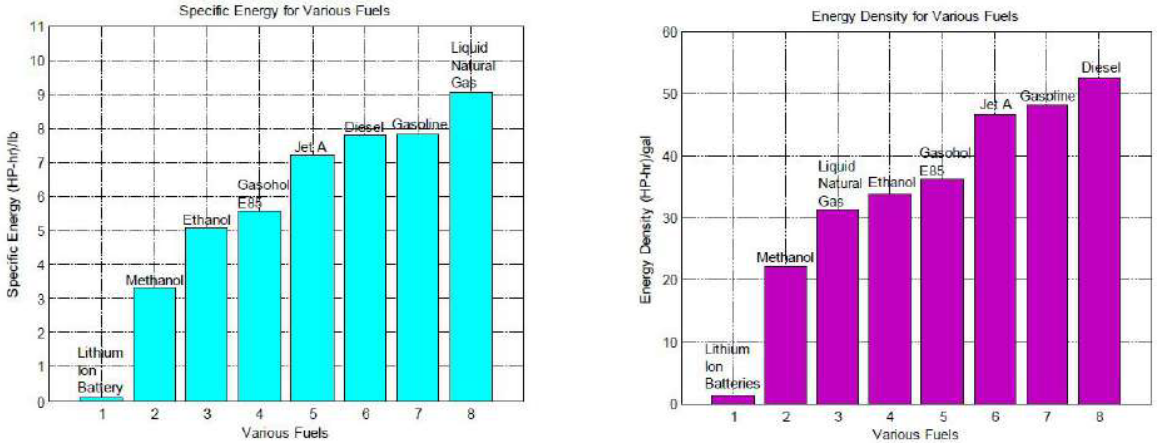

(a) (b)

Figure 1.12: Specific energy and Energy Density of various fuels. [46]

In addition, lithium-ion (Li-ion) battery discharge characteristics are such that voltage drops with higher current draw. In the figure below, the typical discharge characteristic trend for Li-ion batteries is represented, with several 'C-ratings' for increasing discharge rates. It should be noted as well that

Li-ion batteries cannot be over-charged or over-discharged without causing damage to electrodes, so the effective usable energy range is limited, as indicated in the figure.

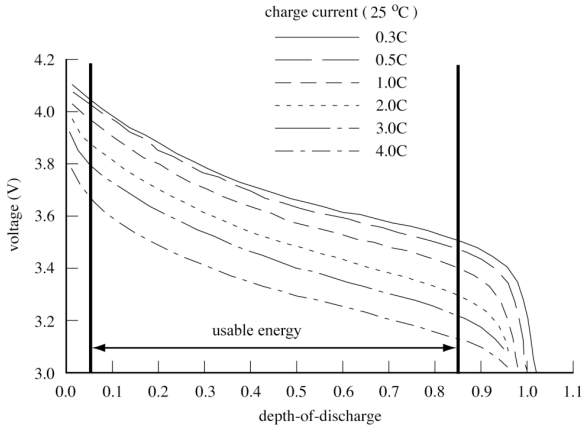

Figure 1.13: Lithium-Ion typical discharge curve. [47]

With scale-up in application size, the impacts of voltage drop for high-current applications is increasingly difficult to handle. As a result, systems tend toward higher voltage systems at lower current draw. However, high voltage systems have difficulties of their own, including thermal management and electromagnetic interference, as explained in Challenges Associated to High Power Hybrid Electric Propulsion in Aerospace. [48] Progress is being made to accommodate the design challenges at Airbus, identifying that at higher voltage, circuits that experience short-circuits have potential to damage aircraft structures. In an experiment comparing short-circuit arc tracking (in tens of milliseconds tripping), a 270V circuit melted and damaged cable jacketing, whereas a 3000V circuit vaporized significant lengths of cable. This vaporization and related plasma creation can be an ignition source for flammable gases onboard or can damage nearby structures.

(a) (b) (c)

Figure 1.14: 270V (left) short-circuit testing compared with 3000V (center, right) behaviour showing vaporization of test cable. [48]

1.4.6 Energy Harvesting

Energy harvesting technologies are an intriguing research area for aviation research groups as generating energy from ambient energy sources could mean less mass that must be brought on-board as fuel. These energy sources such as solar, vibrational or thermal can be used for auxiliary power systems, or to augment main power systems for aircraft depending on the application scale.

Solar Energy

The most substantial example of solar energy on a UAV is from the NASA Helios Prototype solar-powered aircraft. In August 2001, this impressive aircraft reached record setting altitude of $96,863 ft$. The 247 foot wingspan aircraft combined solar power and hydrogen-air fuel cells in a unique high-dihedral wing design and conducted several test campaigns. [49]

Figure 1.15: NASA Project Helios HP03-2 on Takeoff. (top) HP01 High-Altitude Configuration of NASA Project Helios. (bottom left) HP03-1 NASA Project Helios Fuel-Cell Variant flight in 2003. (bottom right) [49]

Freestream and Braking Energy

Research conducted with the University of Toulouse and Airbus explored the possibility of energy harvesting using braking energy of landing gear systems of the aircraft. Also in this analysis, the potential of using the propeller to 'wind-mill' energy during the descent phase was explored. In the simulations, it was found that large components would need to be added to the aircraft braking system and would only yield a 0.19% energy recovery. [50] The additional drag associated with windmilling the propellers during descent affects the aircraft's performance severely. For these reasons, and due to the limited time frame in which the aircraft has the opportunity to harvest the energy, this technology is not being further explored.

Fuel Cell

Fuel cell research for use in UAS is typically explored when combining with conventional lithium polymer batteries. Polymer electrolyte membrane fuel cells (PEMFC) are good candidates for UAV designs because of their low cost and operating temperature, as well as efficiencies of $40-60\%$. Although further development and research is required into practical application of fuel cells on UAS, the Heliplat Project proved that a $400Wh/kg$ system was possible when combined with energy harvesting technologies. [51]

Thermal Electric Generators

Thermal electric generators (TEGs) convert thermal energy to electrical energy using a phenomenon called the 'Seebeck Effect.' The larger the temperature gradient between each side of the TEG, the greater the electric potential. The methodology for using TEGs on aircraft would be to make use to the large thermal gradient between the combustion engine exhaust and the freestream air. During normal operation of the aircraft, these two thermal sources of heat and cooling would be consistent without impacting the propulsion system's behaviour. Most commercially available TEGs achieve a relatively low conversion efficiency of 5% due to limitations in semiconductor materials. However, an approximation of an analysis of a combustion engine yielded that 40% of a fuel sources energy is expelled to the environment in the form of exhaust thermal and kinetic energy. [52] As exhaust systems on small combustion engines typically have plentiful surface area, and temperature gradients between ambient air of $800^\circ C$, they are prime candidates for TEG technology.

Since aircraft vehicles are always mass constrained, there has been limited experimental research for TEGs on aircraft. However, Fleming, Ng and Ghamaty investigated thermoelectric power systems for micro air vehicle applications. [53] Flight testing of a thermoelectric power system, as well as design modelling and optimization was conducted by Langley, Taylor, Wagner and Morris. [54] In 2018, Matlock, Warwick, Sharikov et al. showed that a TEG system could be feasible on a small scale UAV, with experiments on a $36cc$ Saito engine and a modest $60^\circ C$ temperature difference. Through the experimentation, the optimal resistance for an off the shelf set of 3 small TEGs was determined in order to maximize power and was capable of harvesting $0.5W$ of power. For larger scale applications, the number of TEGs would need to be drastically increased, and with a higher temperature gradient, but then the power harvested could likely run auxiliary power systems, or supplement main power systems on a HEPS UAV.

1.5 Topic Overview - Methodology

In this thesis, the feasibility of a hybrid electric propulsion system for unmanned aerial vehicles will be explored. First, a theoretical model is developed to form baseline results and explore predicted efficiency of UAV with purely electric, purely combustion engine, parallel and series hybrid configurations. The theoretical model will allow for unbiased and parametric study of UAV configurations and explore the design space.

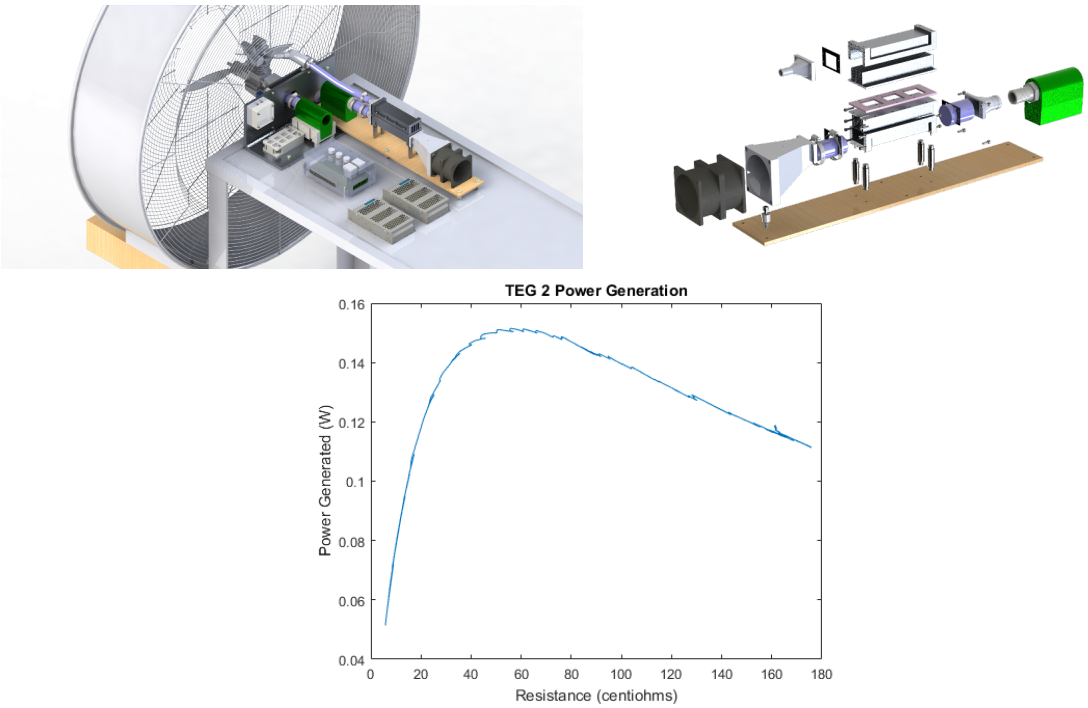

Figure 1.16: Thermal electric generator test apparatus from UVIC CfAR (left) with exploded view of the CAD. (center) The power generation from small-scale TEG was $0.5W$ with a $60° C$ temperature difference. (right)

In order to validate the theoretical results, component level and system level tests must be conducted to create experimental data. Each of the components in the hybrid architecture are tested at the University of Victoria Center for Aerospace Research, and this data is updated back into the MATLAB framework to improve the accuracy of the theoretical model. For the system level testing, a parallel hybrid-electric test bench was developed in order to generate performance data for the UAV's propulsion system. This test bench is designed to be modular to allow for further optimization of the propulsion system in future work. An array of sensors is instrumented to collect critical data points of the propulsion system's performance, which is logged with a custom data acquisition system using National Instrument's LabView. This same LabView program allows for the analysis and control of the test bench itself.

The results of the experimental test bench will be compared against the predictions of the theoretical model to evaluate performance. Various 'mission profiles' can be created to test each propulsion architecture in a range of applications. Further, since the MATLAB model has all of the aircraft design parameters designed parametrically, 'parameter sweeps' can be conducted to explore the design space with various trade studies. Each of these experiments will be run for the propulsion configurations to observe trade-offs between each architecture.

1.6 Framework Need Identification

With the many different hybrid-electric UAV projects being conducted around the world, it becomes difficult to make direct comparisons between projects. The first contributing factor to this complication is

the wide range of scales of which UAVs are designed for. It is clear that with the wide range of project presented in the State of The Art section of this report that it is incredibly difficult to evaluate HEPS aircraft against one another for efficiency and endurance metrics since their scale can be so drastically different.

Another contributing factor to this difficulty is the wide range of applications UAVs are typically used for. For instance, even if two UAVs being compared are of similar take-off weight, wingspan and design, their main objective application can be drastically different. Some UAVs are designed for maximum endurance and efficient flight, where others are specifically designed for large payloads and much shorter mission segments.

Another factor is the application of which hybrid-electric propulsion systems are being evaluated. Not only are there various architectures (series, parallel, power-split, push pull etc) there are also various strategies on how to execute these architectures. For example, two parallel hybrid architectures could be drastically different in how they share power requirements, where one architecture could use the EM just as a small buffer for the ICE, where another could have the EM supplying the majority of power for most of the duration of the mission with the ICE only supplementing a few loiter sections. It is not sufficient to simply compare two hybrid architectures of the same type.

It is clear that without eliminating variables of the aircraft designs and mission purposes, it is not a useful exercise to compare UAV projects against one another. For evaluation of an aircraft design, it becomes increasingly difficult to assess performance if there is no baseline design to compare against. A much more useful comparison of a hybrid-electric UAV performance would be to compare the hybrid architecture performance against baselines of more conventional propulsion systems, like electric or combustion engines. This way, external factors of varying size, mission applications and objectives are eliminated, and only the propulsion system performance remains. An unbiased comparison such as this would allow for critical analysis of the impacts of adapting and changing the design based on specific parameters rather than external factors.

During the literature review of this project, several HEPS comparison frameworks were discovered being worked on by groups around the world, but have limited access. The majority of the projects were in initial stages of development as this research project began, and had restricted access as they were closely involved with industry partners. [40] [41] [42] [43] In 2019, the Stanford University *SUAVE* program explored HEPS aircraft and is the first framework known to the author that will become open source but is not currently available. [44] As such, the need for the design and implementation of a MATLAB framework was identified. The framework must be able to analyze typical aircraft dynamics, load in information about the aircraft design, and separate out the propulsion system performance in its own module. This will allow for simulations to be run for different mission cases or parameter sweep exercises independent of the selected propulsion system. Furthermore, scripts must be included to automate the sequence of simulation to allow for multiple missions to be run with parameter sweeps and multiple propulsion systems against each other.

1.7 Objectives

The main objective of this research is to open the pathway for research and exploration at the University of Victoria Center for Aerospace Research on energy efficient and emerging propulsion technologies for Unmanned Aerial Vehicles. This research will bridge the gap of capabilities for the University of Victoria Center for Aerospace Research to design, evaluate, build and test hybrid-electric propulsion systems for use in UAVs. The primary objective is to determine if efficient propulsion technologies can be proved as viable solutions for small-scale aircraft so that the technology can be adapted and scaled up for use in much larger aircraft applications. Proving that hybrid-electric propulsion systems are feasible for small unmanned aircraft, and have potential performance and operations benefits is critical for the future of aviation technology at CfAR and across the entire aerospace industry.

Objective 1: Can a hybrid-electric propulsion system be proven as a viable solution for small UAVs?

The MATLAB framework will allow for comparison of propulsion technologies independent of the aircraft design. This tool will allow for unbiased and quantitative results to drive engineering design decisions for hybrid-electric propulsion systems on UAVs. This framework may potentially provide results that do not favour hybrid electric systems, but will provide clarity on which propulsion technology is the correct choice for the aircraft and application. Based on parameter sweep exercises, certain aspects of the aircraft design may be explored as well to compliment the hybrid system. For instance, when sizing an aircraft in the conceptual design stage, it is critical to estimate the mass of the propulsion system and power output capabilities when sizing fuselage and main lifting surfaces. Using the designs in this research as a baseline, and tweaking parameters with the MATLAB framework will allow future groups to become better informed in their engineering design decisions.

Objective 2: Can the design space of hybrid-electric propulsion systems be explored to advise design engineers and provide insight for mission planning?

With the recommendations and predictions of propulsion system performance created in the MATLAB framework, it is imperative to validate the theoretical results with experimental data. The end goal of this research project is not just to provide theoretical recommendations from simulated propulsion systems, but also to provide insight and tangible experimental results of HEPS performance. Thus, the objective is set to create a hybrid-electric test bench.

Objective 3: Can a hybrid-electric propulsion system be implemented in a controllable test bench in order to experimentally evaluate performance? What are the challenges associated with implementing a functional hybrid system?

Building upon the objective of creating a controllable test bench, can the two propulsion systems in a parallel configuration be effectively combined under the control of a supervisory controller?

Objective 4: Can a supervisory controller be implemented with the hybrid test bench in order to effectively combine the two different propulsion types and optimize performance?

CfAR and the rest of the aerospace research community holds high interest in investigating energy efficient propulsion systems for use on UAVs. Not only could this potentially reduce operational costs

of the aircraft, it can also make a substantial reduction in harmful greenhouse gas emissions. As outlined in the Motivations section of this report, there are aggressive goals set by the aerospace industry to improve aircraft performance over the next several decades. [4] As is true in most sectors, proof of concepts experiments typically lead the way for large-scale adoption and integration of new technologies. Experiments with smaller scale unmanned aerial vehicles are an excellent approach for mitigating financial risk and optimizing systems before tackling large scale applications.

Objective 5: Can a hybrid-electric propulsion system be experimentally proven to operate at equivalent or superior operating conditions to baseline propulsion systems while reducing green-house gas emissions?

The final objective of the research project is to make a comparison of the results collected in the experimental test bench with the results collected from the theoretical modelling in the MATLAB framework. This comparison will provide insight into the accuracy of the models developed in framework and allow conclusions to be drawn on the theoretical mission results.

Objective 6: Can the experimental results collected on the test bench be compared against the theoretical results of the MATLAB framework?

The data collected in this research, as well as the experimental apparatus, will open the doors of possibility for future research, improvements and optimization to hybrid architectures to be implemented at CfAR. The MATLAB framework tool will allow for qualitative analysis of the trade-offs and impacts of varying system parameters, which can then be validated by running experiments on the hybrid test bench. Data collected from the experimental work can then be implemented back into the MATLAB framework to further improve predictions of the hybrid system performance.

1.8 Thesis Outline

Chapter 1 - Introduction

The introduction section of this report captured the necessary background information of UVIC CfAR, and the motivations of pursuing hybrid-electric propulsion system technologies for UAVs. In the state-of-the-art section details were included from projects around the world in small-scale UAV and large commercial aircraft that are participating in energy efficient propulsion technologies in the aviation sector. Hybrid-electric propulsion systems have a history in development mostly in the automotive and marine applications, and are still emerging in the aerospace sector. Since UAVs are built at a wide range of scales and for a wide range of applications, it is difficult to directly compare one vehicle to another. Past research and development has indicated the feasibility for HEPS on UAVs, but there is no available optimization framework to inform engineering design decisions. Thus, the need for a framework to analyze component and system performance of a HEPS is clear for this research project to make direct comparisons of various propulsion architectures. The objectives section introduces the tasks and goals outlined for the scope of this research.

Chapter 2 - Theoretical Overview

A theoretical overview will be discussed for how a hybrid-electric propulsion system could replace conventional electric and gasoline configurations. The concepts of operation for a hybrid electric propulsion system will be discussed, as well as potential advantages of using a hybrid system. The series and parallel hybrid-electric configurations are the most common applications for UAVs, and their differences are discussed. Explanations and examples of the major components in a HEPS are introduced to review their function in the system. Finally several control scheme models are shown that will form the basis of the controller used in this project.

Chapter 3 - Simulation and Modelling

Each of the components of the electric, combustion, and hybrid electric configurations must be modelled in the MATLAB framework. In addition, other aircraft components like the propeller or battery systems must be modelled to gain a better understanding of how the entire system will perform. The numerical models used in this research are described, as well as the methods used to construct the MATLAB framework, and how the aircraft simulation framework functions. Component-level bench testing will also take place in order to update and validate these first order models. Further, the Simulation and Modelling chapter details the various mission profiles developed in the framework so that the UAV propulsion systems can be compared against each other in realistic operating cases, rather than steady-state comparison.

Chapter 4 - Experiments - Test Bench

The Experiments section will explore how the parallel hybrid test bench was designed and assembled. Detailed component level testing must be conducted to ensure the performance of each of the propulsion system components is modelled correctly. Further, in order to model the interaction of components with each other, for friction and heat transfer losses, system level testing is conducted. In order to observe these interactions, a modular hybrid-electric test bench had to be designed. This test bench allows for various components of various sizes to be tested together to evaluate system performance. This test bench is instrumented with an array of sensors to monitor and record system performance, and is used in the controller design which is described in this chapter. The bench testing experiments represent the bulk of the work required for evaluation of a hybrid electric system, and is how the theoretical predictions of a hybrid electric propulsion system will be validated. There were many design challenges to overcome in the design of this test bench, and many complexities in the instrumentation and control of the system. Finally, a brief exploration of the feasibility of implementing a parallel HEPS into a small-scale UAV is discussed. Several modifications need to be made to accommodate the additional systems on board, but these upgrades will allow for the parallel hybrid system to be explored and tested on an actual aircraft.

Chapter 5 - Results

The results section of this report first reviews the evaluation and trade studies section looking into the trade-offs of predicted system performance for changing and sweeping certain aircraft parameters. Using the MATLAB framework, the theoretical performance of each propulsion type can be explored and compared against its competing propulsion types. The next section of results presented are for the component level testing for the various HEPS components. After the construction of the test bench, the results of the system-level design are evaluated for each of the 4 operating modes: EM Only mode, ICE Only mode, Dash mode and Regen mode. Next, the supervisory controller that was developed in this project is analyzed for performance for three different controller modes: EM Controller, ICE Controller, and the Hybrid Controller. To validate the results collected on the parallel HEPS test bench, the theoretical results are compared to see how accurately performance is modelled. Using this information, critical engineering design decisions can be made to optimize the aircraft's performance.

Chapter 6 - Conclusions and Recommendations for Future Work

In this section, the achievements of this project will be discussed, as well as a critical look at the results found. In addition, recommendations for future work will be discussed which will include hybrid-electric propulsion system potential improvements and upgrades, areas or components for optimization, as well as future work with aircraft implementation and eventual flight testing.

Chapter 2

Theoretical Overview

In this section of the research, the theoretical information required for the analysis of a HEPS is presented, including descriptions of the operation concepts. In the formulation of the MATLAB framework in order to compare different propulsion architectures, the numerical equations to evaluate component performance was created, as well as logic for the system to function as expected. Topics introduced in this research are described in this section with sufficient information and external sources to form a complete understanding of the topic.

2.1 Concept of Operation

The concept of operation for a HEPS in a UAV is to combine the power from an electric motor and another propulsion type in such a way to optimize the efficiency of the overall system, extend endurance, or increase the output power. Depending on the requirements of the mission for the UAV, the hybrid system can enter into different operating modes in order to meet goals. For the purposes of this research, the electric motor is combined with a two-stroke internal combustion engine.

One of the main objectives of a HEPS is to extend the range of the UAV by operating efficiently, or by combining power sources to supplement the power requirement coming from a single source. Typically, for this scale of hybrid propulsion system, the ICE provides the majority of power with an electric motor providing support. In this manner, the ICE can be held to operate at its most efficient point, while the electric motor provides the remaining amount of required torque. In this way, the ICE of the HEPS can be sized smaller for sustaining cruise requirements, and the EM can be combined during high power segments like climb-out or dash.

The two energy sources used in a hybrid-electric UAV are batteries and hydrocarbon fuels like gasoline. Gasoline is a widely available and energy dense energy source which makes it extremely popular for propulsion systems in a wide range of applications. However, the combustion of hydrocarbons releases CO_2 and other harmful gases into the atmosphere. On the other hand, although electricity is consumed in the charging of battery systems which may come from non-carbon-neutral sources, no additional greenhouse gases are produced during operation. For this reason battery technologies of

all types are extremely appealing, but come at the cost of large manufacturing expenses and a lower energy density compared to hydrocarbons. As shown in Figure 2.1 below, the energy density of Lithium Polymer batteries are well below that of diesel or gasoline fuels, despite being one of the most energy dense battery technologies.

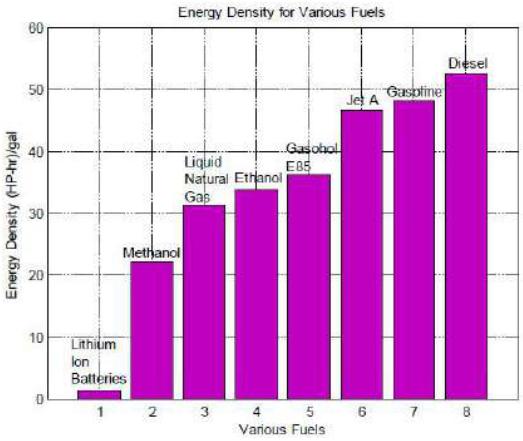

Figure 2.1: Energy density of fuels. [46]

However, if utilized properly, a hybrid architecture could extend the overall range of a UAV platform. For instance, for use in some military applications, a HEPS could be advantageous to extend the operational range of a stealth aircraft. Typically, small scale UAVs used for Intelligence, Surveillance and Reconnaissance (ISR) missions are electric propulsion to exhibit a small thermal and acoustic signature, but are hampered by a short flight endurance, thus limiting their operational range. This means that military groups must deploy the UAV close to areas of interest which may prove difficult. However, with a HEPS UAV, a combustion engine can be used to extend the cruising segment of the mission by carrying energy dense hydrocarbons instead of massive battery packs. During cruise, where the thermal and acoustic signature of the aircraft is of less importance, the ICE can consume fuel and achieve long ranges.

Then, once the aircraft enters the area of interest, the UAV can transition to fully electric operation, and idle or fully stop the ICE, effectively removing thermal signature and drastically reducing the acoustic signature in the absence of exhaust noise. Once the ISR mission is complete, the aircraft can transition back to ICE or a hybrid mode in order to travel back to the launch location.

Research groups at the University of Victoria are developing a hyper-spectral camera and a LIDAR system to analyze agricultural health. This system is being designed to attach to a small-scale UAV that can fly over and scan large areas of land and extrapolate the levels of nitrogen content in the soil, which is used as a metric of plant health. The instrumentation used in this project is sensitive, and needs an extremely low vibration environment in order to capture accurate data. For applications such as this one, a hybrid-electric architecture would be beneficial since the internal combustion engine could be idled during phases of sensitive data capture, but switch on in segments to extend the aircraft's overall data collection range.

Furthermore, in civil aircraft applications, hybrid-electric configurations could reduce the amount of

acoustic noise generated during the take off sequence where the power demand is often highest. As mentioned in Section 1.4 State of the Art, FlightPath 2050 is looking to reduce commercial aircraft take-off noise by 65% to minimize the amount of noise pollution experienced by nearby industrial and residential areas.

The final concept of operation is simply to reduce the overall fuel consumption for long-range commercial applications. For set routes of air travel, where the aircraft has a very specific flight operation envelope, a hybrid-electric system at any degree of hybridization could prove to be extremely beneficial and drastically reduce annual operation costs. It is clear that there is substantial interest from commercial groups at looking into energy efficient propulsion technologies for commercial aircraft.

2.2 Potential Advantages

There are a number of potential advantages that a HEPS poses when compared to conventional EM and ICE propulsion systems. The first and most prominent advantage is the reduced fuel burn and corresponding emissions of a hybrid system compared to an ICE Only system. The future of aerospace technology favours technologies that limit the amount of pollutants produced as well as extend the operational range of the aircraft.

Another advantage that HEPS offer over conventional aircraft types is redundancy in the case of failure. In a parallel hybrid configuration, the ICE or EM could fail and the other system could take over control. Although the single propulsion system may not be sufficient for sustained flight, depending on the sizing of the system, a partially operational propulsion system could make the difference in landing the aircraft safely because it would extend the range compared to a zero-propulsion glide.

As combustion engines increase in size, they exhibit larger acoustic noise from exhaust. In minimizing the size of the combustion engine on board, the produced noise from engine exhaust is also minimized. Furthermore, with larger combustion engines it becomes difficult to fully dampen and control the amount of vibration produced, especially in a UAV application where volume in the aircraft to support and mount the engine is limited. A smaller engine in the same aircraft would allow for more supporting structure, and increased vibration dampening control.

Electric motors have the advantage over combustion engines of having extremely quick dynamic response to fluctuations in demanded power. For this reason, electric propulsion aircraft can be incredibly nimble and agile and react quickly to mission power requirements. Further, an EM is capable of providing a high torque across a larger operating range compared to an ICE, which is able to deliver torque at very low RPM ranges. This in turn corresponds to higher efficiency. In a HEPS, the EM can allow the system to experience an increase in dynamic power response, and torque delivery for the entire operating range. In fact, a hybrid system can tend towards EM only in low speed high torque requirements, ICE only in high speed low torque requirements, and a combined power mode in high speed high torque requirements.

HEPS in UAVs also allow for advanced configurations that have new and novel characteristics, including distributed propulsion. Rather than a single power source for the entire aircraft, a single energy

source can deliver power to a variety of smaller power sources that can be arranged throughout the aircraft. In recent years, proliferation in the multirotor aircraft sector and massive increases in popularity have brought technological advancements in small brushless DC motors, speed controllers and flight controllers. As such, many different research groups and companies are exploring vertical take-off and landing (VTOL) configurations for all ranges of UAVs by adding small BLDC motors. Typically, these small motors are used for the VTOL phases in flight, and are left dormant, stowed, or rotated for use during horizontal flight. In these applications, exploiting a central HEPS systems can allow for generation of power for the VTOL motors, as well as providing the main source of power for cruise.

2.3 Hybrid Configurations

There are two types of hybrid-electric configurations considered for UAVs in this project: series and parallel. The objective is to combine electric motors and internal combustion engines in such a way that increases the performance of the vehicle. Although many of the components are similar in these two configurations, their architecture and performance is quite different. In a series architecture, one power unit is used to propel the aircraft while the energy storage is hybridized. In a parallel configuration, two power sources are mechanically combined to drive the propeller directly. There exists configurations more advanced than series and parallel, including power-split or 'series-parallel' configurations which combine the two architectures, but are not considered for UAV applications due to the additional mass of the planetary gearset and additional generator. [55]

Series Hybrid Configuration

In a series configuration, the ICE and EM are not directly mechanically coupled. Instead, a separate generator is directly attached to the combustion engine in order to generate onboard power. This power can be used to directly power the EM which connects to the propeller, or can be used to charge onboard batteries. The main advantage to a series configuration is that the ICE is mechanically decoupled from the EM, meaning that it can be operated independently. The ICE can be programmed to operate at the most ideal operating point where it provides the required power for the least amount of fuel consumption. This configuration also allows for the simplest control as the hybridization considerations are only between the energy sources. However, the main disadvantage to a series configuration is the inherent energy conversion losses in the system. Chemical energy stored in the hydrocarbon fuel is converted to mechanical energy in the combustion engine before being converted to electrical energy in the generator. From here, the power is transmitted through the system where there are minor transmission losses, and then is converted again by the EM to mechanical power of the output shaft connected to the propeller.

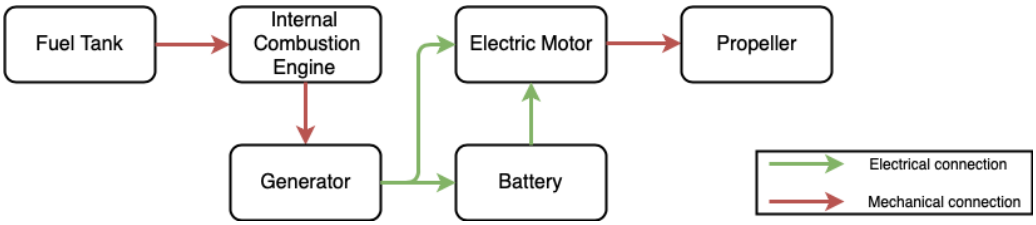

Figure 2.2: Series hybrid energy flow diagram.

Parallel Hybrid Configuration

In the parallel hybrid electric propulsion system, two power sources are combined through some form of a mechanical coupling which often contains a clutch mechanism. To fulfill the power requirement of the system, the power can be delivered by the EM or ICE exclusively, or through a combination of the two. There are several complex operating modes that can be achieved with a parallel architecture that are made possible through a clutch mechanism in order to isolate or combine power sources. When the clutch system combines the two power sources, the torque from each source is added together. When using a one-way bearing, the two sources must be rotating at the same speed for torque to be effectively combined. In addition if the clutch is combining the power sources, the EM can be used as a generator for regenerative brake mode in which the EM draws power from the ICE into the onboard batteries. Since a power-sharing mode is possible in a parallel configuration, each power source can be sized below the total power requirement which is not possible in a series configuration. Although the individual power sources may not be able to provide sufficient power for the entire operating envelope, each source could be sized for cruise requirements or for extended glide which could act as redundancy in the case of a power source failure. This reason, as well as the additional generator component of a series configuration, leads to an estimated 8% mass penalty compared to a parallel configuration for a $13.6kg$ UAV. [12] The main disadvantage of a parallel HEPS is that the mechanical transmission adds complexity to the system and controller design.

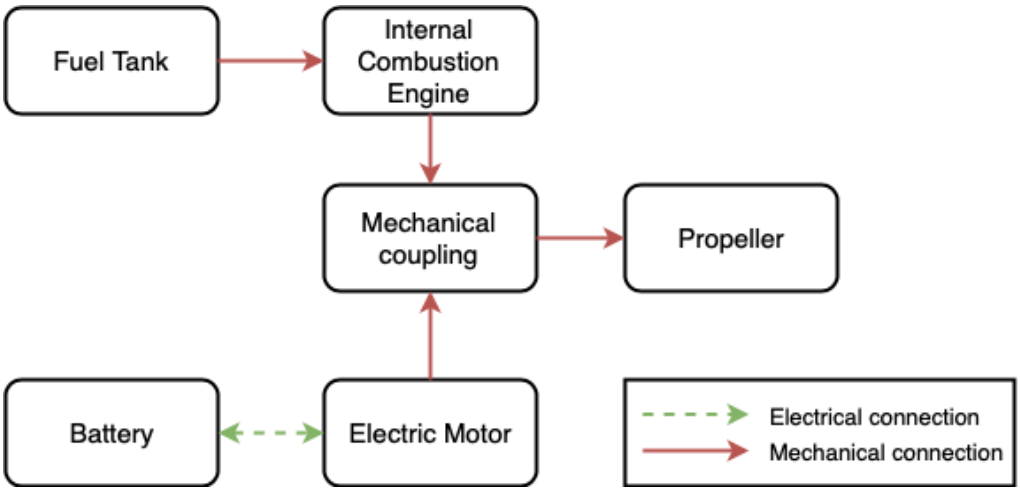

Figure 2.3: Parallel hybrid energy flow diagram.

2.4 Hybrid Electric Propulsion System Components

There are several main components which make up the core of a parallel hybrid electric propulsion system: the combustion engine, electric motor, batteries, mechanical coupling and propeller. This section will discuss the theory behind operating these components together, in order to maximize performance and minimize fuel consumption. Many of the components for this research project were sourced as commercial-off-the-shelf components making use of hobby-grade and professional grade equipment where available.

Internal Combustion Engine

The core of the power of a parallel hybrid electric propulsion system is the internal combustion engine (ICE). The ICE operates on the principle of converting hydrocarbon fuel chemical energy to mechanical energy by burning the fuel with an air mixture in order to drive a piston. A two-stroke engine is typically selected for small-scale aircraft applications since the engine is lighter-weight (higher power-to-weight ratio) and simpler compared to a four-stroke engine. The following figure indicates the stages of a two-stroke engine where the cylinder in the engine head moves to open or close ports.

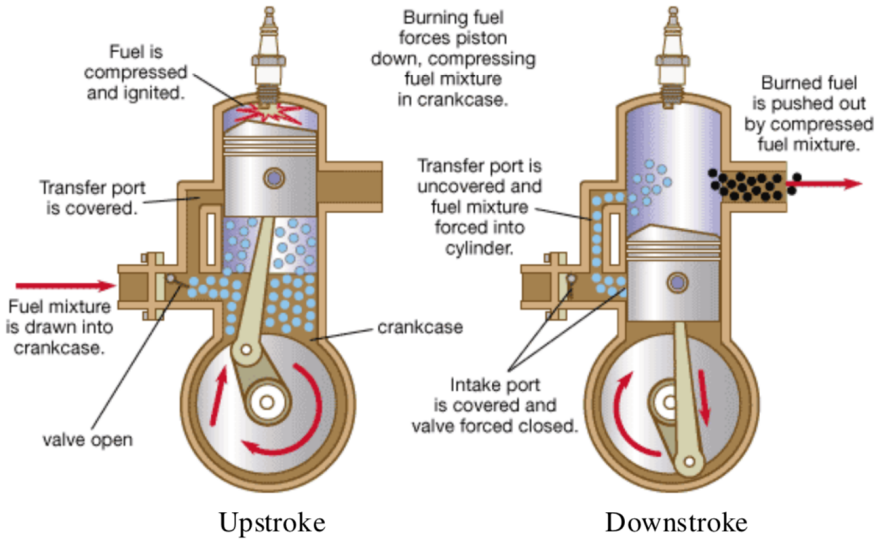

Figure 2.4: Diagram of a two-stroke engine strokes. [56]

In the upstroke of the engine, when the cylinder is at the Top Dead Center position, the crankcase port is open to allow for fresh fuel and air mixture to enter the crankcase. At the same time, a spark is used to ignite the compressed fuel and air mixture. This ignition drives the downstroke of the engine where the cylinder is forced downward to the Bottom Dead Center position. Here, the intake port is closed while the transfer port and exhaust port are opened for the fuel mixture to enter the cylinder. Simultaneously, the the burned fuel is expelled out of the engine exhaust port. Since it is difficult to completely displace the burned fuel mixture with fresh fuel mixture in the cylinder, the engine suffers a lower efficiency compared to four-stroke engines. In fact, two-stroke engines can exhaust some of the unburned fuel mixture out of the cylinder before it gets a chance to combust.

There are typically two types of fuel-delivery strategies used in small-scale combustion engines: naturally aspirated carburetors or fuel injection systems. To minimize the cost and complexity of the system, the combustion engine in this project was selected with a carburetor system, although it is not the most fuel efficient option. The amount of air that is able to enter the carburetor is controlled by two butterfly valves for the choke and throttle control. The choke valve is manually controlled and only closed during start up when a higher fuel-flow rate is desired to assist with initial start up. The throttle valve is connected to a servo, and can be controlled during operation from a fully open perpendicular orientation for Wide Open Throttle (WOT) to an idle position. At the idle position, the valve rests against an 'idle pin' which is manually adjusted to the minimum position in which the engine can run without stalling.

In addition to the two fuel valves, the carburetor contains trimming needles to adjust the rate at which fuel is pulled into the carburetor. The high-RPM pin and low-RPM pins will adjust how rich or lean the fuel to air mixture is at the high and low end of the engine's RPM range, and are typically adjusted experimentally or following manufacturer's instructions. A successfully tuned two-stroke engine will run smoothly at idle position, without 'miss-fires' or rough torque spikes, and transitions easily to higher RPM without overheating. A properly tuned engine will extend the working life by reducing the amount of carbon residue build up or dirty spark plugs, and prevent high-temperature operations which can lead to early fatigue.

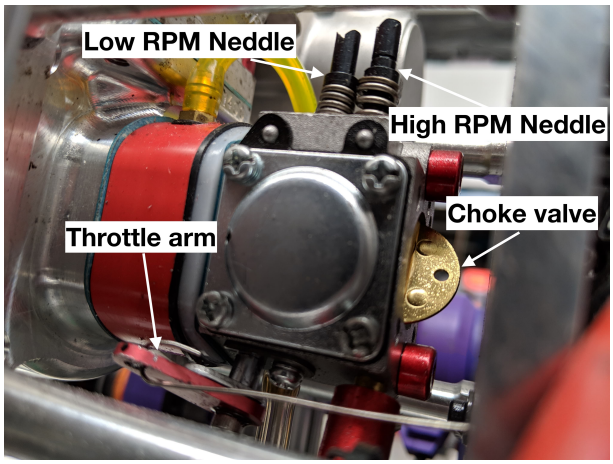

Figure 2.5: Walburo carburetor used in the Desert Aircraft DA-35 engine.

In small two-stroke engines, typically a capacitive discharge ignition (CDI) is used to reliably create a spark that is correctly timed with the cycle of the engine. Internally, a microprocessor calculates the RPM of the engine based on a hall-effect sensor input, and a large capacitor releases a high-voltage spark across the terminals of the spark plug. If the spark is not igniting at precisely Top Dead Center, the timing of the spark can be adjusted to slightly lead or lag by adjusting the position of the hall-effect sensor with respect to the crankshaft of the engine. In the Desert Aircraft DA-35 engine, three small magnets on the crankshaft are used by the CDI to create a more accurate RPM measurement. Disconnecting power to the CDI will prevent the engine from running any further because the fuel cannot be ignited without a spark, but the engine typically will continue to rotate for a short period of time because of the angular momentum of the system.

Following recommendations from suppliers, two-stroke gasoline engines typically combine a high octane gasoline fuel with a lubrication oil. The lubrication used in this research was a two-stroke engine oil mixed with 50:1 94 octane gasoline. This mixture is specified by the supplier in order to provide adequate cooling to the engine and to prevent piston deposits or sticking that can lead to premature damage to the cylinder walls. There are other possible additives for two-stroke engines, for example anti-freezing agents to prevent fuel freezing in cold operation environments. No additional additives were added in this experimentation.

For large combustion engines, torque estimation is possible through multiple sensors or by measuring Top Dead Center as proposed by Khiar. [57] However, in small scale UAVs, measurement of Top Dead Center presents several complications as outlined by Wilson. [58] In order to properly analyze the performance of an ICE, the power and fuel consumption must be determined as a function of the engine's speed (RPM) and output torque τ. An engine's output power is defined as:

$$P = \frac{\tau \cdot 2\pi \cdot RPM}{60} \tag{2.1}$$

$$BSFC = \frac{\dot{m}_{fuel}}{P} \tag{2.2}$$

The brake specific fuel consumption (BSFC) of an engine is defined as the amount of fuel consumed for a power $P\,[kW]$, where mass of fuel consumed $\dot{m}_{fuel}$ is measured in $[g/hr]$. Typically, manufacturers will run the engine on a dynamometer and vary the speed of the engine through its capable range, and apply varying braking power to the output shaft with a DC generator.

Electric Motor

The brushless DC motor (BLDC) is used in this application of a parallel hybrid electric propulsion system since it offers high reliability and longevity compared to the brushed counterpart. A brushed DC motor tends to wear out substantially more quickly than a brushless DC motor since the brushes required for commutation will degrade with regular use. In a parallel system, the BLDC can be used as both a motor and a generator depending on the required operating mode of the system. The permanent magnets in the BLDC are excited with electromagnetic coils in the stator to attract and repel the poles of the motor. In an inrunner BLDC the rotor runs within the stator, which can provide high-torque at low rotational velocities but offers a lower torque at high rotational velocities.[55] An outrunner BLDC has the rotor spinning around the stator which provides lower torque capabilities at low RPM, but a higher torque capability at higher rotational velocities. However, the additional rotational inertia of an outrunner BLDC will limit the maximum speed of the EM. The BLDC used in this design, and the majority of small scale aircraft, is an outrunner BLDC since it requires lower energy magnets, has larger rotor inertia, and has lower production costs.

To control a BLDC motor, a switching power circuit in the form of an electronic speed controller (ESC) is required. ESCs are typically comprised of metal–oxide–semiconductor field-effect transistor (MOSFET) where the voltage will determine the conductivity of the device. In the simplified description

from Dejan [59] for a motor with 2 rotor poles and 6 stator poles, it is shown that current is applied to the coils on the stator that will attract or repel the rotor. Combining the stator coils and commanding the 6 intervals can be achieved by activating the correct 2 MOSFETS as shown in Figure 2.6.

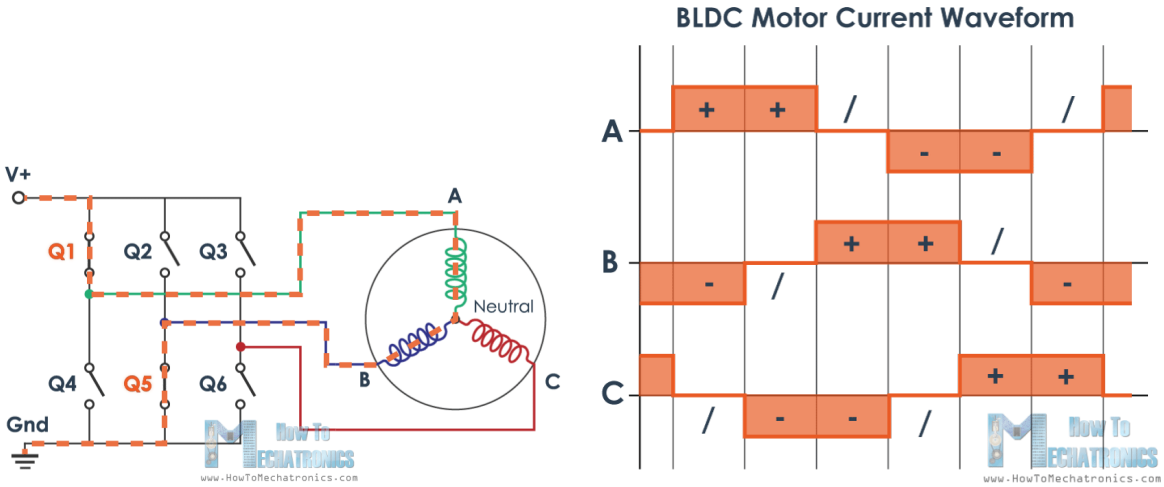

Figure 2.6: BLDC theory with simplified ESC theory. [59]

The ESC selected for this experimentation is the FOCBOX speed controller from Enertion Boards. This ESC was built up based on the VESC Open Source Project, and was selected for its detailed documentation and large regenerative braking capability. This speed controller is typically used in hobby electric skateboard applications where there is a very large current draw demand for normal operation, as well as regenerative braking. The motor selected for this project is the AXI 4130/20 from AXI Motors. Various products from this vendor have proven to be reliable based on experience from past projects at UVIC CfAR and motor performance data.

Batteries

There are many different types of batteries that have various characteristics that make them suited for certain applications. In this project, a battery type was selected that has a high energy density, and can handle large charge and discharge rates: Lithium Polymer (LiPo). LiPo batteries are available in a wide range of capacities, and in packs with varying number of cells in series. Further, suppliers such as Tattu / GensAce batteries provide LiPo cells with extremely high coulomb ratings (C) for both charging and discharging. Tattu batteries are extremely popular in multirotor and small aircraft applications based on their high discharge capabilities and energy densities.

However, there are several downsides to using LiPo batteries. Typical LiPo battery cells will have minimal protection against puncture damage which can cause them to rapidly overheat and combust once the lithium is exposed to oxygen. LiPo cells have a nominal voltage of 3.7V per cell, and should not be discharged below 3.0V per cell, or charge above 4.2V per cell. The anode and cathode of each LiPo cell can degrade over time if exposed to high temperatures, or charged above or below safe levels. In fact, it is possible to decrease the lifespan of a LiPo cell if it is stored for long periods of time fully charged or fully discharged, even if the measured voltage is within the recommended range. (For long

term storage LiPo cells should be charged to 3.7V per cell).

Mechanical Coupling

There are a number of different options that could be used in a parallel HEPS for the mechanical coupling of the ICE and the EM. Larger scale applications that can accommodate large and heavy components commonly use a clutch system, either mechanical our electromechanical, in order to mechanically couple components. The slippage behaviour of a clutch system is desirable in many applications where the difference of torque or RPM between two interfaces can be 'smoothed' using a clutch. However, based on the mass restrictions in small scale aircraft, a lightweight mechanical coupling is sought after in the form of a one way bearing. There are several different variations of one way bearings including a variant called a 'Spraug' bearing. In a Spraug bearing, the cam-shaped roller components of the bearing allow for smooth and free operation of the inner race in one direction, but prevent rotation in the opposite direction. As shown in Figure 2.7, each of the Spraug roller elements rotate and lock into place when rotational direction is reversed.

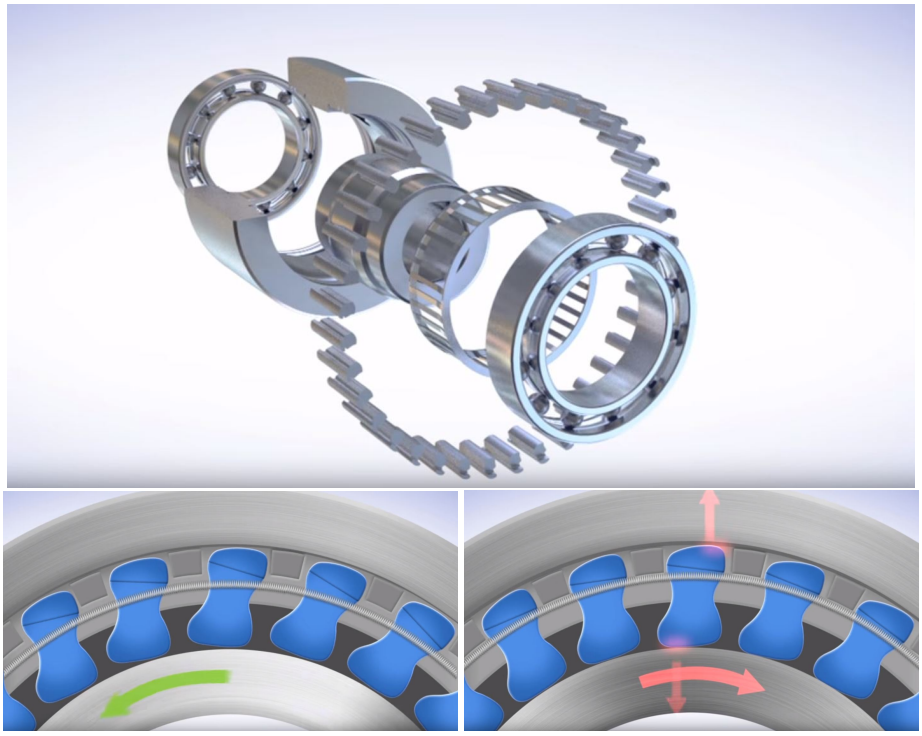

Figure 2.7: Spraug bearing description that is used in the parallel HEPS. [60]

When the ICE is the dominant power source, and rotational speed exceeds that of the EM, the one way bearing engages and torque is directly transferred to the output shaft. However, when the EM is the dominant power source, and the rotational speed exceeds that of the ICE, the one way bearing disengages, and torque is transferred from the EM directly to the output shaft. In operation modes when the EM and ICE are operating at the same speed, the one way bearing is engaged so that the torque can be shared between the power sources. This is also true for the regenerative braking mode, however the EM is removing torque from the system as opposed to supplying it in the combined mode. Using this

characteristic, it is possible to combine the ICE and EM of the hybrid system together.

Propeller

The performance of a hybrid electric propulsion system to be used for an aircraft must have a propeller which is correctly sized to produce the desired amount of thrust. At UVIC CfAR, a thrust test stand was developed in order to test and characterize different combinations of electric motor and propellers. The thrust test stand can accommodate propellers up to 22 inches in diameter, and is capable of measuring both thrust and torque. The power electronics of the thrust test stand are also capable of measuring and recording the power drawn by the electric motor, and contains safety cut-offs if the current drawn by the motor exceeds the pre-programmed threshold. In this way, it is possible to test and analyze various different propellers to assist in the optimal sizing.

The manufacturer of the combustion engine recommended propellers of varying pitches between 17 and 21 inches in diameter. The propeller that provided the correct torque and speed combination that was closely matched to the IOL for a desired thrust was a 19x10" wooden propeller from FlightModel RC. Although a variable pitch propeller could provide the ability to vary the amount of torque on the system, the added mass and complexity caused it to be ignored.

Control Schemes Model

The optimization of a hybrid propulsion control scheme is a critical component of achieving the highest possible efficiency. Comprehensive studies conducted by Harmon, Frank and Chattot suggest that fuel savings between 20% and 60% can be achieved compared to pure-gasoline conventional aircraft. [23] The simplest of the control schemes for hybrid propulsion systems are called 'on/off' or 'Thermostat' models. [13] These models are controlled entirely by monitoring the state of charge of the energy systems. Once a specific percent of charge is reached, the controller switches modes depending on the architecture. For example, in a series hybrid propulsion system, a thermostat controller may command the ICE to be idle until a charge of 20% is reached, at which time it is switched on to supply power to the main motor as well as charge the energy storage systems.

A rule-based controller developed by General Motors in 1997 saw a decrease in fuel consumption for a series hybrid vehicle of approximately 6 percent for highway and 11% in urban settings. [61] Although this data and controller were developed for ground vehicle hybrids, the same principles can be applied to aircraft to optimize performance and similar results are expected. Rule-based controllers are simple to implement, and provide reliable control for hybrid propulsion systems.

Fuzzy-logic controllers are based on the same principles as rule-based controllers, but instead of binary variables 0 and 1, they use any value between 0 and 1. The designer of the fuzzy-logic controller can input preferences and bias into the control scheme, unlike in a rule-based controller. However, the fuzzy-logic controller is not suited for high-input systems since it is susceptible to "exponential rule expansion" on non-linear problems. [13] Recent research in 2019 suggests that a fuzzy-logic controller on a UAV can save up to 11% fuel consumption for certain flight missions. [62]

Harmon, Frank and Joshi made breakthroughs in the development of hybrid propulsion systems control schemes with their work on cerebellar model arithmetic computer (CMAC) Neural Network controller. [12] This control scheme uses 67.3% less energy than a purely gasoline powered UAV of the same size for a 1 hour mission, and 37.8% less energy in a 3 hour mission. The CMAC controller is essentially a look-up table that is capable to adapt and generalize, and requires substantially less memory. Compared to a baseline rule-based controller, the CMAC controller could use 6.3% less fuel. CMAC controllers represent the State of the Art in hybrid propulsion system controllers, albeit the most complex to implement.

There exists two main operating strategies for HEPS of parallel or series architectures: charge sustaining (CS) and charge depleting (CD) strategies. [12] In a CS strategy, the objective is to maintain an overall state of charge (SOC) in the battery storage system, and will prioritize entering regenerative modes to accomplish this. This means that the electric motor only mode would not be prioritized. On the other hand, in a CD strategy, the SOC is decreased overtime by prioritizing the modes which consume battery. CD strategies are typically used in applications where the mission or drive cycle is well defined and the device can be recharged after each use, such as in electrified scooters. The CD strategy fits well with small scale hybrid UAVs as the aircraft can be recharged from an external power source after missions are completed. However, if only a CD strategy is utilized for the entire duration of the flight, the aircraft will not be optimized to handle variance in power requirements and will be constantly depleting the battery source. For example, if a hybrid UAV experiences large power fluctuations during a mission, it may be advantageous to alter the operating strategy to accommodate the mission requirements and design goals for endurance or fuel consumption. A control strategy that utilizes both CD and CS strategies will provide the most robust system. Thus, it is clear that a supervisory controller is required to assist in the decision making of energy management on a HEPS.

In the open-loop rule-based controller implemented in this project, the objective is to match the speed reference and output. As depicted in Figure 2.8, a reference speed is read by the UAV operator which will initiate a torque request. From here, the supervisory controller finds the optimal combination of ICE and EM throttle which corresponds to the lowest fuel consumption rate, and the information is sent to the UAV. From here, the speed output can be measured, and compared against the reference speed, completing the loop.

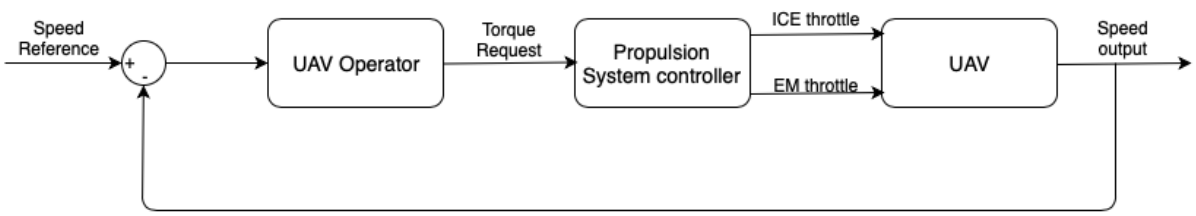

Figure 2.8: Controller feedback loop description. [63]

Chapter 3

Simulation and Modelling

The Simulation and Modelling section of this report will describe the modelling techniques for each of the components and systems developed in the Aircraft Simulation Tool implemented in MATLAB.

3.1 Aircraft Simulation Tool - Architecture Description

The framework developed in MATLAB has various components. The highest level is the aircraft class which contains aerodynamic and aircraft operation data. Depending on the aircraft type being analyzed, the propulsion module contains component data for the electric, gasoline, parallel or series hybrid architecture. Within this module, the propulsion performance is calculated based on the required power for the time-step. The MATLAB framework also allows for the design of complex mission profiles for the simulated aircraft to run in. This allows the various propulsion types to be compared in an unbiased and realistic manner rather than direct steady-state comparisons. The framework allows for high detail control over the mission parameters such as climb gradients, cruise speeds and loiter times. To reduce complexity and minimize computational time, the time-steps for each mission can be specified for each mission section and increased for sections where the aircraft is in nearly steady state (for example in cruise or loiter sections with constant altitude.)

The MATLAB framework is divided into two main sections: the propulsion module and the aircraft module. The propulsion module was designed to interface directly with the aircraft model by sharing variables, but can be defined independently. This means that the propulsion module can be swapped out for different propulsion types without influencing the aircraft aerodynamics aspect of the simulation. Several command arguments are loaded into the main propulsion method including throttle percentage, velocity and 'time-step.' These variables will determine the amount of power output required, the desired vehicle horizontal velocity as well as the resolution of the simulation by varying the 'time-step' interval. Outputs from the propulsion module is data for debugging code, as well as a structure 'propulsionOutput.' This structure contains many variables including:

- Forces produced in xyz axis
- Moment produced in xyz axis
- Mass of propulsion system
- Remaining charge of battery system
- Estimated remaining endurance
- Estimated emissions produced
- Propeller RPM
- Battery voltage
- Battery current
- Battery power
- Shaft power of propeller

For each propulsion type, (electric, gasoline, series hybrid and parallel hybrid) the propulsion module calls functions to calculate 'propulsionOutput' unique to that class. Within the hybrid configurations, the control algorithms determine which combination of EM or ICE power to supply the required thrust, and what fuel consumption or energy consumption corresponds to the calculation 'time-step.'

The aircraft module of the framework includes all of the characteristic properties of the aircraft itself, including the maximum take-off weight, mass distribution, lift, drag, fuel and dynamics such as velocity, climb/descent rates as well as mission segment. A flight data recorder 'FDR' captures the values of each of these aircraft properties determined for each time-step of the simulation. Based on the configuration selected, the aircraft module is configured accordingly to include appropriate component masses associated with that architecture. Finally, the simulation can run different 'mission scripts' where the aircraft is exposed to different environments or flight conditions.

The following figure shows a simplified overview of the MATLAB framework.

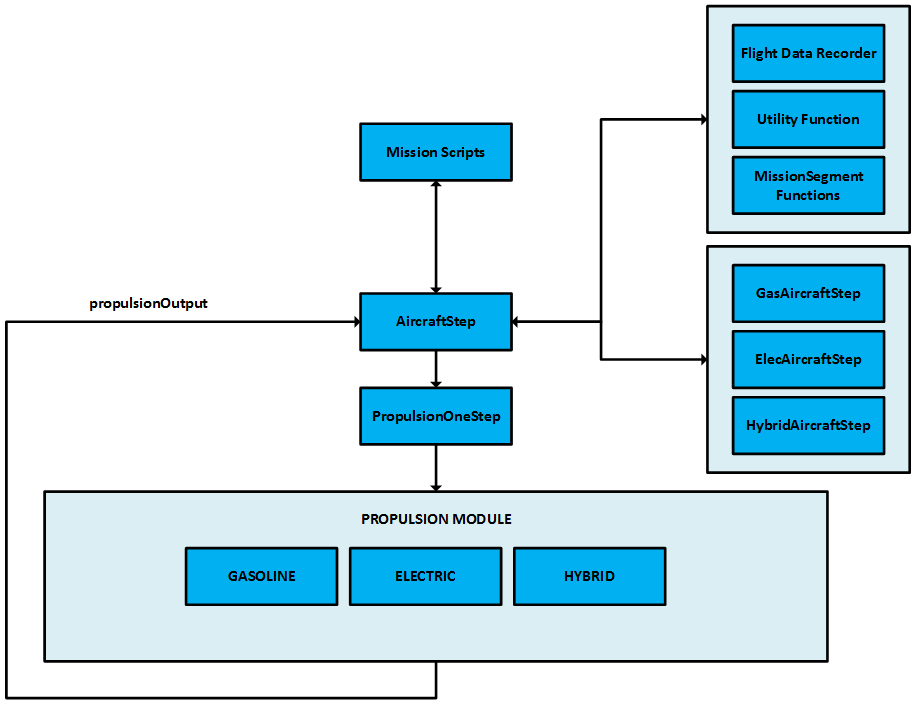

Figure 3.1: Flow chart of the information flow between the various modules in the Aircraft Simulation Tool.

3.2 Numerical Model - Components

In order to effectively predict the performance of the various UAV propulsion systems, including the hybrid systems, it is imperative to properly model each of the components in the system. This section reviews the description and details of component models used to calculate and predict the overall system performance.

Lithium Polymer Battery Model

Many different research groups are exploring the performance and behaviour of lithium polymer (LiPo) batteries as they become increasingly prolific in modern technology applications. The majority of this research is focused on the pursuit of maximum efficiency and power capabilities of battery systems. MathWorks has developed a Simulink model for the charging and discharging characteristics of many common battery types including LiPo batteries. The following equations form the basis of the battery charge and discharge curves of the electric module, and is used in both parallel and series hybrid framework modules. [64]

Charging ($I_n < 0$)

$$V(I_t,\ I_n,\ t)\ =\ V_0\ -\frac{K\ \cdot Q\ \cdot I_n}{I_t \cdot t\ +\ 0.1Q}\ -\ \frac{K \cdot Q \cdot I_t \cdot t}{Q\ -\ I_t \cdot t}\ +\ A \cdot exp(-\beta \cdot I_t \cdot t) \tag{3.1}$$

Discharging ($I_n > 0$)

$$V(I_t,\ I_n,\ t)\ =\ V_0\ -\frac{K\ \cdot Q\ \cdot I_n}{Q\ -\ I_t \cdot t}\ -\ \frac{K \cdot Q \cdot I_t \cdot t}{Q\ -\ I_t \cdot t}\ +\ A \cdot exp(-\beta \cdot I_t \cdot t) \tag{3.2}$$

Where I_n is nominal battery current (A), I_t is battery current during the time-step, t is the time-step, Q is battery capacity (mAh), V_0 is nominal battery voltage, V is output voltage, β is exponential capacity coefficient, and K is polarity voltage.

The model used for LiPo batteries requires several coefficients which can be determined by analyzing the voltage curve of a battery discharging at a constant rate. To determine the coefficients used in these equations, battery testing was conducted with the CfAR Thrust Test Stand to discharge batteries at constant current. An example of one of these voltage discharge curves is shown in Figure 3.2. Using the exponential zones, the coefficients can be determined.

The following figure depicts the results of the battery discharge curve estimation. Shown in the dotted blue line, experimental data for a $1A$ discharge curve of a six cell $8000mAh$ TATTU LiPo battery was collected by UVIC CfAR using a National Instruments Data Acquisition System. The nominal discharge area is shown in orange, but the exponential areas shown in green are of particular interest in order to determine the discharge curve of the battery. These exponential zones are used to determine the coefficients in the equation above and allow for the determination of voltage draw at each time step of the model. Shown as green and red markers, the voltage approximation at the beginning and end of an example simulation are also shown in the figure, and exhibit high precision with the experimental data.

From this model, the charging characteristics of a lithium polymer battery can be approximated using

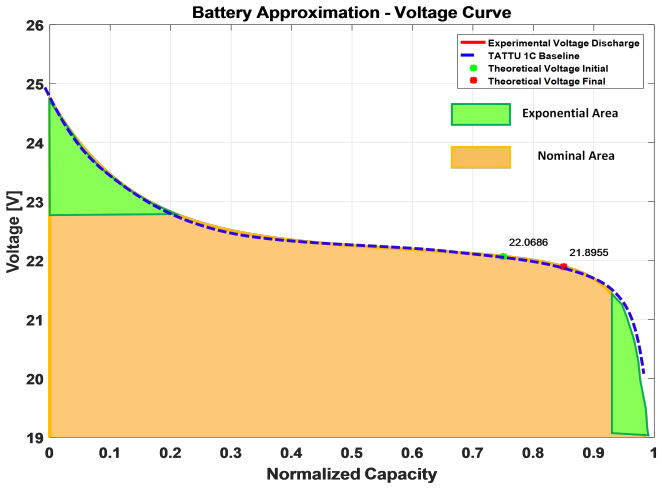

Figure 3.2: Lithium polymer battery discharge curve estimation for voltage drop of Tattu batteries.

a negative current. Using this model, the state of charge (SOC) can be approximated using the state of charge equation shown in Equation 3.3.

$$SOC \ = \ 100 \left(1 \ - \ \frac{\int_0^t I_t \cdot t}{Q} \right) \tag{3.3}$$

Propeller Model and Database

The propeller model in the MATLAB framework is a blade-element code developed by Dr. Jenner Richards. Blade element and momentum theory was the basis of this modelling, where the propeller geometry is divided into 25 sections and *XFOIL* is used to predict lift and drag. [65] Further, the APC propeller database was used in the generation of the parametric model based on the 481 propellers geometry, efficiency and thrust and power coefficients. A baseline 20x8" propeller was measured for airfoil coordinates, twist distribution, chord distribution and sweep distribution. Using this information, a parametric model was developed that could be morphed for desired geometry for a range of propeller sizes.

BLDC Electric Motor Model

A brushless direct current (BLDC) electric motor is the basis of the electric motor model in the aircraft framework. BLDC motors have proved to be extremely popular in unmanned aerial vehicles due to their inherent high efficiency and reliability by removing the necessity of commutation brushes. To model these electric motors, a simplified Kirchhoff's Law equivalent circuit is used to calculate performance.

The EM model includes the internal resistance R_m measured in ohms (Ω), and the no-load current I_0 measured in amps (A). The motor's back-EMF is given by the following equation:

$$V_m \ = \ V \ \ - I \cdot R_m \tag{3.4}$$

V_m is used to determine the motor's shaft rotation ω_m with the motor's speed constant K_v.

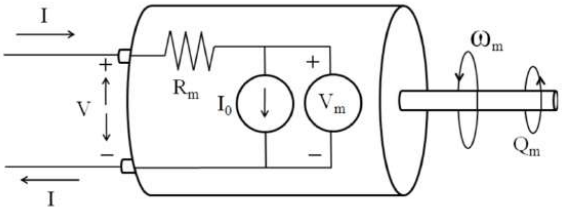

Figure 3.3: Simplified diagram of a brushless DC motor using simplified equivalent circuit. [8]

$$\omega_m \ = \ V_m \cdot K_v \tag{3.5}$$

The torque produced by the motor is a function of the current applied I and is calculated:

$$\tau_{out} \ = \ \frac{I - I_0}{K_v} \tag{3.6}$$

The no-load current of the AXI 4130/20 motor used in this research is $I_0 = 1.1A$ and the speed constant $K_v = 31.94$. To determine the power that is provided to the EM, it is the sum of supplied voltage and current.

$$P_E \ = \ I \cdot V \tag{3.7}$$

And finally, the output power of the EM is calculated by the sum of the output torque and rotational speed of the motor.

$$P_{out} \ = \ \tau_{out} \cdot \omega_m \tag{3.8}$$

Internal Combustion Engine Model

The internal combustion modelling is based on both manufacture and experimental engine maps. Data was collected for a range of two-stroke combustion engines ranging from $28cc$ to $50cc$ displacement. These engine maps include fuel consumption, power output, RPM and torque. From the data points of the engine maps where the engine is tested with a dynamometer, surfaces were extrapolated in MATLAB to allow parametric modelling of the engine. This parametric modelling allowed for elastic scaling of the engines, based on maximum engine power. The following figures represent the engine performance data for the main candidate engine, the Desert Aircraft DA35. This information will allow the simulation framework to return estimates for engine torque, power, BSFC or RPM based on inputs for any scale of engine within the modelling range.

As is typical with two-stroke engines, the DA35 is most inefficient at low speeds and low throttle positions, and is suited more for high RPM high throttle setting applications. In larger scale applications or automobiles, a gearbox is utilized to maintain the engine running in higher RPM zones, while adjusting the output power as required.

In order to properly map the ICE provided by Desert Aircraft, the Ideal Operating Line (IOL) had to

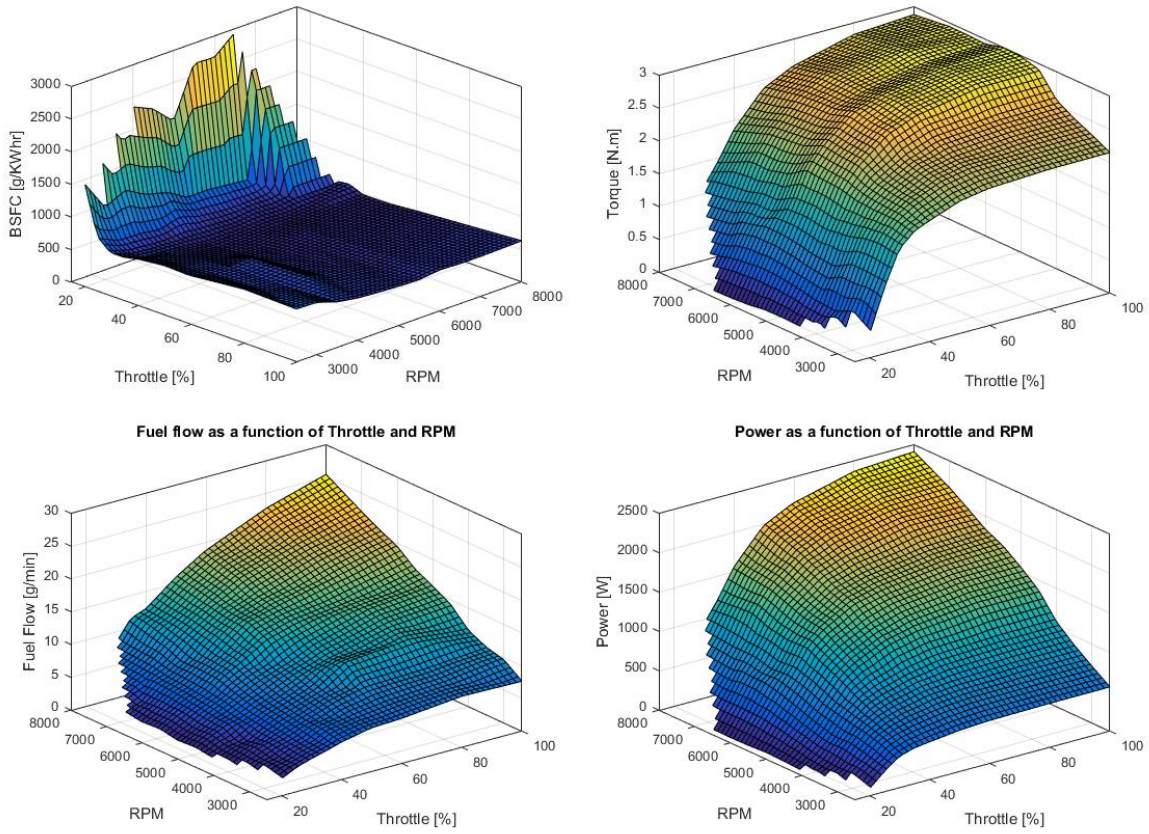

Figure 3.4: DA35 engine BSFC (top left) torque (top right), fuel flow (bottom left) and power as a function of throttle and RPM.

be determined first theoretically and then experimentally. The IOL is a trend line on the fuel consumption map of an engine that is the combination of each torque and RPM set that corresponds to the lowest BSFC. As seen in Figure 3.5, the engine map for the DA35 is shown with the IOL which is an extrapolated third order polynomial created by selected discretized power points throughout the engine's operation range.

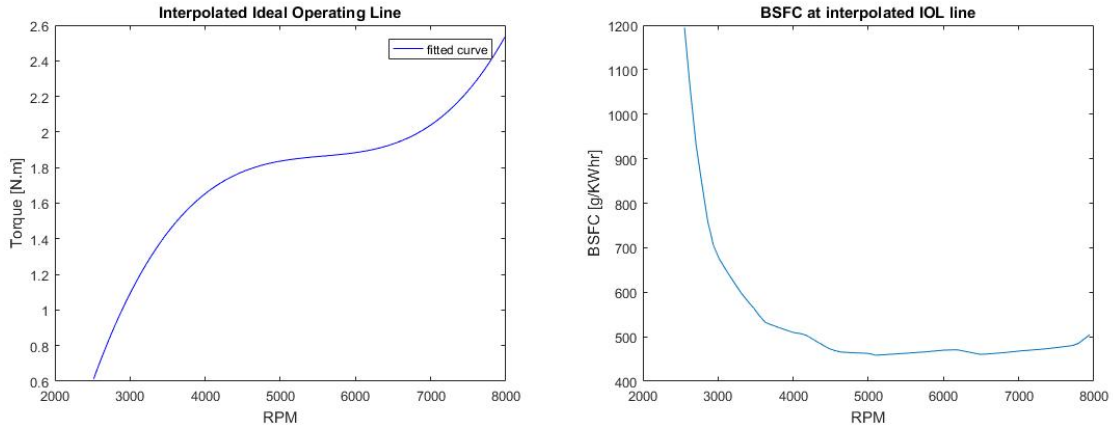

Figure 3.5: DA35 engine IOL and BSFC vs RPM following the IOL. Overlaying the 19x10" propeller curve and IOL onto the DA35 torque-RPM map.

As shown in Figure 3.6, the DA35 engine operates most efficiently in high torque and high RPM

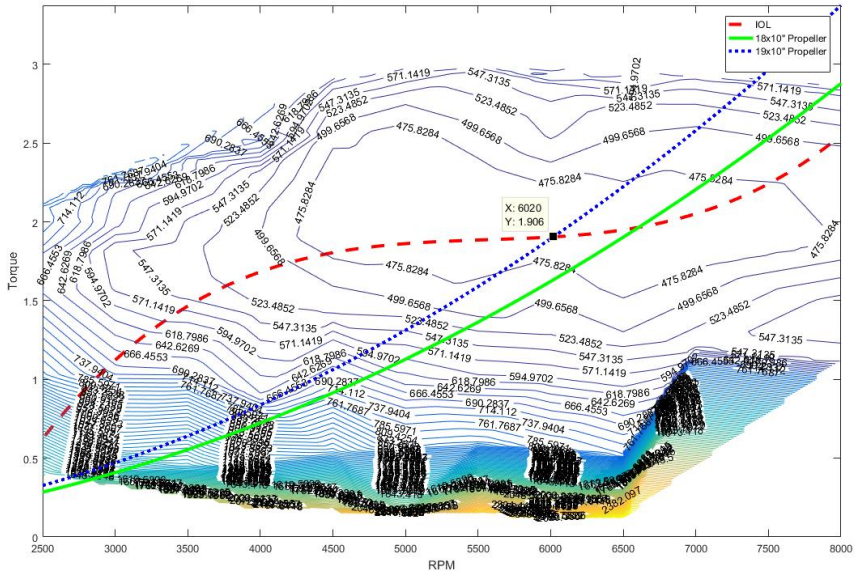

Figure 3.6: DA35 engine BSFC with IOL, 18x10" and 19x10" torque curve.

ranges of the engine map. This shifts the operational range of the engine to be limited within 4000 and 6000 RPM, and for torque values between 1.7 and $2.0Nm$. The engine must be held within this zone or it will suffer substantially lower performance at high speed / low torque zones, or any low speeds.

Electronic Speed Controller Model

The electronic speed controller can be modelled for efficiency based on the energy dissipation in the ESC. The factors to calculate the ESC efficiency include the internal resistance R_i, input voltage $V_{in,ESC}$, input current $I_{in,ESC}$, power input $P_{in,ESC}$ and maximum power capacity of the ESC $P_{max,ESC}$. Finally, the part-throttle factor in the equation is for relating part-load efficiency, k_{PTF}. For simplicity, the model for electronic speed controller in this module has been simplified for a set 90% efficiency of the speed controller for all voltages and load capacities.

$$\eta_{ESC} = \frac{V_{in,ESC} - R_{i,\,ESC} I_{in,ESC}}{V_{in,ESC}} - \frac{k_{PTF}}{V_{in,ESC}} \left(1 - \frac{P_{in,ESC}}{P_{max,ESC}}\right) \tag{3.9}$$

Sizing and Optimization

There are many options described in literature for the sizing and optimization of a hybrid propulsion system. As noted by Perullo and Mavris, the inclusion of hybrid systems makes the problem a multi-variable optimization rather than a root-finding problem in conventional aircraft design. [66] The variance in time-scales also adds complexity to the model where the controller decisions are on the order of micro-seconds, engine performance on the order of seconds, and the flight endurance on the order of minutes or hours.

The purpose of this report is not to review complete aircraft design techniques. However, one of the main drivers of aircraft design is the power requirements to overcome mechanical, electrical and

propeller efficiencies of the aircraft, and achieve a minimum velocity for a specified lift-to-drag ratio, aspect ratio and wing area. Basic equations of aircraft sizing are written by Bagassi, and more extensive equations can be found in Corke. [67][68]

The optimization of a single energy source UAV is a simple process, as described by Choi and Reynolds. [69] [70] Pornet, Kaiser and Gologan developed a metric called Cost-Specific Air Range or 'COSAR' to compare different aircrafts and technologies. [41] This method takes the aircraft dynamics into account, and can be set to minimize energy use, maximize endurance or to maximize gross weight for predetermined mission criteria. The AeroPropulsion System Department at the Korea Aerospace Research Institute identified that power management is a critical factor in the sizing and optimization of multiple energy-storage systems, based on the simulated behaviours of fuel cells, batteries and solar cells working together. [71]

The most successful strategy in the sizing and optimization of hybrid UAV systems was put forth by Glassock and Hung. [72] This strategy is based around the estimated mission endurance for ICE only, ICE with generator and a parallel hybrid system. This approach allows for parametric study of factors such as payload, maximum engine power and battery size, and the study contains a large amount of data that will form the baseline of comparison for ICE only, electric only and parallel hybrid systems.

Since the CfAR QT1 aircraft in this research had sizing information available for both electric and gasoline configurations, the hybrid propulsion systems had a strong baseline to refer to. Other influences on the sizing of components in this project were also based on commercial-off-the-shelf parts, availability, cost as well as complexity to integrate. All of these factors contributed to the selection of the components described in Section 2.4.

Electric Propulsion Module

The electric propulsion module is quite simple compared to some of the other propulsion modules, and is all driven by a power requirement input command. This command can be either a throttle setting, thrust value or a power requirement. Mission variables are loaded into the module to include information such as climb gradients or velocities to achieve, as well as individual component data for the motor, propeller, electronic speed controller (ESC) and the battery system. Each of the components of the system are modelled individually based on existing models found in the state of the art research. Further, these models can be updated with bench-testing data, as was done with the lithium-polymer battery model discussed in the component model section of this report. The following image depicts the simplified flow of information of the electric propulsion module.

At each step of the simulation, the amount of power requested by the motor is found by either fixed throttle or fixed thrust demand. The amount of voltage supplied by the battery and required current is calculated in the battery module. The battery module uses a sophisticated script to predict the voltage drop of the cells based on the required current draw based off of experimental results from varying discharge rate tests, and decrements the battery capacity state of charge accordingly. The power requirement calculation considers the inherent efficiencies of each of the components to ensure sufficient power remains after losses. Output from the electric module are the moments and forces exerted on the

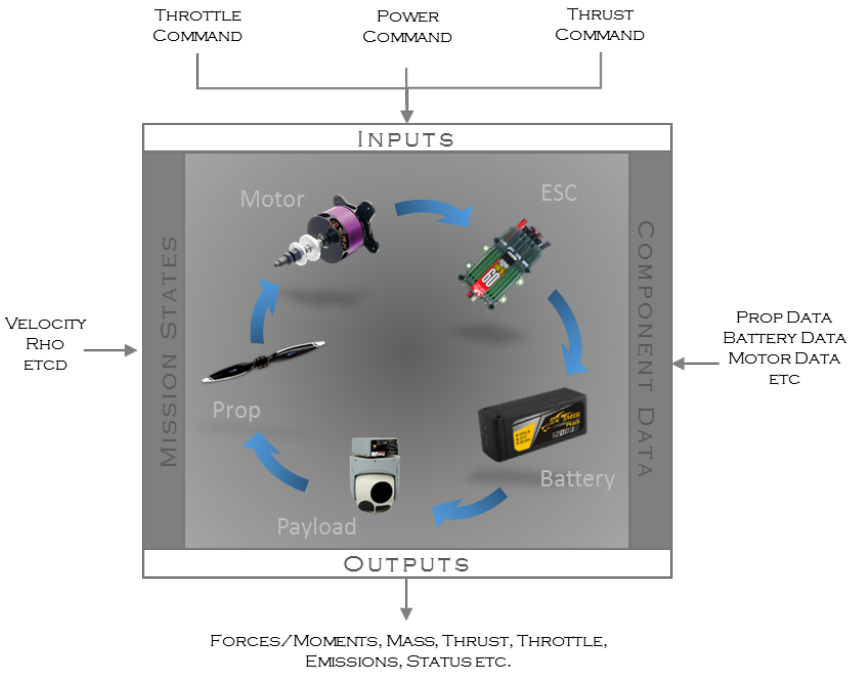

Figure 3.7: System modelling figure for electric propulsion module.

aircraft, aircraft mass, thrust produced, throttle position, emissions and battery status.

Gasoline Propulsion Module

The gasoline propulsion module follows a similar flow of information as the electrical module with several differences. The gasoline model is capable of collecting an RPM command as an input, as well as throttle position or thrust command like the electric model. Mission conditions are contained in the gasoline model just as in the electric model, including climb gradients, altitudes or speeds. Component data is loaded into the module for engine parameters, propeller data, and fuel capacity. To achieve the optimal fuel efficiency, the speed and torque of the engine is selected in order to achieve minimal fuel consumption, or 'Brake Specific Fuel Consumption,' BSFC. The following image is a simplified model of the flow of information in the gasoline model.

This model will output the forces, moments, thrust produced, throttle position and engine status of the aircraft. Unlike the electric aircraft, the mass of the aircraft changes overtime as the fuel is consumed. The difference in aircraft mass has an impact on the aircraft performance, and is also captured to measure the amount of emissions produced by the aircraft.

Hybrid Propulsion Module

The architecture in the hybrid propulsion module is slightly more complex than the electric or gasoline modules, and contains portions of each. As with the other modules, the framework receives a throttle or thrust requirement at each time step in order to achieve the mission parameters. Using the parameters defined in the mission requirements for the aircraft velocities, flight conditions and current aircraft attitudes, the power requirement can be defined. The two main configurations of hybrid propulsion systems

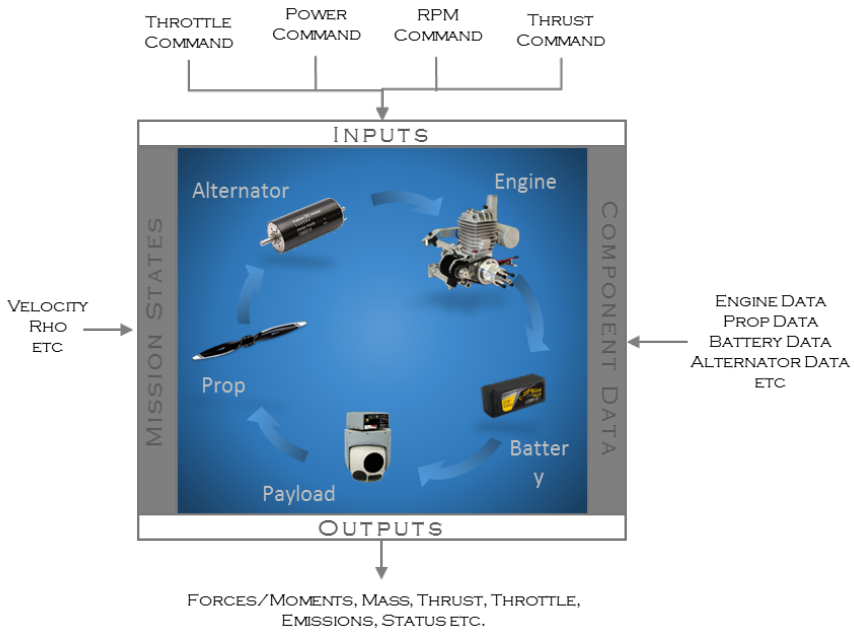

Figure 3.8: System modelling figure for gasoline propulsion module.

are broken into series and parallel systems. In Chapter 2 of this report, the various different types of hybrid propulsion technologies were explained for high-level operation and differences in components. In the MATLAB framework, the hybrid module operates much like both the electric and gasoline modules. Power requirement is determined as either a throttle or thrust command, mission variables and component information are loaded in depending on the sizing and configuration of the hybrid type. The hybrid module outputs forces, moments, masses and emissions data just like the electric and gasoline modules, but the overall state of the module is determined in an independent state controller.

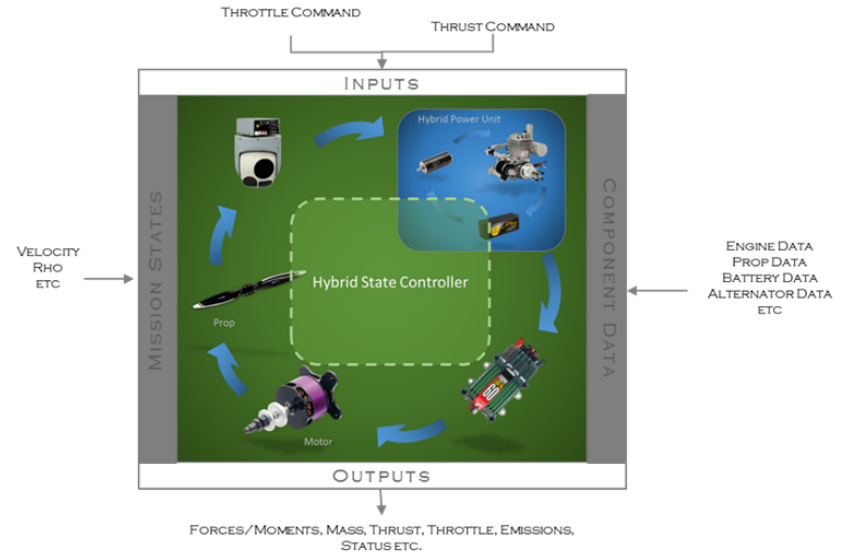

Figure 3.9: System modelling figure for hybrid propulsion module.

Series Hybrid State Module

The series hybrid state module includes a rule-based controller which is used to determine the state of the aircraft at each time step of the simulation. The considerations of this controller include the required power to provide thrust, battery SOC, and the Ideal Operating Line (IOL) of the ICE based on its speed. At any given time during the mission, the state of the aircraft can be forced into a charging state regardless of mission factors, but may suffer a performance decrease. The ICE will operate in the IOL unless the maximum power is requested, and this should only occur when the battery systems are depleted and a dash or climb sequence is requested. Finally, the battery is constantly in a slow state of charge when the power requested is slightly below the IOL of the ICE. The battery will discharge when the aircraft is requested to be in an electric-only 'stealth mode' or during extreme climb modes where the battery systems will provide the balance of the requested power. The following image describes the basic flow diagram to determine the operating state of the aircraft.

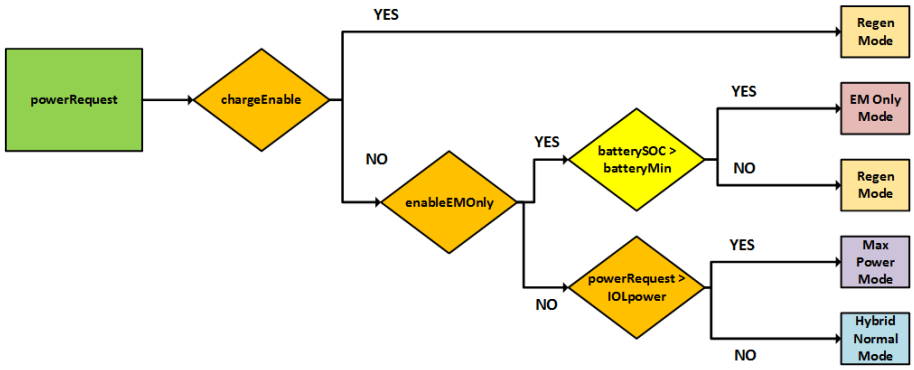

Figure 3.10: Series hybrid controller in aircraft simulation framework.

Parallel Hybrid State Module

The parallel hybrid state module includes a rule-based controller based on 3 decisions: state flags, battery charge percent and power requirement. Depending on the power requirement, certain hybrid modes may be unavailable, such as the EM Only 'stealth' mode. The battery SOC also dictates which hybrid state the propulsion system operates in, and finally there are state flags to force the system into charge or stealth modes. The following diagram shows how the power requirement at each time step is divided into sections based on IOL 'optimal power' for the ICE to supply and the maximum motor power. Using this strategy, the ICE is kept at an ideal operating point whenever possible, and the electric motor will provide the extra power required, or recharge the battery as a generator when the power requirement is below 'optimal.'

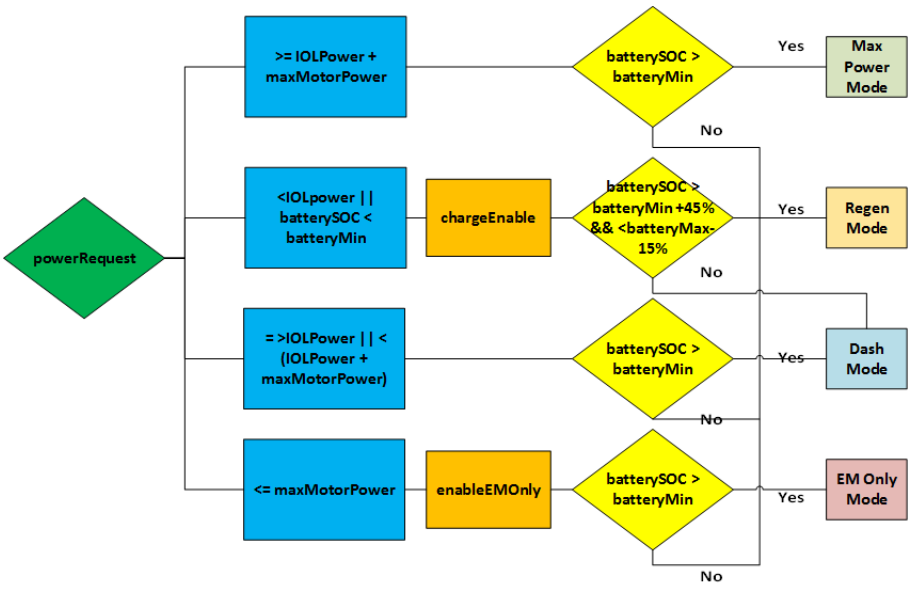

Figure 3.11: Parallel hybrid state controller in aircraft simulation framework.

3.3 Mission Profile Development

The electric, gasoline and series and parallel hybrid architectures were evaluated for several mission profiles to better analyze their performance. Rather than steady-state comparison between propulsion systems, these mission profiles provide a wide range of operating points, and simulate typical use cases for UAVs.

Interceptor

The first mission is a high-speed Interceptor Mission which could simulate a Search and Rescue type mission, such as monitoring naval traffic in distress travelling through the North-West passage. The objectives of the mission will be to climb-out at maximum rate-of-climb, and dash at high speeds to the interest area. Next, the aircraft is to loiter over the interest area for as long as possible before dashing back to base. This mission will favor aircraft configurations that can dash at the highest speeds, sustain the longest loiter times, and consume the least amount of fuel.

Communications Relay

The second mission is a maximum endurance Communications Relay where the aircraft can relay a signal to a distant receiver from high altitudes. Communication relays are a very practical and common application for small UAVs and drones, which is why this mission was selected for comparison. In this mission, the main parameter requirement is an initial steep climb-out gradient. The aircraft is to sustain this gradient until the set altitude is reached, and then maximize the amount of time loitering 'on station.' Once the loitering stage is completed, the aircraft will descend back to base. The main goal of this mission is to maximize loitering time.

Pipeline Inspection

The next mission is a terrain following mission where the aircraft does a Pipeline Inspection flying a prescribed distance above the ground. Terrain following missions are common among small aircraft and UAVs, and this mission type is for a pipeline inspection in Northern British Columbia. The mission profile has each different aircraft configuration travelling between Hope and Darfield, with a varying altitude to match the terrain. Since there are steep climb gradients, the aircraft must be sized with a large enough propulsion system to achieve these climb rates to avoid collision with obstacles. The main objective of this mission is to traverse the most distance with the set amount of take-off fuel, and must travel as efficiently as possible.

LIDAR Mission

Finally, a path-optimization mission was developed for a LIDAR Data Collection mission type. In the LIDAR data collection mission, the aircraft must carry an $8kg$ payload which represents sensitive instrumentation including a LIDAR system. The main objective of this mission is to collect data over a large area using sensitive imaging equipment. To ensure high-quality data collection, it is imperative that the data be collected with minimal on board vibrations, so a hybrid aircraft must be able to enter 'EM Only mode' where the internal combustion engine is idle or disabled. For this reason, the ICE configuration is omitted. This mission requires the aircraft to takeoff and cruise to the interest area, collect as much data over the largest space possible, and then return cruise to base. There are no high-speed dash or large climb-out requirements in this mission, with the main goal of reducing fuel consumed.

Figure 3.12 illustrates simplified diagrams of each of the missions developed for the framework.

(a) Interceptor Mission

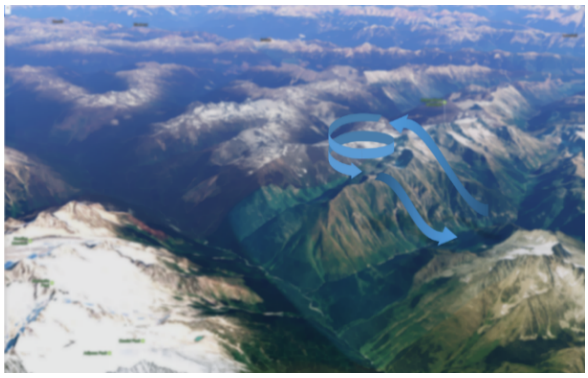

(b) Communications Relay Mission

(c) Pipeline Inspection

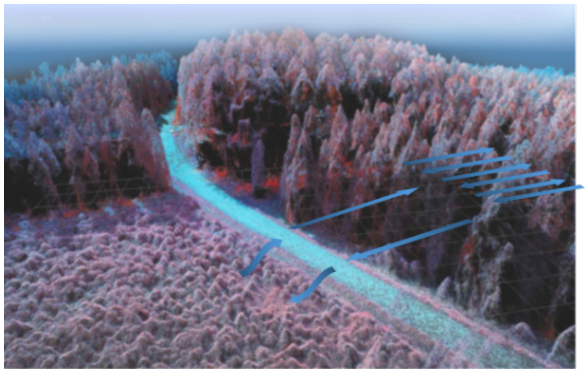

(d) LIDAR Data Collection

Figure 3.12: Depictions of various mission profiles for UAV evaluation in MATLAB framework.

Chapter 4

Experiments - Test Bench

This chapter outlines the design and development of the parallel HEPS test bench, and the proof of concept testing and issues discovered throughout the process. Discoveries made through the design process influenced the final design of the system, and improvements were made by the author that ultimately increased the performance of the HEPS. Due to timeline and budget restrictions, not all of the findings made by the author were able to be implemented, but are outlined in the future work and recommendations section of this report.

4.1 Experimental Procedure

Various procedures were followed to ensure safe and consistent testing of the parallel HEPS test bench and associated experiments. Before beginning each experiment, a test procedure was created to ensure the test operators followed safety protocols. In addition to safe testing, these protocols helped assist in maintaining accuracy between tests. At the beginning of each experiment, sensors were calibrated and zeroed as necessary, and battery systems fully charged. After each test, the mechanical components and all rotating components were checked for damage and all fittings inspected for correct tightness and that fastener thread-lock had not come loose. Variables for data analysis included rotation speed (RPM), battery $Current[A]$, $Voltage[V]$, as well as fuel mass $m_{fuel}[g]$. In post processing, motor torque $\tau_{EM}[N \cdot m]$, propeller torque $\tau_{prop}[N \cdot m]$, propeller power $Power_{prop}[W]$, battery power $Power_{bat}[W]$, fuel flow rate $\dot{m}_{fuel}[g/min]$ as well as brake-specific fuel consumption $BSFC[g/(kW \cdot hr)]$ were able to be calculated.

4.2 Proof Of Concept Testing

Before designing the full scale test bench, a proof-of-concept (POC) test bench was created to monitor the operation of an electric motor with the Enertion RC VESC electronic speed controller. To mitigate risk, and simplify the POC test bench, small 2206 brushless DC electric motors were used. Two motors were coupled with a timing belt to explore the regenerative braking mode. In this experiment, one EM is

driven by a standard ESC, and then the second EM is connected to the Enertion RC VESC ESC which is capable of regenerative braking.

Although the POC test bench was successfully able to generate current with the small motor acting as a regenerative brake, the motors were quickly damaged. The author believe that the damage was caused because the motors are much smaller than the size motors the Enertion VESC ESC is typically used with, and a larger POC experiment was pursued. This larger experiment used a cordless drill mounted directly to the AXI motor shaft to drive the motor. The drill is powered on, then the ESC is activated for increasing levels of regenerative brake.The current drawn from the EM was first tested with a programmable electric load to ensure safe operation as large current spikes could damage battery packs. Later, the experiment directly connected the ESC to batteries and validated the design.

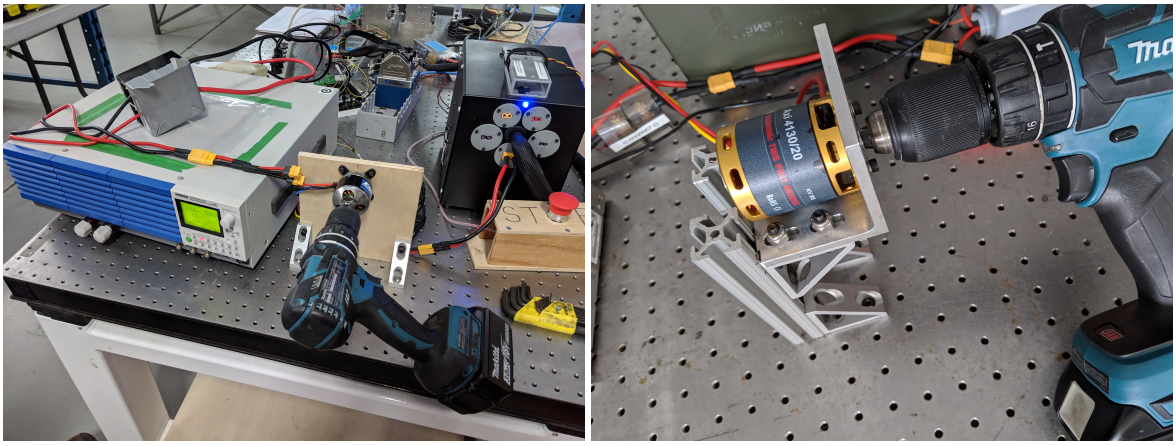

Figure 4.1: Proof of concept testing of the regenerative braking mode of the EM using an electric drill as mechanical power source, and a programmable load to safely measure current and dissipate generated power.

4.3 Bench Testing and Model Updating

The parallel hybrid-electric test bench was designed to be modular to allow for the experimentation of multiple different components of various sizes, and was adaptable for future improvements or optimization. Many of the structural components selected would not be present in the final design of the system to be implemented on a small UAV, but were used in the modular test bench to ensure system rigidity, ease of assembly or maintenance. Further, the ability of the test bench to quickly swap out components for several iterations would not be present in a fully optimized and integrated system. The ability to conduct sensitivity analyses with the test bench was a requirement set by UVIC CfAR, but this requirement would not be necessary for implementation into an aircraft.

The experiments conducted for this research were always static flow tests where the test bench did not have any incoming flow over the propulsion system. For these experiments, this did not cause any problems, but could be a factor to consider in future testing within a wind-tunnel or similarly controlled enclosure/ environment where ambient air flow, temperature and pressure conditions are repeatable.

To mitigate the limitations of the test bench in an open environment, experiments were conducted

many times to eliminate bias and outlier cases in the data. In this way, the results captured and conclusions drawn could be made with higher confidence as the standard deviation of test points between experiments was reduced. Repeatablity of the test bench performance was crucial in order to draw useful conclusions from the results recorded on the hybrid test bench.

Throughout the design, construction, and testing with the parallel hybrid test bench, there were various complications or difficulties to overcome which will be discussed in detail in this section. Some of the constraints of this test bench with manufacturing time, component costs and available machinery placed limitations on the design strategies implemented. With an extension to this project, further experimentation would be possible in addition to test bench improvements to increase usability, increase accuracy of measurements, increase the working life of components and also increase performance of the system.

4.3.1 Safe Operation of Apparatus

The most critical requirement in the experimental testing of the UAV HEPS system was to conduct tests in a safe environment that posed no threats to the personnel conducting the tests. Although safety is paramount on all projects conducted at UVIC CfAR, the experimental nature of this project meant that many prototype components were being tested in unique configurations. Additional measures were put in place to ensure the safe operation of the tests. Plexiglass shields were placed between the test bench and members conducting the tests so that the performance of the test bench would not be impacted by restricting flow, but provided protection in the case of a component failure. In this way, zones around the test bench were controlled using high-visibility tapes and blocked markers to ensure a safe area radially around the test bench rotating components, especially around the large propeller. At high rotation speeds the tips of the rotating propeller are incredibly difficult to see, so the entire experimentation area was sectioned off from viewers or employees not directly working on the project. Furthermore, the area in front of the propeller was marked off so that no objects could be ingested by the propeller and cause damage to the system or test participants. During the startup procedure, the starter mechanism requires direct contact with the flywheel where the operator holds the starter in position. During startup, the operator has to carefully remove the starter away from the system once the ICE starts, and so a mounting plate was installed to brace against.

Due to the high vibration noise in the test bench system, several different strategies were applied to reduce the overall effects. Firstly, the ICE was supported in multiple locations: behind the carburetor with long standoffs, as well as perpendicular mounting tabs that connect close to the piston actuation. In early revisions of the test bench, it was found that the forces of the piston actuation would cause large vibrations in the system and damage the support behind the carburetor, so additional mounts were added to the system.

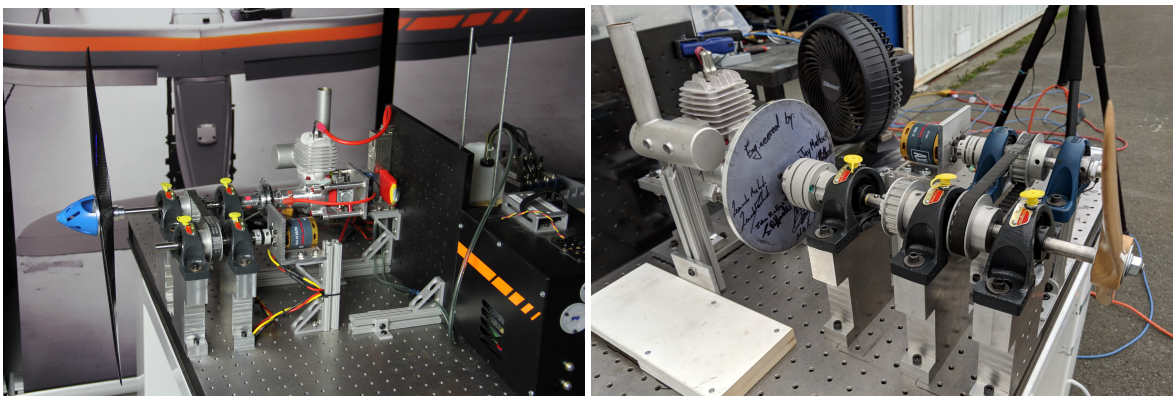

Figure 4.2: Parallel hybrid-electric propulsion system test bench for UAV.

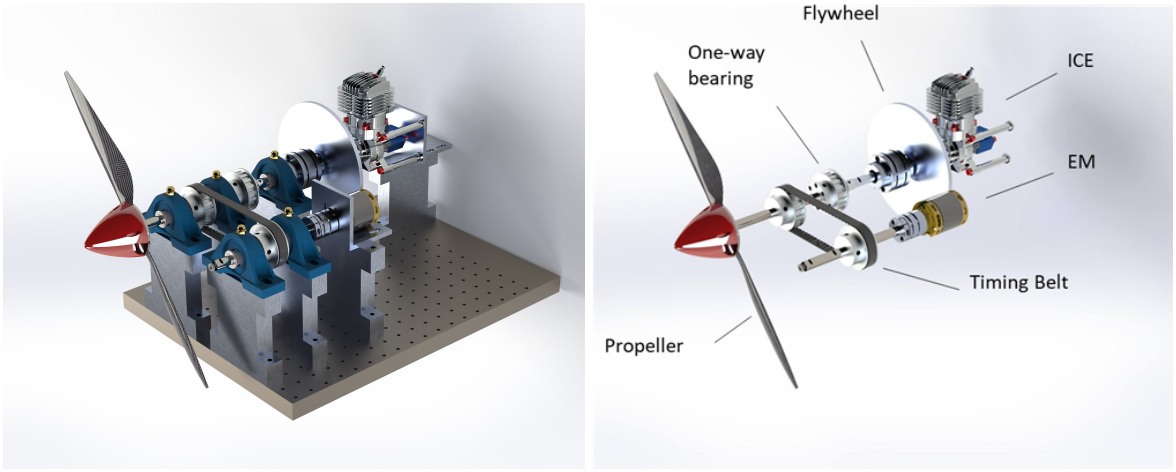

Figure 4.3: Parallel hybrid-electric propulsion system CAD model.

4.3.2 Assembly

Electric Motor

As shown in Figure 4.3 the parallel test bench is comprised of two major components, the electric motor (EM) and internal combustion engine (ICE) joined together with a mechanical coupling to the output shaft and propeller. The 4130-20 V2 from AXI Motors was the EM selected for this project. This EM has a substantial amount of power at $1.65kW$ and is the most powerful motor of this stator-size class available from AXI motors which have been proven reliable for CfAR in the past. This motor is capable of supplying sufficient power for electric-only mode, and maintains high efficiency across a large torque band.

Electronic Speed Controller

The electronic speed controller used in this project is based off a design by Vedder, called the VESC - FOCBOX by Enertion RC. [73] This electronic speed controller is typically used in hobby electric-skateboards and was selected for its high-current capacity as well as regenerative braking performance. The FOCBOX includes features like over-voltage and over-current protection, RPM limits as well as field-oriented control. The manufacturer recommends that the regenerative brake current be limited to $-15A$

Figure 4.4: AXI 4130/20 V2 BLDC

Motor	AXI 4130/20 V2
Max power	$1.650kW(2.2hp)$
Poles	14
Weight	$0.410kg$
kV	$305RPM/V$
Max efficiency	90%
Max motor current	$56A, 60s$
Max generator current	$40A$
Internal resistance, R_m	0.99Ω
No load current	$1.1A$
Number of cells	6-8 Li-Po

Table 4.1: AXI 4130/20 V2 Specifications.

Figure 4.5: Enertion RC FOCBOX electronic speed controller capable of regenerative brake mode. [73]

Electronic Speed Controller	Enertion FOCBOX
Max Power [W]	3000
Voltage Range [V]	8-50
Peak Current [A]	120
Continuous Current [A]	60
Recommended Regen Current [A]	30

Table 4.2: Specifications for Enertion FOCBOX ESC.

for testing (below the rated $-30A$), whereas it can drive motors at $60A$ continuously, $120A$ peak at $50V$].

Internal Combustion Engine

The internal combustion engine in this test bench is the Desert Aircraft DA-35. Desert Aircraft has a history of reliable engines that are used in many UAV applications. This single cylinder two-stroke engine has a displacement of $35cc$ and is capable of $2.34kW$ of power output with a 19x10" propeller. This engine is intentionally sized to provide sufficient power for cruise requirements, and extended loiter in the case of an EM failure, but is not powerful enough to sustain the climb-out requirements.

Figure 4.6: Desert Aircraft DA-35 two-stroke combustion engine.

Engine	Desert Aircraft DA-35
Type	Single Cylinder, two-stroke
Displacement	$35cc$
Weight	$0.935kg$
Max Power	$2.344kW(3.14hp)$
Max Torque	$2.99Nm$ at $5500RPM$
RPM Range	$1500 - 8200RPM$

Table 4.3: DA-35 Specifications.

Mounting of the ICE

Special attention was given to on the mounting methods of the ICE in the parallel HEPS as the amount of vibration created by the small two-stroke engine was substantial. Initially, the engine was mounted on $1/4$" aluminum angle bracket bolted to a large aluminum base. However, through the stages of testing the angle bracket mount was damaged when a shaft coupler failed, and needed to be replaced. At this time, the ICE mount was also reinforced with additional stiffening members to help support the ICE, and the test operators noted a reduction in system vibration. Preventative measures were taken in the operation of the ICE to ensure smooth operation which included regular inspection, temperature readings of the cylinder head, and careful concentricity measurements to prevent excessive vibration in the system. In addition, the ICE was mounted with robust supports that were assembled with thread-locked fasteners to prevent any supports coming loose in the high-vibration environment.

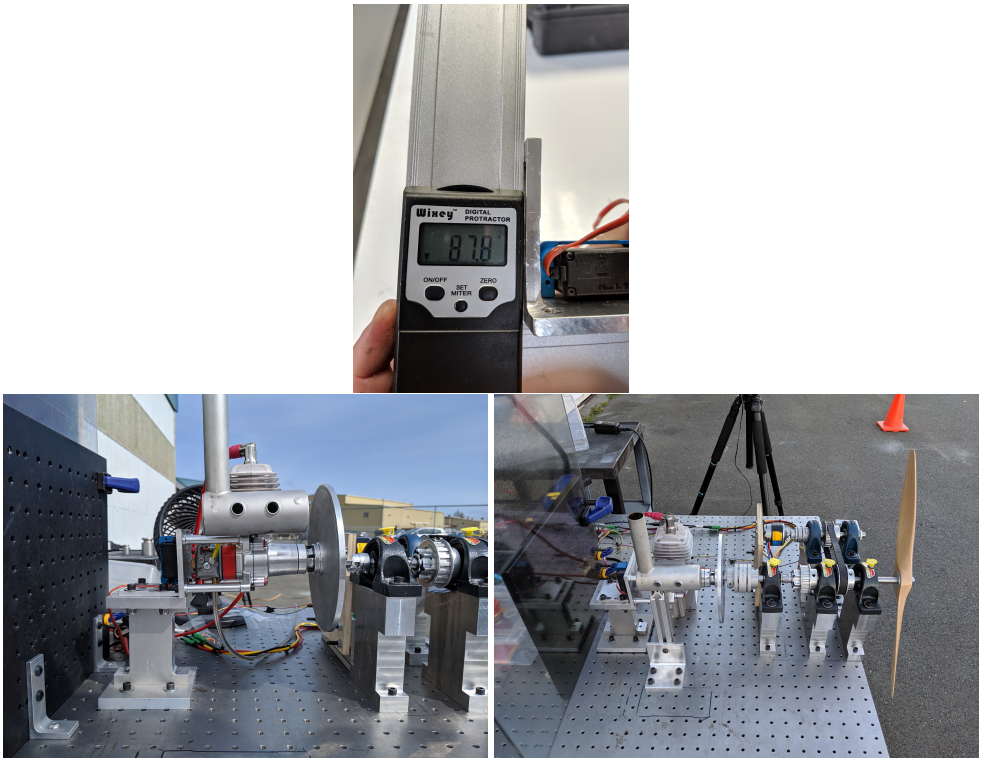

Figure 4.7: Damage of ICE aluminum bracket during mechanical coupler failure, and reinforcement to decrease system vibrations.

FlyWheel

Typically when a small two-stroke engine like the DA-35 is operated, a propeller is attached directly to the crankshaft. The propeller dissipates the energy produced by the engine to produce thrust as it rotates, and also acts as a mechanical capacitor to effectively dampen out torque inconsistencies or spikes delivered by the engine. These spikes are called rotatum, or the derivative of torque with respect to time.

$$Rotatum = \vec{P} = \frac{d\vec{\tau}}{dt} \tag{4.1}$$

In the hybrid electric test bench, since the ICE is not directly coupled with the propeller, the one-way bearing cannot effectively transfer rotatum since the spraug bearing will slip when the output shaft has a higher torque than the engine crankshaft. To circumvent this behaviour, a flywheel was mounted directly to the crankshaft of the engine. Due to space limitations on the test bench, the flywheel was designed as a thin 1/4 inch aluminum disk and approximated in *Solidworks* for the same inertia as the 19x10" propeller. To minimize the amount of vibrations added to the system, the flywheel disk had to be machined to very precise concentricity tolerances of $0.001"$ to the crankshaft. Further, the interfaces between the flywheel and the crankshaft casing had to be machined to extremely high perpendicularity to ensure no axial vibrations were induced with the addition of the large flywheel. Without the flywheel in the test bench, the ICE had difficulty starting. With the system starter running, the ICE could be driven through the compression cycle and properly fire. Once the starter was removed, the ICE could get through the expansion stroke, but did not have sufficient inertia to successfully get through the compression stroke. As a result, the engine would misfire with combustion away from Top Dead Center, possibly leading to engine damage. Once this issue was identified, and with the flywheel addition to the system, the ICE was able to successfully start and maintain a strong idle.

Figure 4.8: HEPS starting method of pressing hobby ICE starter against system flywheel.

Coupler

To connect multiple shafts together inline, several different couplers are used. These couplers typically connect two shafts of differing sizes between various components. These couplers use a friction fit to attach to each end of the shaft, and can be easily accessed for quick removal. If there are small amounts of axial or in-plane misalignment, these couplers are also helpful in dampening the effects out, at the expense of a slight energy loss due to friction. As shown in Figure 4.9 below, the coupler contains a small rubber 'spider' which is compressed slightly when the coupler experiences rotatum, or 'torque spikes.' However, after approximately 20 working hours of testing on the test bench, these couplers deformed and failed, causing damage to several system mounts. As shown in Figure 4.9, the spiders compressed and allowed the end coupler joints to move freely and misaligned the system. A new type

of coupler was used that uses metal-leaf springs to allow for misalignment, and absorb axial loads and torque spikes. However, this coupler also failed after several hours of testing. The prevailing solution was to use a higher torque rated metal-leaf coupler, as detailed in Appendix A of this report. In addition, the ICE mount stiffness was increased to reduce system vibration.

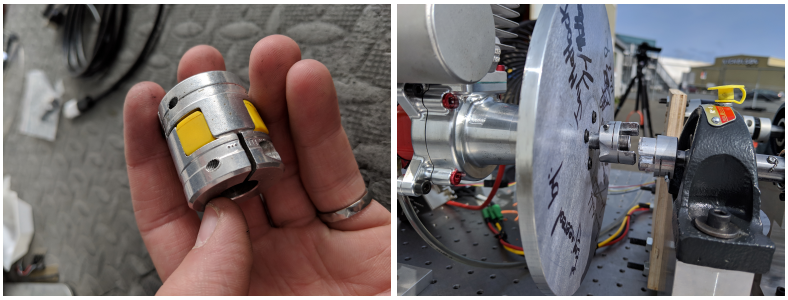

Figure 4.9: Mechanical coupler used in the HEPS that clamps between shafts using rubber 'spider.'

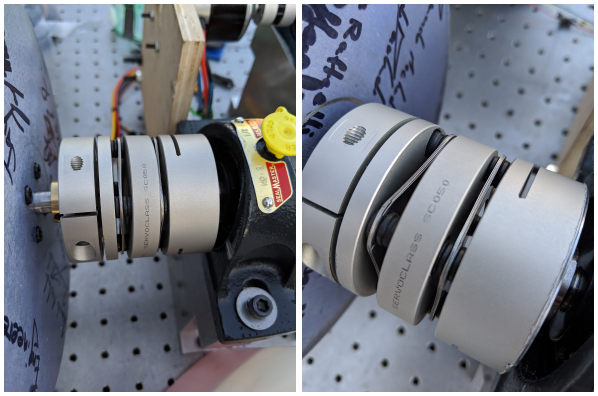

Figure 4.10: Flexible mechanical couplers used in the HEPS that clamp between shafts with metal-leaf springs.

Shafts and Alignment

Each of the steel shafts, mounts and components used in the HEPS test bench were carefully machined to ensure concentricity and alignment. However, as is typical in many prototype projects, there were still small amounts of misalignment that needed to be accounted for. Each of the shafts in the system were supported on large bearing blocks. These blocks can accommodate discrepancies in shaft alignment relative to the mounting base, but provide substantial rigidity with the integrated mounting features. These mounts allowed for the test bench to be assembled easily. However, these bearing blocks are still rated to support the axial thrust produced by the propeller at full speed.

One-Way Bearing

The ICE has a one-way bearing connected to the crankshaft which is a Spraug Bearing from Align RC. As explained in the Theoretical Overview chapter, this bearing type allows for rotation in one direction, but the uniquely shaped cams internally restrict rotation in the opposite direction. Taking advantage of this bearing's operation allows for the ICE to provide main power to the propeller in ICE Only mode, Dash

Mode, and Regenerative Braking Mode, but is 'disconnected' when the EM RPM exceeds that of the ICE in EM Only mode. This allows the ICE to idle while the EM provides all the power to the propeller.

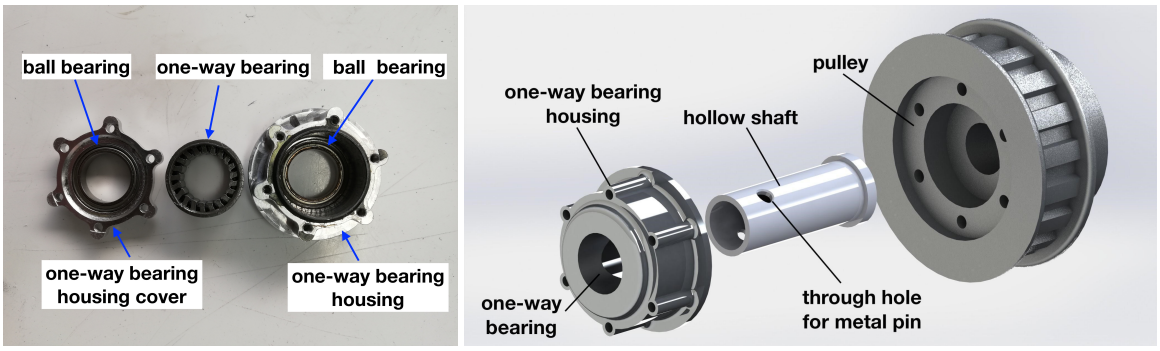

Figure 4.11: Align RC one-way bearing assembly with exposed spraug bearing and ball bearing supports encased in modified aluminum enclosure. (left) One-Way Bearing Assembly CAD from HEPS. (right)

The spraug bearing is mounted within a bearing housing as shown in Figure 4.11. The one-way bearing housing covers the internals which consists of two thin ball bearings on either end of the spraug bearing. Since spraug bearings are not designed to encounter large axial or radial loads, these ball bearings work to protect it. However, with the limited space inside the Align RC one-way bearing housing, these small ball bearings are not designed to operate under sustained large axial loads. The hollow shaft that interfaces with the spraug bearing must be machined to incredible precision since even the slightest undersized shaft would cause slippage between the shaft and the spraug bearings, rendering the one-way bearing useless. For this reason, the precision shaft that was included from Align RC was incorporated into the hybrid test bench.

In the initial design of the test bench, the one-way bearing assembly was housed inside an aluminum pulley that was used with a timing belt to transfer the torque from the EM. However, in preliminary testing, it was found that the radial loading on the one-way bearing assembly was too high for the ball bearings inside the Align RC one-way bearing assembly, which led to failure. The small ball bearings had broken the interface between the bearings and the inner race, causing binding. This binding of the one-way bearing shaft caused continuous engagement, and led to improper operation of the spraug bearing. (The EM was not able to exceed the RPM of the ICE in EM only mode because the failed one-way bearing was acting as a solid coupler).

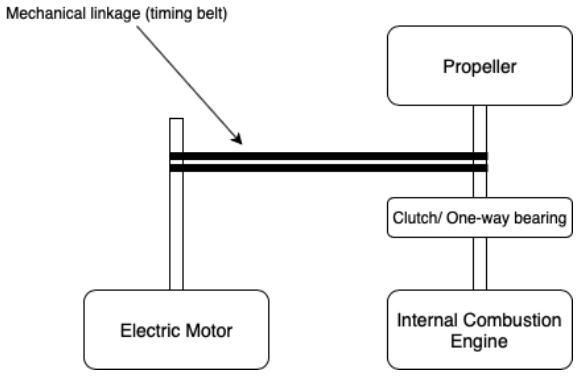

Figure 4.12: Installation of the one-way bearing acting as a clutch in the HEPS test bench.

To eliminate this effect, an additional section was added to the test bench with a separate timing belt pulley. The other side of the one-way bearing is mounted to the output shaft through a set screw which interfaces with a flat on the output steel shaft. Each of the pulley blocks and timing belt pulleys have a set screw which interfaces with a slotted flat on the corresponding shaft. To transfer the torque from the electric motor to the output shaft, a $0.5inch$ timing belt is used with timing pulleys (toothed gears.) This pulley allows for the torque to transfer with no slippage, and minimal frictional losses. As opposed to v-belt pulleys, this timing belt does not need to be pre-loaded or tensioned down with an additional pulley.

Propeller

Before testing, each of the propellers to be evaluated had to be balanced using a propeller-balance jig. This jig balances a pin through the center of the propeller on an extremely-low friction magnetic bushing. From here, the furthest edges of each propeller blade are lightly sanded by hand until the propeller is able to balance along its center axis. A propeller that is correctly balanced will perform most efficiently, and minimize induced vibrations in the system. Bushings were machined for each test propeller so that they could all mount to a standard output shaft quickly.

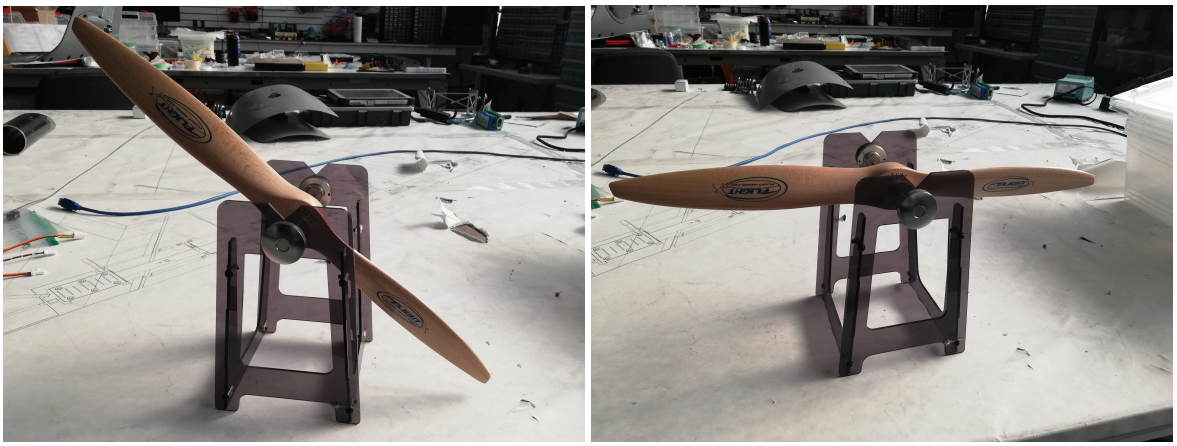

Figure 4.13: Balancing of propellers to ensure stability and performance.

Starter

In order to start a small ICE engine on traditional hobby aircraft, a small electric hand-starter is used. This starter has internal gearing for maximum torque, and a rubber cup which friction fits to the spinner on the propeller, and initiates rotation of the combustion engine crank shaft. At the correct rotation rate, the spark plug receives properly timed signals from the capacitive discharge ignition (CDI) to ignite the fuel and air mixture in the cylinder head, starting the engine. The starter can then be manually removed and put aside during operation.

However, due to the unique design of this hybrid propulsion system, the one-way bearing will not allow for conventional starting methods. If the RPM of the propeller exceeds that of the ICE, the one-way bearing disengages from the ICE shaft and freely spins, transmitting none of the power to the ICE.

To circumvent this behaviour, a separate starting mechanism was explored. In preliminary design, a 3D-printed gear assembly was connected to the ICE shaft to allow the hand-starter to directly connect to the ICE shaft.

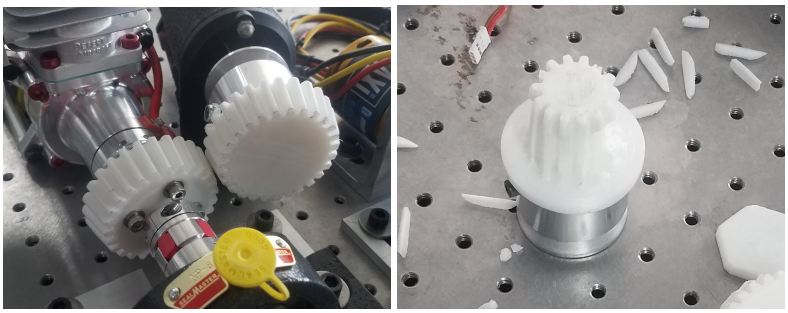

Figure 4.14: ICE starting method with direct drive 3D printed gears, shear failure from the high starting torque requirement.

However, due to the large torque requirement of these gears, the strength of the 3D printed gears was insufficient and were damaged in testing. Further revisions of the 3D printed gears yielded results similar to the result shown in Appendix A, including 5 different sizes and gear ratios. A pull cord concept was explored but abandoned due to the pull strength required and entanglement risk of the cord. The next mechanism for starting explored was a bicycle sprocket and chain directly coupled with the starter, as shown in Figure 4.15. After several tests, the timing belt inside the starter failed and required replacement since the torque required to start the ICE was too high for a direct coupling system.

The prevailing design for successfully and consistently starting the ICE was to use the flywheel with a custom friction disk mounted on the starter. As shown in Figure 4.16 the starter is pushed against the outer surface of the flywheel and held in place as the starter activates. Once the ICE starts, the friction disk can slide freely against the flywheel, and is set aside during testing.

Ideally, this test bench would be equipped with a simpler and more compact starting mechanism, such as a small in-line motor which could be incorporated in the final airframe design. The author recommends that the final design of the air-frame incorporates a clutch mechanism of some kind so that the EM can be used for starting of the engine.

Optical Table

The entire parallel-electric hybrid test bench is supported on an optical table. This table is equipped with a imperial 1” spacing $1/4” - 20$ bolt pattern for simple placement of components, an extremely rigid stainless steel surface that minimizes deflection and contains rubber materials of various durometers beneath to dampen vibration in the system. Not only will this table allow for the convenience of adding new components to the system, the vibration dampening effects will increase the accuracy of the instrumentation used by eliminating some background noise. Furthermore, the entire table is equipped with 4” caster wheels to allow the entire test bench to be moved with ease. Since this experiment will be producing noxious exhaust fumes from the combustion engine operation, it is imperative to be testing in environments with high air-flow.

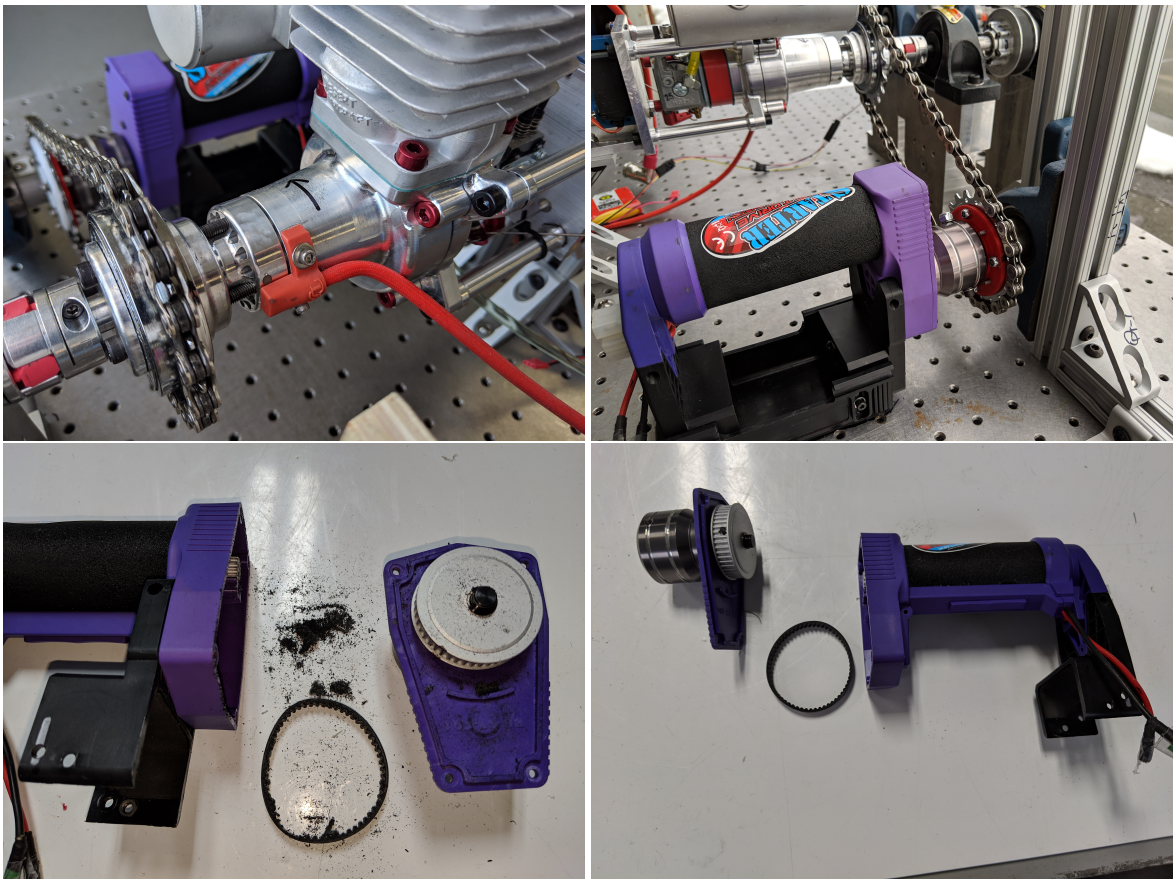

Figure 4.15: ICE starting mechanism using bicycle sprocket and chain. This method yielded failure of internal timing belt in starter and required replacement.

Figure 4.16: Final design for ICE starting mechanism.

Sensors

The main sensors used in this test bench were hall-effect sensors to collect information on the RPM of the various shafts used throughout the hybrid electric propulsion system. The battery was equipped with a shunt resistor to calculate the voltage and current going to the ESC. Further, there was a strain gauge-load cell used to collect information on the fuel consumed weight of the engine in operation. Figure 4.17

shows an output torque sensor for the propeller that was not implemented in this research as the sensor on-hand was an in-line sensor from FUTEK that was oversized and did not have the required resolution.

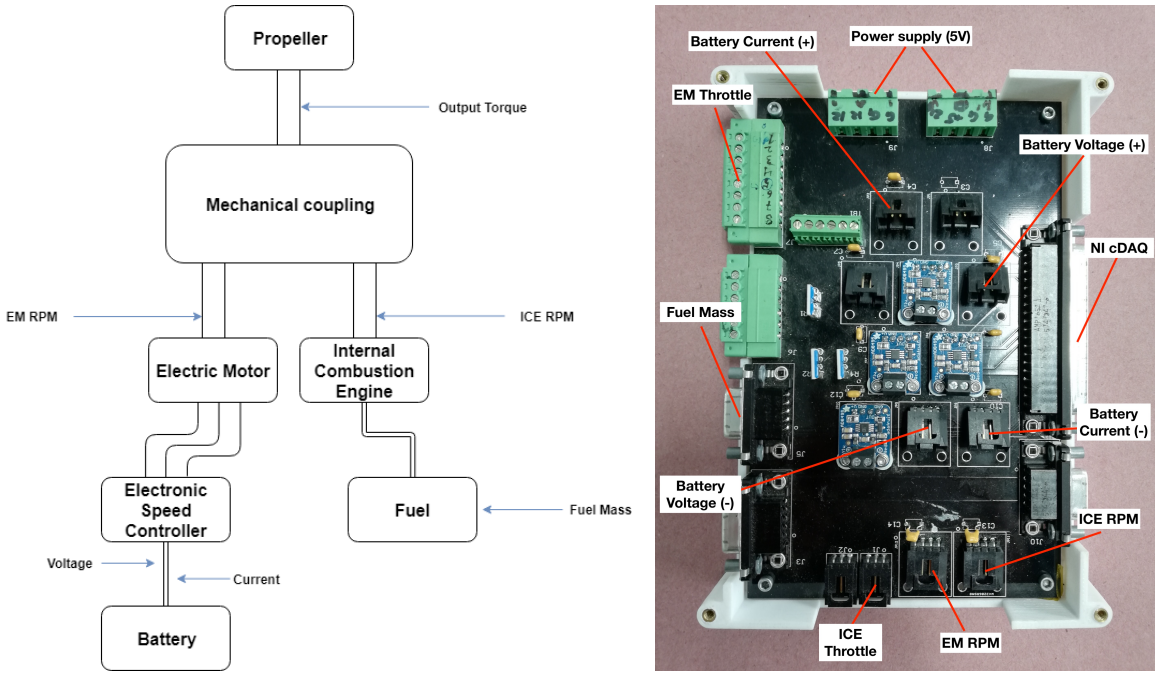

Figure 4.17: Sensor setup diagram for parallel HEPS test bench.

4.4 Airframe Development

The results of the experimentation in this research will be analyzed for practical use and application of integration into small unmanned aerial vehicles. Although the hybrid test bench was not designed for direct integration into an aircraft, many of the components and design techniques will be identical. A first attempt was made by the author to outfit the QT1 aircraft at UVIC CfAR with a parallel HEPS similar to the system developed for the test bench. In this exercise, the same scale components were assembled into the aircraft for feasibility with conservative estimates for unknown masses of components. As can be seen in Figure 4.18, the components for a parallel HEPS can comfortably fit inside the fuselage of the QT1 aircraft, with sufficient space for several large battery packs, a fuel tank and remaining area for avionics systems. An exercise was conducted to explore the possibility of implementing a HEPS on a UAV, the QT1 aircraft at CfAR. It was estimated that a parallel HEPS could be configured on this scale of aircraft with a mass penalty of 24.5% compared to the electric configuration. Further, since the series configuration must contain an EM as well as a generator, the mass penalty is 37% compared to the electric configuration. (This corresponds to a 10% mass penalty for the series HEPS relative to the parallel HEPS, which aligns closely with the theory from [12].) The summary of this exercise with propulsion systems and corresponding fuel and battery masses are shown in Table 4.4.

Parameter	Electric	Gasoline	Parallel	Series
Empty Mass $[kg]$	10.2	12.7	12.7	14
Payload $[kg]$	5	5	5	5
Fuel Mass $[kg]$	0	7.3	3.4	2.4
Battery Mass $[kg]$	9.8	0	3.9	3.6
TOW $[kg]$	25	25	25	25

Table 4.4: QT1 Aircraft Example Propulsion System Comparison.

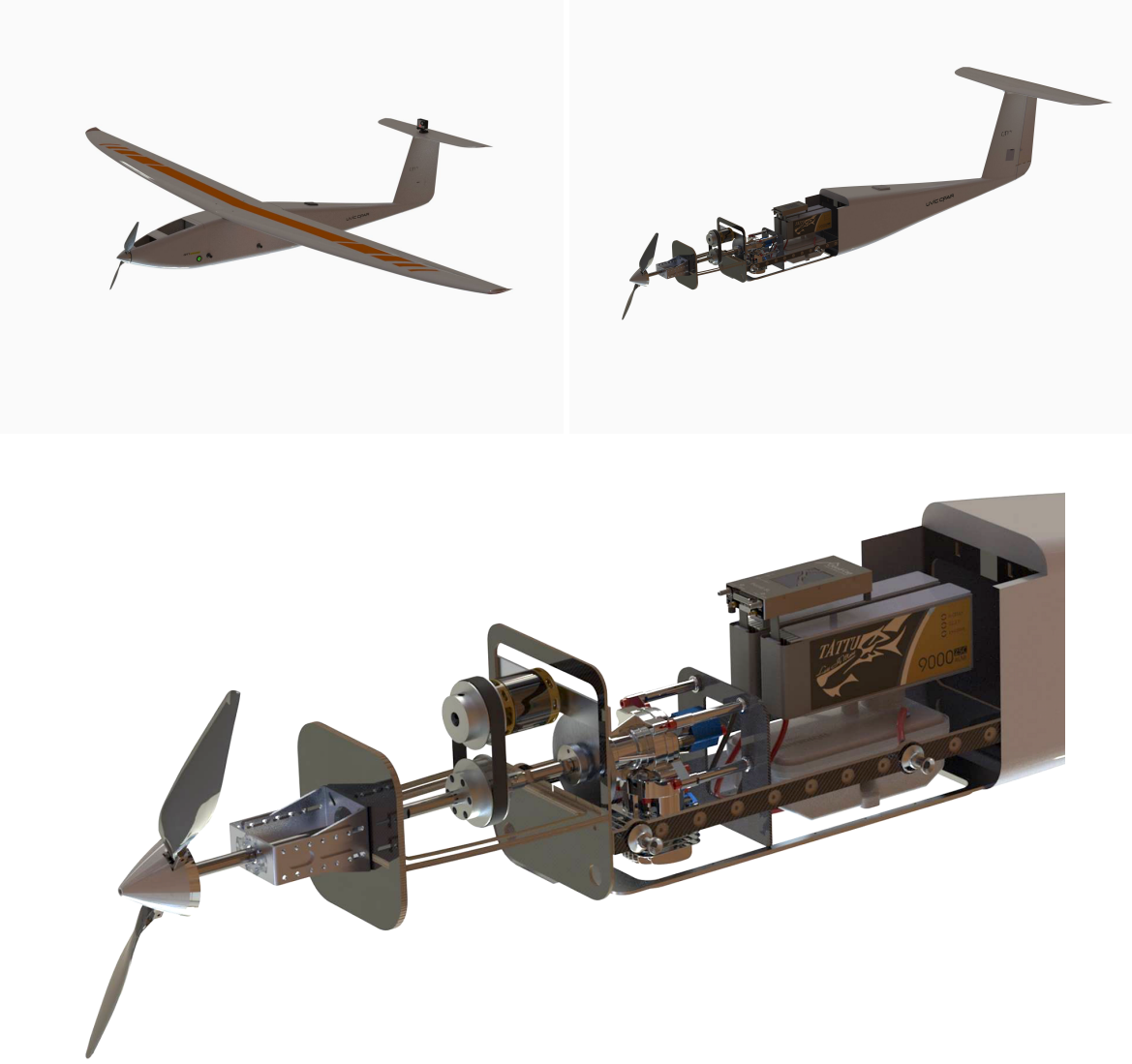

Figure 4.18: Parallel hybrid-electric propulsion system conceptual design into UVIC CfAR's QT1 UAV fuselage.

4.5 Controller Design

The controller used in the test bench is intended to operate each of the components in their most efficient region to maximize the efficiency of the HEPS. As described in the Theoretical Overview chapter of this report, the rule-based controller was selected as the simplicity and functionality was well suited for this project. For the control of the test bench, the controller controls the throttle servo of the ICE, the throttle of the EM, as well as the 'throttle' for regenerative braking when the EM acts as a generator. The

'throttle' position is best described by Greiser as the linear relation of the requested torque divided by total available torque. [74] The basic concept behind the hybrid state controller implemented on the parallel HEPS is the torque request is supplied by the ICE up until the IOL torque. Above the IOL, the EM and ICE work together until the EM outputs maximum torque, and then the ICE supplies additional torque. This concept is illustrated in Figure 4.19.

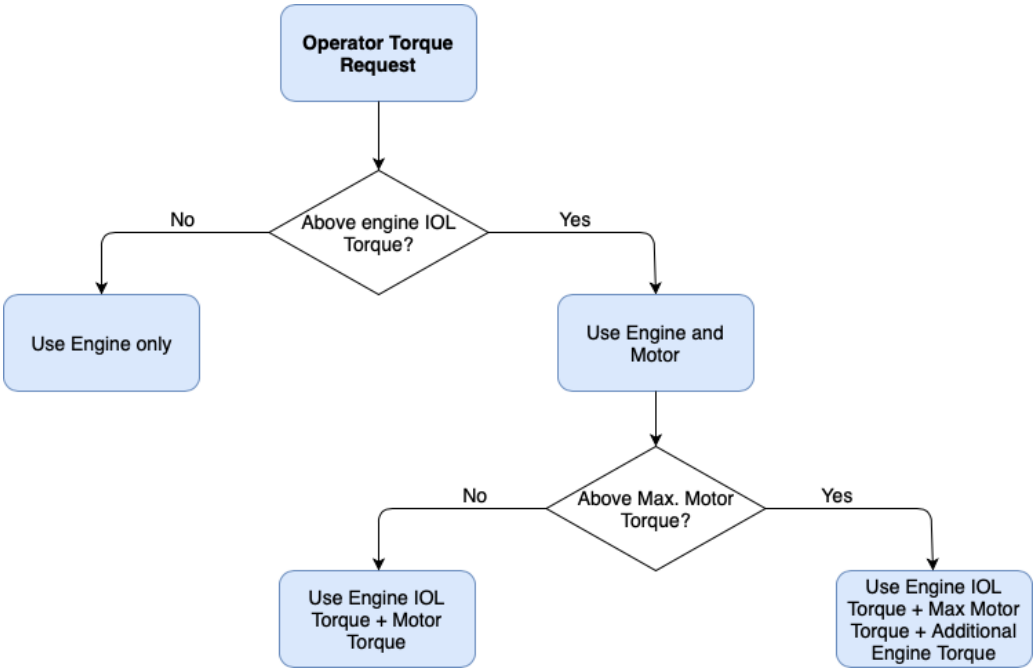

Figure 4.19: State controller decision tree implemented on the parallel HEPS test bench.

All of the components of the controller can be controlled and monitored in a graphical user interface (GUI) developed in LabView. This GUI, shown in Figure 4.20 allows for the selection of each different operating mode: EM Only, ICE Only, Dash Mode or Regen Mode. In addition, the GUI is where the supervisory controller is activated for the EM Controller, ICE Controller and the Hybrid Controller. Here, the test operator can send torque requests, or run mission profiles. All the required controls are implemented in the GUI for data acquisition, sensor readouts and associated calibration, as well as warning and error codes if issues arise in the test bench. A full description of the LabView GUI, and operational instructions and review of built in features and associated error codes was completed by Machado. [63]

Figure 4.20: GUI developed in LabView to control and monitor performance of the parallel HEPS test bench. [63]

Chapter 5

Results

The results section of this report first explores the performance of a UAV simulated in the Aircraft Simulation Tool. These results model the aircraft with various propulsion systems to analyze trends that can be used to drive engineering design decisions of future hybrid-electric UAVs. Next, the results are presented for the performance of a HEPS at the component level and system level with the developed parallel test bench. Each of the four different operating modes were evaluated, as well as the performance of the developed supervisory controller. With the data collected from experiments on the HEPS test bench, it is possible to compare the theoretical performance with the experimental performance of a parallel-hybrid.

5.1 Evaluation and Trade Studies - MATLAB Framework Results

This section explores the theoretical results collected for UAVs with various propulsion systems using the MATLAB framework for each of the four mission types. Although many trade studies were conducted by the author to evaluate the HEPS performance against conventional propulsion systems, the results shown in this report were selected because they portray interesting findings.

5.1.1 Mission Profile - Pipeline Inspection

The Pipeline Inspection mission offers a wide range of operating conditions for the UAV with steep climbs, slow descents, and long cruise segments, and was used extensively in the tuning and evaluation of the hybrid state controller. The objective of this mission was to follow a path along mountainous terrain, maintaining a prescribed altitude above the ground. This means that the vehicle must make constant adjustments to maintain altitude when following the terrain.

To explore the performance of the various aircraft configurations in this experiment, the coefficient of lift during cruise was swept defined by Equation 5.1.

$$C_L = \frac{L}{\frac{1}{2}\rho_\infty V_\infty^2 S_{ref}} \tag{5.1}$$

Parameter	Electric	Gasoline	Parallel	Series
Empty Mass $[kg]$	10.2	12.7	12.7	14
Payload $[kg]$	0	19.3	15.69	13.93
Fuel Mass $[kg]$	0	3	2.64	3.1
Battery Mass $[kg]$	24.8	0	3.97	3.97
TOW $[kg]$	35	35	35	35
Climb Gradient $[^\circ]$	10	10	10	10
Cruise C_L	0.55	0.55	0.55	0.55
Distance $[km]$	195	288	288	288
% Complete	68	100	100	100

Table 5.1: Pipeline Inspection Mission baseline results summary.

Where L is lift $[N]$, ρ_∞ is freestream density$[kg/m^3]$, V_∞ is freestream velocity $[m/s]$, and S_{ref} is the reference area $[m^2]$. Figure 5.1 describes the aircraft performance of the amount of fuel-burn mass when sweeping the $C_{L,cruise}$ from $0.55 - 0.9$. This analysis allows for the exploration of trade-offs between the gasoline configuration and both hybrid-electric configurations comparing the amount of fuel burn through the duration of the mission. As can be seen, the series hybrid configuration will burn less fuel than the gasoline configuration for higher C_L values, and the parallel configuration is the most efficient with the lowest fuel burn for the entire C_L range.

For this type of mission, an electric configuration would be useful if the endurance requirements were reduced below $195km$ as it would perform well in the steep climb gradient portions of the mission. However, the gasoline and hybrid configurations would allow for long range and high payload capacity.

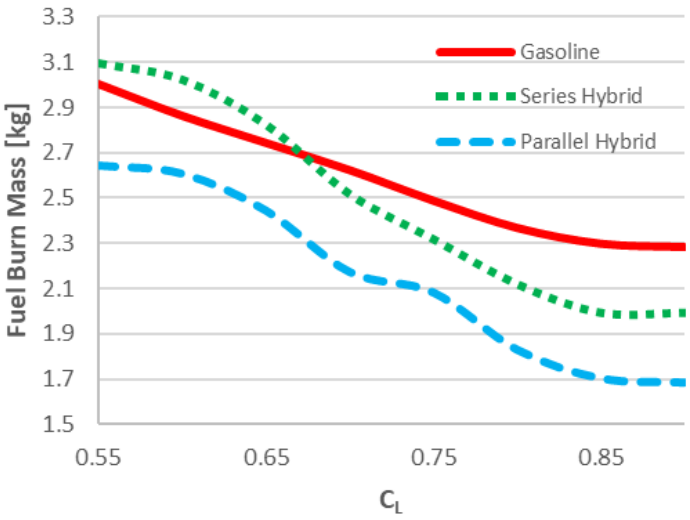

Figure 5.1: Framework design study example: Pipeline Inspection Mission $C_{L,cruise}$ versus fuel burn mass.

At $C_L = 0.55$, the gasoline configuration has the highest payload capacity at $19.3kg$ while the parallel HEPS has $15.69kg$, and the series configuration has a 13.93 payload capacity. At $C_L = 0.90$, the parallel configuration burns 26.1% less fuel at $1.7kg$ whereas the gasoline configuration burns $2.3kg$. Sweeping through the cruise C_L range, the payload capabilities for each configuration can be calculated as shown in Table 5.2. Therefore, the parallel HEPS configuration has an average of $3.52kg$ lower payload capacity for the $35kg$ aircraft (17.6%), but has a fuel consumption reduction of up to 26.1%.

Cruise C_L	Gasoline Payload $[kg]$	Parallel Payload $[kg]$	Series Payload $[kg]$
0.55	19.3	15.69	13.93
0.67	19.6	16.03	14.33
0.9	20.0	16.63	15.08
Average ΔPayload	-	-3.52	-5.19

Table 5.2: Payload capacity for various aircraft configurations in the Pipeline Inspection Mission with varying C_L cruise.

Parameter	Electric	Parallel	Series
Empty Mass $[kg]$	10.2	12.7	14
Payload $[kg]$	8	8	8
Fuel Mass $[kg]$	0	5.4	4.03
Battery Mass $[kg]$	11.8	3.9	3.9
TOW $[kg]$	30	30	30
Climb Gradient $[^\circ]$	10	10	10
Op Altitude $[m]$	1000	1000	1000
Cruise C_L	0.7	0.7	0.7
Range $[km]$	7.5	7.5	7.5
LIDAR Collection Endurance $[hr]$	3.11	22.03	18.81

Table 5.3: LIDAR Data Collection Mission baseline results summary.

The accurate prediction of fuel burn mass for a aircraft through an entire mission is extremely advantageous when designing a UAV. The novelty of having the ability to precisely predict the required amount of fuel means that the additional payload capacity of the UAV can be exactly calculated, and the fuel reserves minimized. This would allow for the maximum amount of payload on board for additional sensor arrays or equipment. Typically, UAVs of this size class must be flight tested several times before an accurate fuel consumption metric can be established.

5.1.2 Mission Profile - LIDAR Data Collection

The main objective of the LIDAR Data Collection mission is for the aircraft to carry an $8kg$ payload containing highly sensitive instrumentation and precise equipment over an area of interest to collect data. The remaining payload capacity is filled with fuel or batteries. In this mission, the intended payload would be a LIDAR system capable of scanning agriculture areas, but the results are applicable for any payload. Due to the high-vibration nature of an internal combustion engine, the ICE Only configuration was excluded from analysis due to the detrimental effect of the vibration would have on the equipment's ability to collect data. In further exploration, it may be an interesting exercise to explore if additional mass could be added to the system to dampen the vibrations of a combustion engine, and explore the impacts on endurance.

In this analysis, the variable of 'collection range' is swept to increase until the LIDAR collection time is decreased to 0. Effectively, this analysis will calculate the maximum range that the UAV can take off and cruise out before reaching the data collection area of interest, and the amount of collection time allowed on station before needing to return to base. This information can then be used by the flight engineering team to make plans with mapping areas and range requirements and to build flight sortie plans.

As shown in the Figure 5.2, the electric configuration is well suited for the LIDAR Data collection

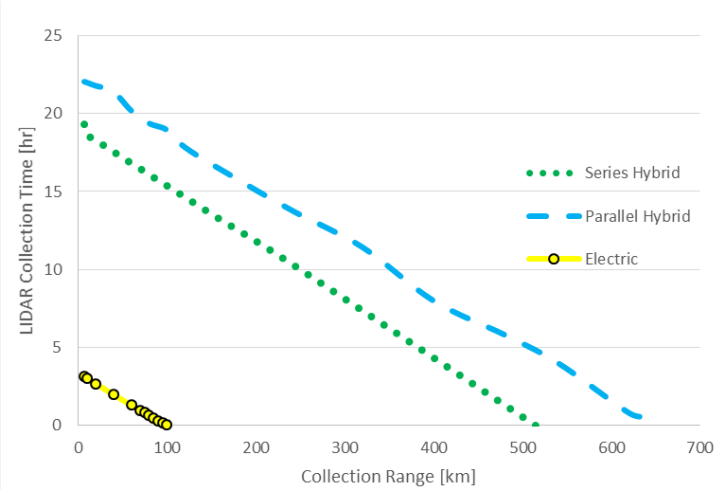

Figure 5.2: Framework design study example: LIDAR Data Collection Mission Time $[hr]$ versus Collection Range $[km]$.

mission, but suffers from a substantially lower endurance than both of the hybrid configurations. A reasonable design point for the electric configuration UAV would only be able to cruise out to a range of $50km$ with a 2 hour LIDAR data collection window before returning. The maximum range of the aircraft with electric configuration is approximately $100km$ but with an extremely limited LIDAR collection time. At this same LIDAR collection range, the series HEPS has an endurance of $16hr$ and the parallel configuration has an endurance of $19hr$. It is clear that HEPS configurations which can make use of burning energy dense hydrocarbons are capable of drastically increasing endurance times compared to electric configurations. In addition, the HEPS configurations are still capable of operating in low vibration noise modes to accommodate the requirements of sensitive instrumentation.

Both the series and parallel hybrid configurations are well suited for this mission type as they are capable of conducting a wide collection range, with very high LIDAR collection endurance. In fact, it can be seen in Figure 5.2 that with a collection endurance of 12 hours for Parallel and 8.0 hours for Series configuration at a collection range of $300km$, this UAV would likely be sufficient for the majority of LIDAR data collection missions. If required, the $8kg$ payload of the LIDAR system could be increased to accommodate additional sensors and the hybrid configurations could still offer large endurance.

5.1.3 Mission Profile - Interceptor

The main objective of the Interceptor mission is to maximize the amount of loiter time the aircraft has once it has reached the target of interest. However, this mission also contains an aggressive climb out segment and high-speed dash segment which will favour propulsion configurations that are capable of high power and high speeds before entering the loiter segment. Once the aircraft has reached the low-speed cruise or 'loiter' segment, the aircraft needs to operate very efficiently to maximize time on station. For this analysis, the take off weight (TOW) of the aircraft is swept from lightest to heaviest possible configuration in the operating envelope, $22 - 35\ kg$, by increasing the amount of fuel sources on board. Intuitively, the aircraft endurance increases in a largely linear trend with additional fuel sources

Parameter	Electric	Gasoline	Parallel	Series
Empty Mass $[kg]$	10.2	12.7	12.7	14
Payload $[kg]$	5	5	5	5
Fuel Mass $[kg]$	0	6.3	2.3	2.4
Battery Mass $[kg]$	8.8	0	4	2.6
TOW $[kg]$	24	24	24	24
Climb Gradient $[^\circ]$	8.4	8.4	8.4	8.4
Op Altitude $[m]$	1000	1000	1000	1000
Cruise C_L	0.8	0.8	0.8	0.8
Endurance $[hr]$	2.4	17.75	11.62	7.24
Endurance/TOW $[hr/kg]$	0.10	0.74	0.48	0.30

Table 5.4: Interceptor Mission baseline results summary.

added, so Figure 5.3 below shows the trend of endurance per mass TOW versus TOW.

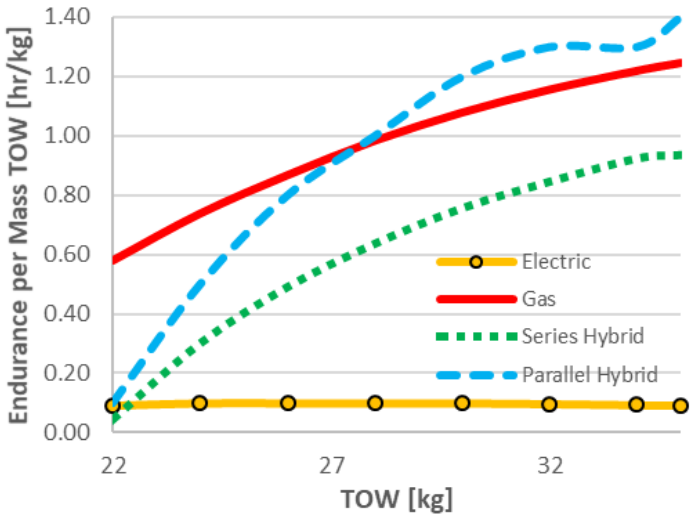

Figure 5.3: Framework design study example: Interceptor Mission Endurance per Mass TOW versus TOW.

For the electric aircraft configuration, the Endurance per Mass TOW is nearly constant for the entire TOW swept range. In addition, the results from the analysis show how the hybrid-electric parallel and series configurations are penalized at lighter TOW because of the additional weight associated with both EM and ICE systems on board, compared to the ICE Only configuration. However, at TOW above the $27kg$ point, the Endurance per Mass TOW of the parallel configuration outperforms the gasoline configuration. At $27kg$ the series hybrid configuration has an endurance/TOW of 0.6 $[hr/kg]$ while both the gasoline and parallel configurations have a endurance/TOW of $0.9[hr/kg]$. This performance can be associated to the smaller-sized combustion engine in the parallel configuration running more efficiently during low-power requirement loiter segments because it doesn't need to be sized for the full power requirements of dash and climb-out like the ICE configuration.

For the Interceptor mission, at $32kg$ TOW, the 10% increase in empty mass of the series configuration compared to the gasoline baseline yields an approximate 26.1% reduction in endurance/TOW. At the same $32kg$ TOW, the parallel HEPS configuration has an endurance/TOW of $1.3[hr/kg]$ compared to $1.15[hr/kg]$ for the gasoline aircraft. This result yields a 13% increase in endurance from $36.8hr$ for gasoline to $41.6hr$ for the parallel HEPS.

Parameter	Electric	Gasoline	Parallel	Series
Empty Mass $[kg]$	10.2	12.7	12.7	14
Payload $[kg]$	5	5	5	5
Fuel Mass $[kg]$	0	7.3	3.4	2.4
Battery Mass $[kg]$	9.8	0	3.9	3.6
TOW $[kg]$	25	25	25	25
Climb Gradient $[^\circ]$	12	12	12	12
Op Altitude $[m]$	2000	2000	2000	2000
Loiter C_L	0.8	0.8	0.8	0.8
Loiter Endurance $[hr]$	1.3	17.85	18.85	8.6
Loiter Endurance/Fuel Mass $[hr/kg]$	0.13	2.45	2.58	1.43

Table 5.5: Communications Relay Mission baseline results summary.

5.1.4 Mission Profile - Communications Relay

In the Communications Relay mission, there is no aggressive dash segment in the mission as in Interceptor. The Communications Relay mission focuses on maximum endurance of the aircraft loiter phase, and has a steep climb out gradient of 12° . For this experiment, the aircraft TOW is swept from $25 - 35kg$ and evaluated against loiter endurance.

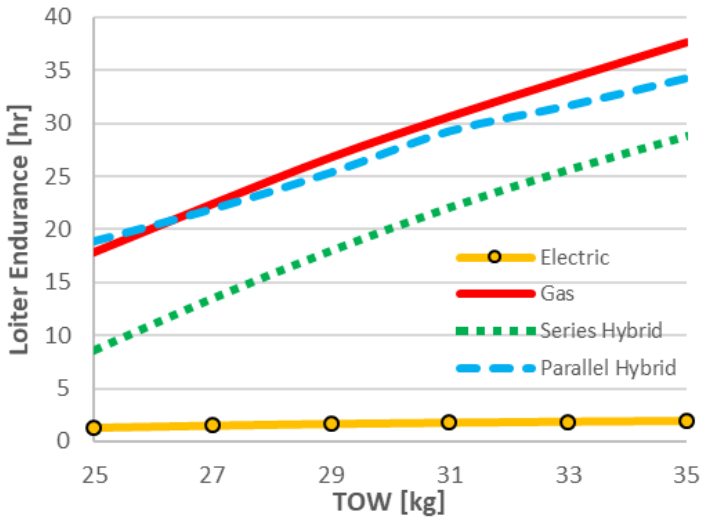

Figure 5.4: Framework design study example: Communications Relay Mission Loiter Endurance versus TOW.

At $25kg$ TOW the parallel HEPS configuration has the highest loiter endurance as it can run efficiently during the loiter phase of this mission, and can use the electric motor for the steep climb out. However, the gasoline configuration has the longest endurance at TOW values above $28kg$. Due to the high energy density of hydrocarbons in the ICE configuration compared to the LiPo batteries in the EM and hybrid configurations, the ICE Only configuration is well suited for this mission. Both of the hybrid configurations are penalized compared to the ICE configuration because they have to bring onboard batteries, and the series configuration has a higher empty weight because of additional components. These factors limit the amount of fuel available to the HEPS aircraft. In addition, the series hybrid configuration suffers a lower loiter endurance compared to the parallel configuration due to the energy conversion losses associated in a series power train. The electric configuration aircraft only saw an increase of loiter

endurance from $1.30 - 1.91$ hours with the TOW sweep, and is unable to compete with the much higher loiter times of the other configurations due to the mass of the battery packs.

In future experiments, an interesting comparison metric would be to compare the aircraft configuration loiter endurance with an assisted take off segment. Aircraft of this size class could benefit from an pneumatic launch system to further decrease the energy requirement of the mission in the climb out segment and explore the full range of loiter endurance.

5.2 Component Level Test Results

EM - AXI Motor Testing

In order to test and characterize small brushless DC motors, UVIC CfAR has developed a thrust test rig shown in Figure 5.5. This setup is capable of testing inrunner or outrunner brushed or brushless DC motors with propellers up to 24 inches in diameter for a wide range of mounting patterns. The power-electronics of the system allow for the testing of any motor with any ESC and battery pairing, with quick-connect bullet terminals, XT90 and XT60 connectors. Further, the power-electronics inside the main electrical box allow for safe testing with current, voltage and temperature cut-offs for up to $150A$, 12S $(50V)$ testing. All critical variables for DC motor characterization are captured with the NI cDAQ data acquisition system, including current, voltage, RPM, thrust, torque and associated mechanical and electrical efficiencies. Torque and thrust are measured using a FUTEK MBA500 bi-axial sensor which is rated for $890N$ of thrust and $23Nm$ of torque. A thrust test experiment GUI was developed in LabView in order to interact with the test bench, set safety parameters, monitor test performance and record data.

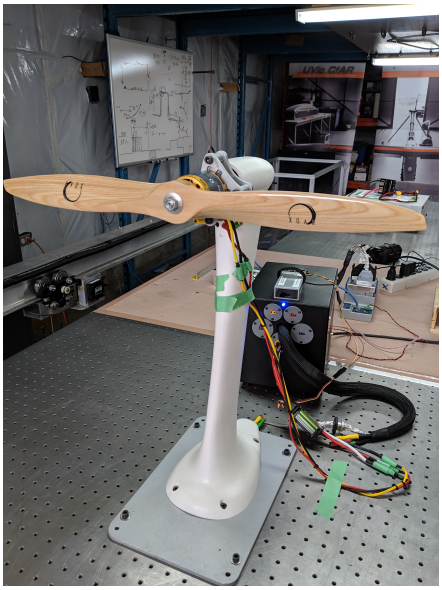

Figure 5.5: Thrust test stand for motor and propeller characterization.

The AXI 4130-20 motor was tested with several fixed pitch propellers in order to fully map its performance. As shown in Table 5.6, the electric motor throttle was swept from $0 - 100\%$ in 10% increments with a 19x10" propeller. It can be seen that even with two large $8000mAh$ 6s lithium polymer batteries

EM_{thr}	RPM	τ_{prop}	$Power_{prop}$	$Current$	$Voltage$	$Power_{bat}$	$\eta[\%]$	$T_{prop}[N]$
0	0	0.00	0.00	0.34	25.16	0.87	0	0
10	756.2	0.033	2.61	0.29	25.15	7.39	35.3	0.36
20	1352.1	0.100	14.22	0.96	25.12	24.12	58.9	2.37
30	1981.4	0.208	43.20	2.40	25.06	60.24	71.7	6.12
40	2595.5	0.351	95.47	4.90	24.94	122.16	78.2	11.41
50	3163.1	0.521	172.66	8.62	24.77	213.52	80.9	17.74
60	3686.6	0.710	274.07	13.57	24.55	333.05	82.3	24.78
70	4155.0	0.899	391.12	19.73	24.19	477.17	82.0	32.08
80	4584.1	1.097	526.66	27.31	23.73	648.22	81.2	39.58
90	4944.8	1.281	663.41	35.93	23.13	831.11	79.8	46.49
100	5161.9	1.402	758.13	42.61	22.47	957.53	79.2	50.92

Table 5.6: AXI Motor Component Testing

used in parallel to power this motor, there is still a decrease in output voltage at the high throttle points. This is due to the nature of LiPo batteries having an exponential curve for voltage drop throughout discharge, especially for high C ratings, as described in the theoretical overview section of this report. It would be possible to decrease this effect by adding additional cells in parallel, or exchange the thrust test power source for a constant voltage supply with a high current rating.

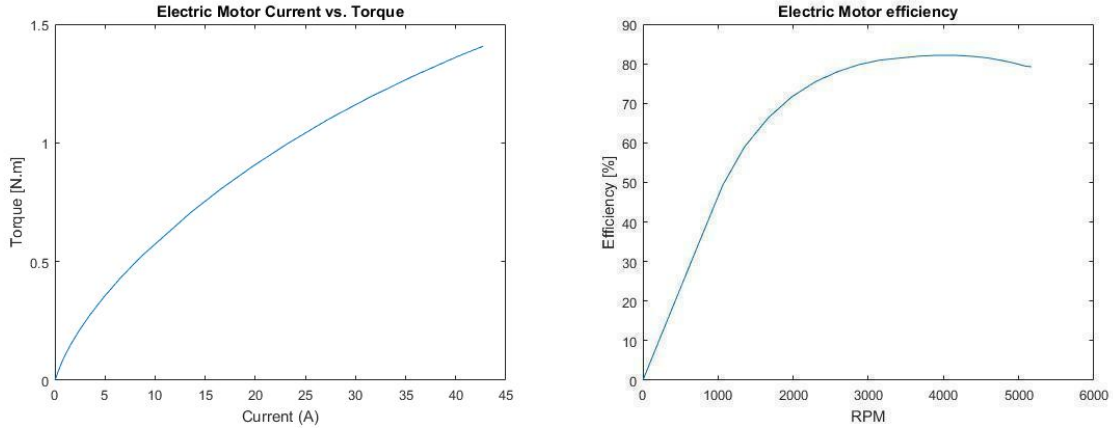

Figure 5.6: Torque vs current for the AXI 4130/20 motor test (left) and Efficiency vs RPM. (right)

Despite the voltage drop, the EM is able to exhibit a generally linear trend for output torque versus current. In the lower region of the plot, below $15A$, the curve has an exponential trend due to the motor's lower efficiency. This result aligns with the theory of direct current motor torque characteristics as described in Appendix A of this report.

The efficiency of the motor was plotted as a function of RPM in order to determine the most efficient point for static thrust. As can be seen in the results of Table 5.6, a maximum efficiency of 82.3% was achieved at $3686.6RPM$. Beyond $3686.6RPM$, the efficiency of the motor begins to drop off but remains relatively high. The efficiency of the motor is an important metric to explore when designing a HEPS as it is a critical factor for component sizing, as well as controller programming. Ideally, the Dash mode of a HEPS would have the ICE and EM components sized to maximize efficiency and minimize fuel consumption when working together.

Propeller Testing

In order to determine the optimal performance of the HEPS system, a range of different propellers were tested with the UVIC CfAR thrust test rig. Together with the AXI motor described in the previous section, each propeller was swept the full power range of the motor to explore the torque and thrust characteristics. Although a variable pitch propeller could provide a larger operational envelope for the UAV, only fixed pitch propellers were considered in this research to minimize component complexity and weight. The performance of the 19x10" propeller is shown in Figure 5.7 for the torque and thrust as a function of RPM. Appendix B of this report includes additional propeller curves, as well as thrust and torque trendline data.

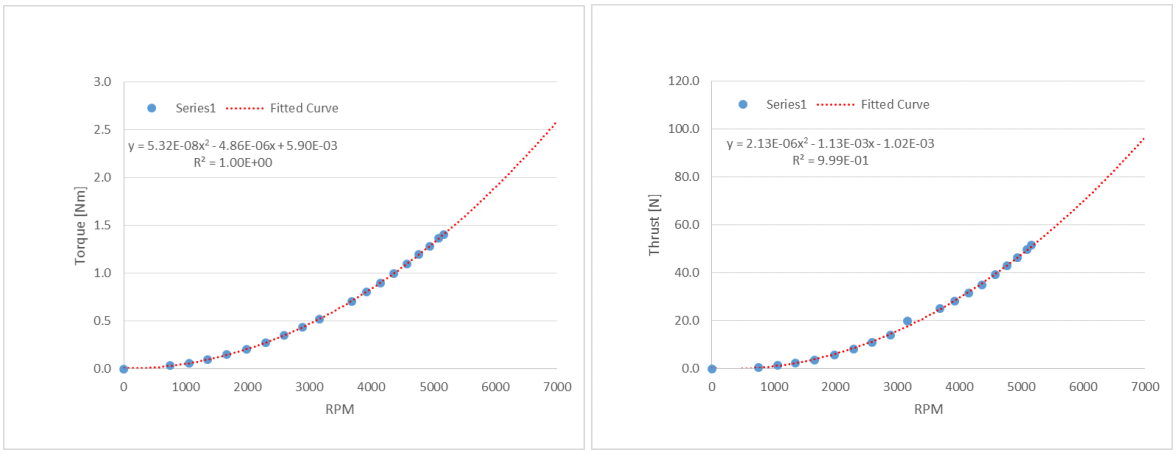

Figure 5.7: Torque vs RPM (left) and Thrust vs RPM (right) for 19x10" propeller.

ICE Testing

In order to create a solid baseline of ICE performance for the HEPS, component-level testing of the DA-35 engine was conducted. This testing was focused on creating an engine map for the two-stroke ICE, and to compare the fuel-flow measurements with those provided by the manufacturer. From the EM and propeller testing conducted before, the ICE could be mapped for torque output just by measuring the RPM of the output shaft. In this testing, a load cell was placed underneath the fuel tank to monitor the difference in fuel mass throughout the test. Since the rotation speed of the small two-stroke engine tended to be noisy with variance in RPM, these tests were conducted multiple times, and fuel flow measurement were averaged to mitigate noise-bias.

It should be noted that even though experimental test conditions were setup to be as consistent as possible between tests, the nature of the test environment contributed to variance between experiments. Since tests were conducted outside of the CfAR shop to properly vent ICE exhaust, the ambient temperature and pressure had slight changes between tests, as well as the test bench was exposed to light winds. Further, small two-stroke engines can exhibit variance in performance after the engine has been 'broken-in' after running for several hours, as well as after warming up. To assist in counteracting these variances, the ICE has two tuning pins for 'high-RPM' and 'low-RPM' for adjusting the air/fuel mixture in the Walbro carburetor. Small adjustments were made to these pins, and recorded in the test documen-

		Experimental Data	Manufacturer Data		
Throttle	RPM	$\dot{m}_{fuel}$ [g/min]	$\dot{m}_{fuel}$ [g/min]	Relative Difference [%]	$\tau_{prop}[Nm]$
10%	3323.0	4.91	-	-	1.052
20%	4029.9	12.97	3.64	71.92	1.551
30%	4293.9	13.19	5.67	56.94	1.762
40%	5033.5	19.83	8.88	55.21	2.425
50%	5698.7	24.57	13.20	46.26	3.112
60%	5800.3	21.26	14.68	30.92	3.225
70%	5828.1	22.59	15.51	31.30	3.256

Table 5.7: Desert Aircraft DA-35 Component Level Test

tation, to make the fuel mixture lean or rich and achieve smooth idle and reliable transition between low and high RPM. Operating small two-stroke internal combustion engines consistently can be complicated, especially with naturally aspirated carburetors.

The other factor that was included in the tuning of the ICE was the ignition spark. The spark plug was regularly removed from the cylinder head for inspection and cleaning, as well as to ensure the spark-plug gap was between $0.38mm$ and $0.50mm$ as per the manufacturer's recommendation. This gap must be maintained to ensure reliable firing as well as correct timing of sparking during the compression stroke. At the front of the DA-35, the hall-effect sensor that tracks the position of the output shaft with a magnet can also be slightly adjusted to advance or delay the spark.

Table 5.7 summarizes the results found in the component testing of the DA35 engine with a 22x10" propeller. These results are averaged quantities from multiple tests in order to eliminate the bias found in inconsistencies of naturally aspirated two-stroke engines. It should be noted that with smaller propellers, including the 18x10" and 19x10", the test operators observed the ICE RPM at extremely high values and the engine was unable to remain at steady idle or low throttle points. The 22x10" propeller better suited the ICE testing and provided consistent performance and engine behaviour. In future experiments, an electronic fuel-injected system (EFI) could provide consistent performance and assist test operators with tuning of the engine. The high cost of EFI engines did not allow them to be explored in this research, but could provide interesting results in future work.

The engine was able to be tested for a range between 3323 and 5828 RPM. As can be seen in Figure 5.8, the fuel consumption measured in this testing is larger than the values provided by the manufacture, and does not follow a close trend throughout the operating range. The ICE test was repeated many times, and had many complications with finding consistent idle behaviour and smooth operation through the RPM range. In addition, the test operators were unable to determine a justification for the high fuel consumption values measured. However, the data collected in this experiment is still used in the programming and tuning of the HEPS controller by providing the necessary torque-throttle curves.

Ideal Operating Line Analysis

Using the provided manufacture data for the engine, the Ideal Operating Line (IOL) can be determined by plotting lines of constant power onto the BSFC map. Along each of the lines, the minima for lowest BSFC can be found as the IOL point for that power-line. Sweeping the entire power range of the engine

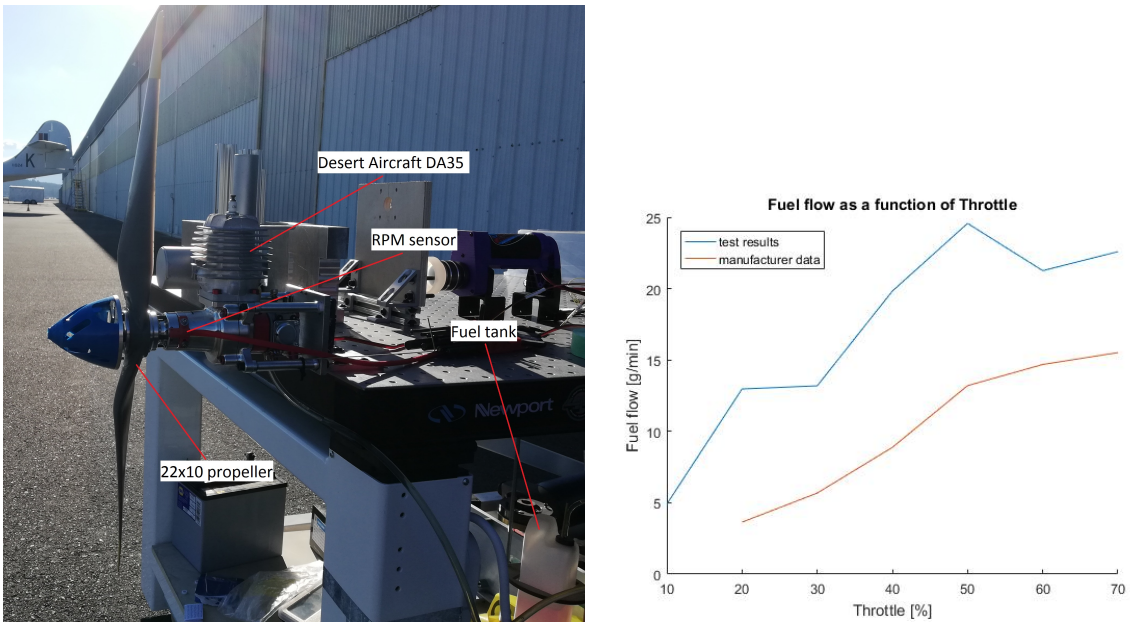

Figure 5.8: DA35 engine component testing to determine baseline performance. (left) Fuel flow rate $\dot{m}_{fuel}$ [g/min] of DA35 component test versus manufacture data. (right)

will create the entire IOL line, as shown in Figure 5.9. Due to the limited number of supplied points for power-lines from the manufacturer, a third order polynomial function was fitted to the line. As shown in Figure 5.9, above $4000RPM$ the BSFC values for the IOL line remain low if the system is held at its most ideal point. From this information, the ICE should be held between $4000 - 7000RPM$ and between $1.7 - 2.2Nm$, and avoid operations in low torque / low RPM ranges.

With the 19x10" propeller pairing, the achievable operating points can be seen in Figure 5.9. Following the dashed curve for the 19x10" propeller, it can be seen that it intersects the dash-dotted IOL line at approximately $6000RPM$ and $1.9Nm$ of torque. Therefore, for the controller development of the system, the ICE will be operable up to $6000RPM$ on its own, and then above the intersection point the EM and ICE will be used together to achieve the desired output torque and the ideal ICE operating point. This allows the system to continue up the propeller curve into the higher regions of the map at higher torque and RPM, while the ICE remains at the IOL line as the RPM increases. The authors found that the 22x10" propeller would also be be well suited for the parallel HEPS, as the results in Appendix B show, however the system was unable to additional torque load of the larger propeller and stalled frequently. With improvements to the HEPS transmission, it may be possible in future work to explore different regions of the engine map, and the engine IOL with different propellers.

5.3 System Level Test Results - Bench Test

Once the bench test was assembled, data could be collected on the system performance of the HEPS for each of the four operating modes. First, the EM Only mode was tested to evaluate the EM performance, as well as determine an estimate for the amount of system losses since the performance can be directly compared to the component testing of the EM on the CfAR thrust test stand. Second, the ICE Only

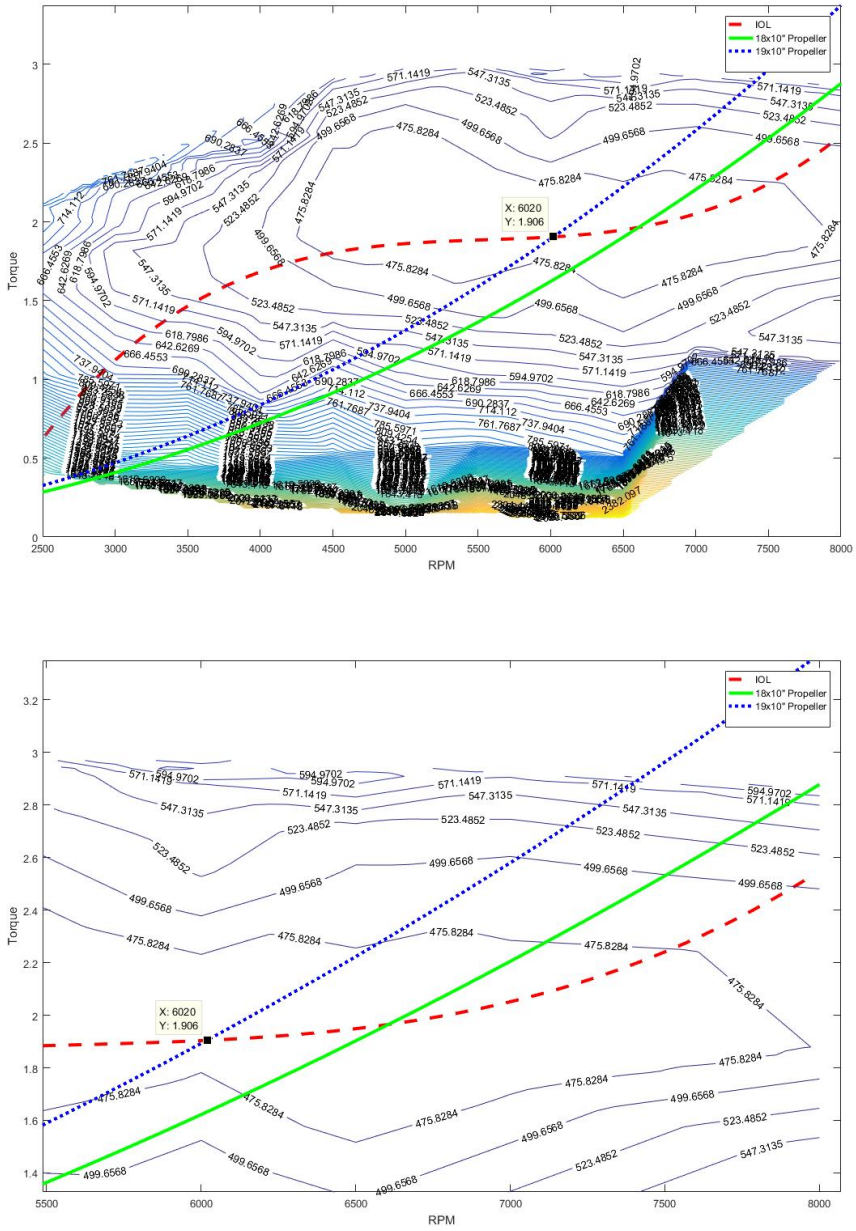

Figure 5.9: Overlaying the 18x10” and 19x10” propeller curves, as well as the IOL of the DA-35 onto the torque-RPM map with BSFC contours.

mode of the HEPS was evaluated to determine the amount of fuel consumption consumed by the HEPS through the operational range. Again, the ICE Only mode would be compared against the component testing baseline to observe the impacts of the HEPS transmission on the component performance. In the third operating mode, Dash Mode, the EM and ICE work together to share the torque load of the propeller. In Dash mode, the ICE is held at a constant throttle point of 40%, while the EM is swept throughout its operating range to gradually increase the torque it provides to the system to observe impacts of system RPM. Finally, the forth operating mode of Regenerative Braking, (referred to as Regen Mode) explores the EM’s ability to act as a generator and supply power to the system batteries. In Regen Mode, the most critical observation is to determine the impact on system RPM as a function of power

EM_{thr}	RPM	$\tau_{prop}[Nm]$	τ_{EM}	$Power_{prop}$	$Current$	$Voltage$	$Power_{bat}$	$\eta[\%]$
0	0	0	0	0	0.001	25.14	0.04	0.00
10	1077.49	0.064	0.000	7.19	0.86	25.10	21.68	33.15
15	1637.60	0.144	0.030	24.78	2.01	25.05	50.26	49.30
20	2079.92	0.231	0.074	50.26	3.47	24.97	86.62	58.03
25	2481.82	0.326	0.130	84.82	5.26	24.88	130.93	64.78
30	2794.68	0.412	0.192	120.62	7.25	24.78	179.51	67.20
35	3033.02	0.484	0.252	153.79	9.17	24.67	226.28	67.96
40	3296.14	0.570	0.324	196.89	11.46	24.55	281.36	69.98
45	3531.59	0.654	0.407	241.69	14.12	24.40	344.52	70.15
50	3774.49	0.745	0.501	294.53	17.10	24.24	414.49	71.06
55	3979.34	0.827	0.596	344.65	20.14	24.07	484.81	71.09
60	4168.71	0.907	0.703	395.78	23.55	23.88	562.26	70.39
65	4317.67	0.972	0.794	439.36	26.48	23.70	627.47	70.02
70	4485.52	1.048	0.901	492.18	29.90	23.50	702.46	70.06
75	4656.81	1.128	1.033	550.27	34.10	23.26	793.14	69.38
80	4672.88	1.136	1.046	555.94	34.53	23.18	800.26	69.47
85	4679.34	1.139	1.056	558.24	34.83	23.12	805.26	69.32
90	4794.73	1.195	1.148	600.24	37.77	22.97	867.63	69.18

Table 5.8: EM Only Mode Test Results on Parallel HEPS Test Bench.

drawn by the regenerative brake.

5.3.1 EM Only Mode and Hybrid Bench Test Friction Loss Estimation

The EM Only testing maps the performance of the electric motor on the hybrid-electric power train. In this testing, since the only difference from the component testing on the CfAR thrust test stand is the additional components of the HEPS power train, it is possible to get an estimation of system losses.

The results collected in this testing were used to update the values in the HEPS controller. In initial development of the controller, values provided from the component only testing were used as they provided more accurate performance than the baseline data provided by the manufacture. However, as the system performance of the EM with the hybrid power train became available, it was used to replace the controller values as it provides the actual system performance.

In this testing, the throttle setting of the EM was swept in increments of 5% from $0-90\%$. To minimize bias between testing, the test was repeated 3 times. In addition, when comparing against the baseline component testing, the power consumption of the EM was compared rather than just the current-draw of the motor. This is due to the fact that even though two large $8000mAh$ LiPo batteries were used to power the system, there is a still a considerable voltage drop when the EM is under full load. Batteries were charged between experiments to ensure results were as consistent as possible. The results for EM Only testing can be found in Table 5.8.

The trends observed in Figure 5.10 exhibit the EM following expected trends for RPM, current, voltage and efficiency. Compared to the baseline values found in the component testing of this project, the most effective comparison is made between motor efficiency curves. The maximum efficiency of the EM on the hybrid bench test was measured as 71.09% at $3979RPM$. In the component level testing of the EM, without the hybrid power train, the maximum efficiency of the motor was 82.9% at a speed of $3687RPM$.

These losses can be attributed to slight misalignment and eccentricity of components in the HEPS

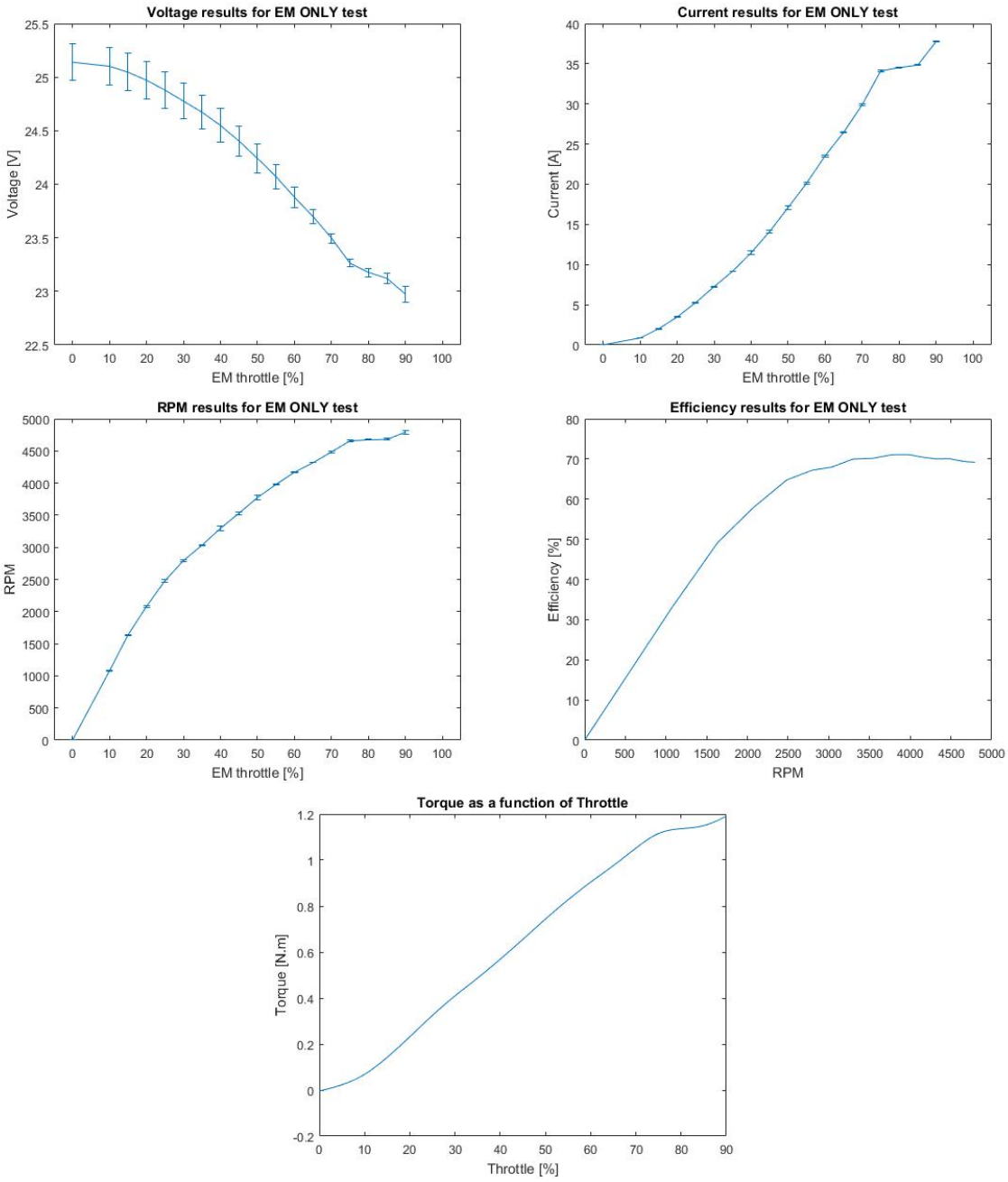

Figure 5.10: Results collected in the EM Only testing on the parallel HEPS test bench.

transmission causing friction losses. The inherent friction losses from introducing various bearings into the system also contributes to these losses. Throughout testing, the friction of the support bearings were reduced as much as possible by using high-speed bearing lubricant instead of high-life bearing grease. In the design of the parallel HEPS test bench, careful machining and assembly techniques were practiced to ensure alignment was as accurate as possible, but slight misalignment is unavoidable. Components of the test bench were sourced from materials with high precision to ensure tight fits with minimal slop and to minimize cumulative misalignment error in the system. All of the HEPS transmission shafts are supported in more than one place, and located with several features.

As shown in Figure 5.10 the standard deviation for this set of testing is low, proving that the EM

runs consistently between tests. Unlike the ICE, the EM is very predictable during testing, and small discrepancies in output power could be attributed to environmental differences between the testing experiments.

Finally, Figure 5.10 shows the relation of the output torque of the EM Only test as a function of input throttle. As can be seen, the EM exhibits very consistent behaviour with a linear trend throughout the operational range, with only small discrepancies at the low end and high end of the range. At the top end of the curve, there is only a small increase in torque for the $80 - 90\%$ range as the efficiency of the EM begins to decline. The test operators observed this behaviour but could not identify the source of the error of the discontinuity in the torque trend above 80% throttle. This figure is critical in the programming and function of the HEPS controller as it uses this data to determine the amount of torque capable for the EM to output during Dash mode.

5.3.2 ICE Only Mode

To capture the data required for the performance of the ICE, the following sensors were monitored:

- Hall Effect Sensor - Propeller RPM
- PWM Signal - Throttle position of butterfly valve of carburetor
- Load Cell - Mass of fuel tank

The main objective of this testing was to provide an accurate estimate to the HEPS controller on the fuel consumption of the system as a function of torque output. The experimental values collected from the built HEPS test bench would replace the estimates from manufacture data as well as component-level testing.

As mentioned in the Test Bench section of this report, the fuel consumption is captured by measuring the fuel mass overtime as the ICE is running. An energy density of $44.4MJ/kg$ was used for the gasoline. [75] To run through power sweeps, the ICE throttle was swept in 5% increments throughout the entire operating range. However, it should be noted that the ICE is susceptible to stalling at low throttle settings before warming up. For this reason the test engineers began the test at higher throttle settings and then decreased gradually as the engine warmed up.

Since small two-stroke internal combustion engines can be unstable in their output RPM, the amount of fuel drawn can vary. As mentioned in the ICE component level testing, naturally aspirated carburetors can have variance in amount of fuel consumed over time even if the air-fuel mixture valve remains stationary. For this reason, the fuel consumption results are represented as average consumption rates over ten-minute testing span windows. Figure 5.11 shows an example fuel mass measurement during a ten-minute window of ICE Only mode testing.

Table 5.9 summarizes the results collected in the ICE Only mode testing of the HEPS. It can be seen that for throttle position values below 15% the ICE is unable to sustain constant running and stalls, compared to the minimum throttle position of 10% in the component-level testing. Further, it can be seen that the maximum efficiency of the ICE Only mode HEPS is at 21.02% at the 45% throttle position. It is

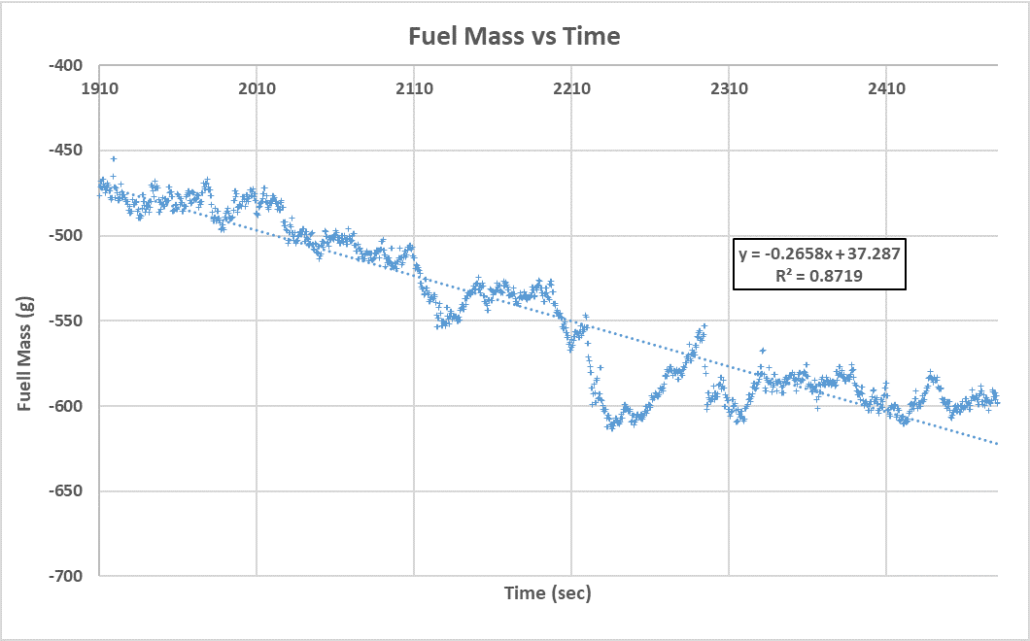

Figure 5.11: Fuel mass data collected in the ICE Only testing on the parallel HEPS test bench.

ICE_{thr}	RPM	$\tau_{prop}[Nm]$	$P_{prop}[kW]$	$\dot{m}_{fuel}[g/min]$	$BSFC[g/kWh]$	$P_{in}[kW]$	$\eta[\%]$
15	4543	1.025	0.532	5.07	572.2	3.754	14.17
20	5415	1.445	0.894	9.94	667.0	7.358	12.16
25	5781	1.643	1.085	11.90	657.9	8.807	12.32
30	6115	1.834	1.282	12.69	594.0	9.390	13.65
35	6319	1.956	1.412	13.09	556.2	9.689	14.58
40	6503	2.069	1.538	15.56	607.0	11.511	13.36
45	6613	2.138	1.616	10.39	385.7	7.687	21.02

Table 5.9: Results from ICE Only Testing on parallel HEPS test bench.

clear that the HEPS power-train offers several operational advantages compared to the component level testing, but the additional friction and rotational inertia added to the system has an influence on overall performance. With the 22x10" propeller, the system was not able to handle the larger propeller load as well as the system friction, so the test bench instead used the 19x10" propeller.

Figure 5.12 shows the results collected for fuel flow, BSFC, torque and power as a function of throttle for the ICE Only mode testing. In the manufacturer supplied data, the engine is capable of providing a maximum of torque of $2.99Nm$ at $5500RPM$. As shown in the testing of the ICE Only mode of the hybrid transmission, a maximum torque value was achieved with the 19x10" propeller at $6613RPM$ which corresponds to $2.138Nm$. The author observed that during the testing of the HEPS in ICE Only mode, the inconsistencies in fuel flow caused difficulties to draw conclusions on the performance of the ICE. Although an EFI two-stroke engine was not explored in this research due to timeline and budgetary constraints, and EFI system would likely provide more consistent ICE performance, as well as a precise means to measure fuel consumption with the integrated fuel pump.

Throughout the experiment, the ICE had a higher fuel flow rate $\dot{m}_{fuel}$ than the DA35 engine maps, but also output more power than the DA35 for equivalent throttle settings. Comparing with the information from the manufacturer, the ICE Only test had a lower BSFC value at the low end of the throttle as well

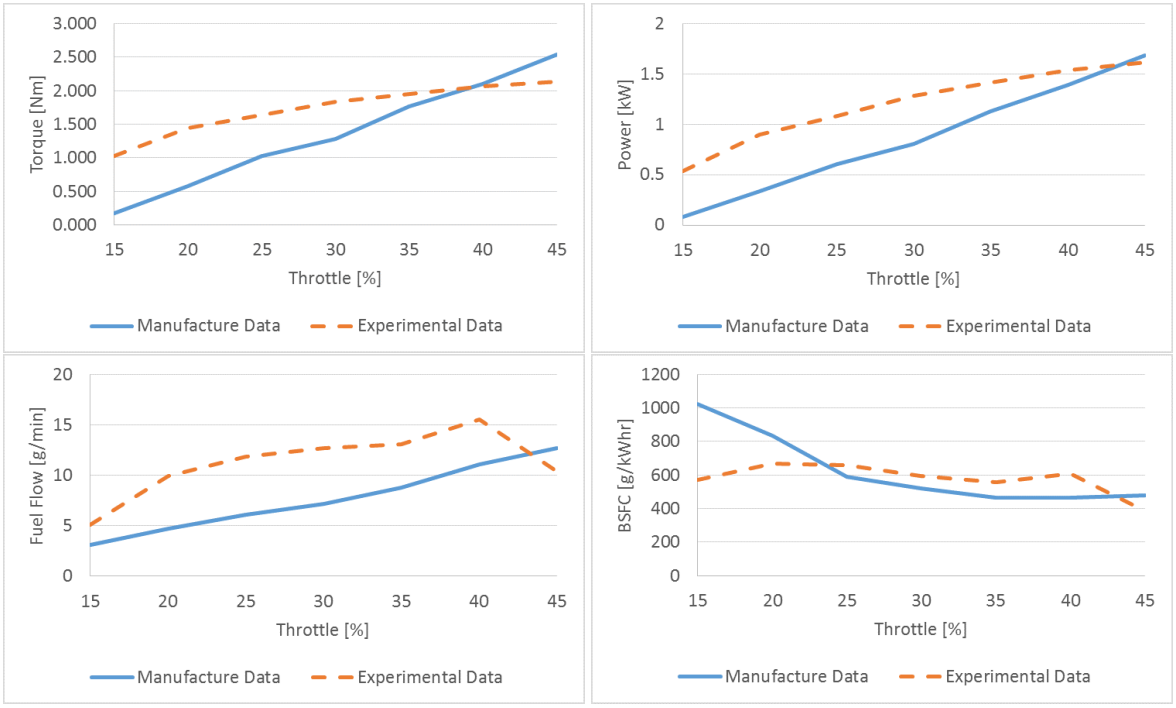

Figure 5.12: Results collected in the ICE Only testing on the parallel HEPS test bench comparing with manufacturer data.

at 45%, but was higher for between $25 - 40\%$ throttle. However, the fuel flow rates at 40% and 45% appear to deviate from the trend of the fuel flow for the rest of the operating range. The 45% throttle test point should be retested several times and an average for fuel flow rate needs to be calculated to determine if this efficiency is representative of engine performance at this point, or if this result is from inconsistent engine performance. Although there are similar trends between the experimental and manufacturer data, they do not closely match. The author recommends full testing and characterization of this ICE, with and without the HEPS test bench, on a dynamometer as it would provide more details on the performance and improve upon the dynamometer data supplied by the manufacturer.

5.3.3 Dash Mode

The most critical test point to validate on the hybrid test bench is 'Dash Mode' where the EM and ICE are working together. In this testing, the objective was to investigate the interaction between the two different propulsion systems and observe the performance and sharing of the torque load of the propeller. In this testing, the throttle valve for the ICE is held constant at 40% while the EM is swept from $0 - 60\%$ in steps of 10%. To observe repeatability, the test was conducted twice. The Table 5.10 summarizes the results of the Dash Mode testing.

As the throttle of the EM is increased, the RPM of the system increases which proves functionality of the Dash Mode operation. The clutch mechanism designed in the parallel HEPS test bench functions correctly and successfully combines these two power sources, despite the complex mechanical interaction. Further, it can be seen that the current going into the EM steadily increases until the 50% throttle position before beginning to decrease. For this reason, the EM throttle was not tested above 60%. Refer-

ICE_{thr}	EM_{thr}	RPM	τ_{prop}	$Power_{prop}$	$Current$	$Voltage$	$Power_{bat}$
	0%	4625.24	1.131	551.82	0.00	24.93	-0.06
	10%	4661.62	1.131	551.97	2.94	24.84	72.98
	20%	4815.54	1.206	608.01	7.26	24.68	179.20
40%	30%	5151.73	1.780	743.41	12.55	24.45	306.91
	40%	5568.72	1.608	937.48	17.49	24.20	423.17
	50%	5728.22	1.700	1019.76	19.88	24.03	477.67
	60%	5741.63	1.708	1026.89	19.07	24.00	457.74

Table 5.10: Results of the Dash Mode on parallel HEPS test bench.

ring to Table 5.10, it is possible to see that above 50% throttle, the current begins to decrease suggesting that the EM has reached a maximum and is no longer able to apply additional torque to the system. At this point, the EM is able to contribute significantly to the torque of the system, drawing $19.9A$ from the batteries. With each increase in the amount of torque supplied by the EM, the system speeds up to the point where above $5700RPM$ where it begins to plateau. However, throughout the testing of the Dash Mode, the current drawn by the EM has a small standard deviation indicating consistency between tests for the EM.

In Dash Mode, the torque supplied by the EM τ_{EM} cannot be directly measured. Instead, as outlined in Numeric Models Section, τ_{EM} is calculated with Equation 5.2:

$$\tau_{EM} = \frac{I - I_0}{K_v} \tag{5.2}$$

An important note to consider in the results of this test is that for the first test point where the ICE is set to 40% and the EM is at 0% throttle, the RPM and corresponding torque output of the propeller is slightly different than the 40% throttle position of the ICE Only test presented in the previous section. A large standard deviation is depicted in the RPM of Figure 5.13 at 0% throttle for the EM. This is caused by large variance in the RPM of the ICE at 40% throttle and reaffirms the observation of inconsistent ICE behaviour which suggests extensive testing of the parallel HEPS in Dash Mode is required.

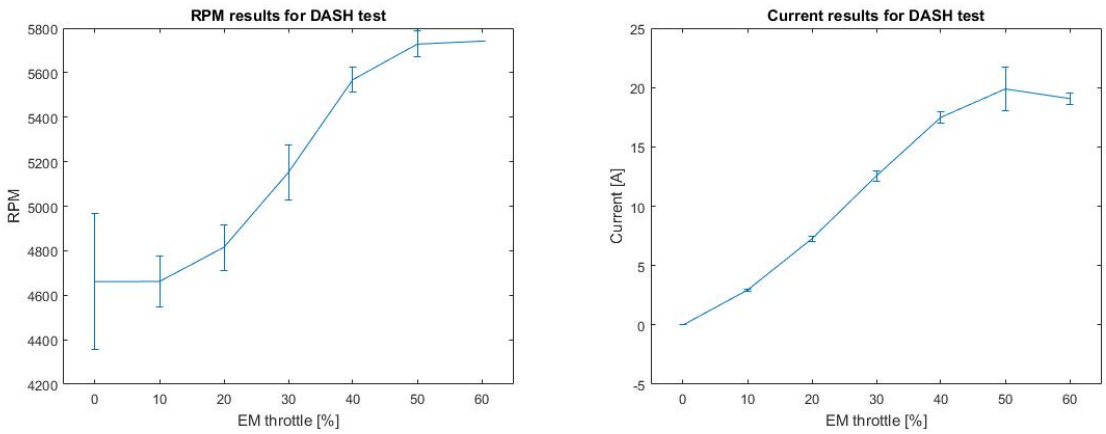

Figure 5.13: Results collected in the Dash Mode testing on the parallel HEPS test bench.

To improve upon the performance of the Dash Mode, there are several strategies that would increase the effective range of the EM. First, the EM could be sized with a higher kV to accommodate higher RPM. Alternatively, the EM could be sized larger to achieve a higher torque for the existing RPM range, and

ICE_{thr}	EM_{thr}	$\Delta\tau_{prop}$	τ_{EM}	$\Delta Power_{prop}$	$Power_{bat}$	$\frac{\Delta Power_{prop}}{Power_{bat}}$	$\frac{\Delta Power_{prop}}{Power_{prop}}$
	10%	0.000	0.050	0.14	72.98	0.19	0.02
	20%	0.075	0.193	56.19	179.20	31.35	10.17
40%	30%	0.248	0.358	191.59	306.91	62.42	31.51
	40%	0.477	0.513	385.65	423.17	91.13	51.87
	50%	0.570	0.588	467.93	477.67	97.96	49.91

Table 5.11: Detailed results of Dash Mode on parallel HEPS test bench.

would be done by increasing stator height and diameter. Besides altering the EM size, the Dash mode performance could be increased by implementing a mechanical gearing between the two propulsion types. This would allow for the EM and ICE to rotate at different speeds, yet still share the torque load of the propeller. For this specific motor sizing, a larger gear on the EM would mean the EM could spin slower than the ICE and still provide torque to the system. Another option would be to change to a more aggressively pitched propeller which would require larger torque for the same RPM. These observations are critical to improving system performance in future work, as well as influencing sizing decisions of other HEPS.

$$\text{Degree of Hybridization} = \frac{\Delta Power_{prop}}{Power_{prop}} \tag{5.3}$$

To further the analysis of the EM influence on the system in Dash Mode, it is critical to explore the degree of hybridization for the system. The degree of hybridization is a useful metric in determining the extent to which the EM is assisting the system, and helps compare HEPS designs against one another. In essence, a very light hybridization factor would mean that the EM only has small influence on the torque of the system, and would operate very differently than a high hybridization factor HEPS where the ICE heavily relies upon the EM's assistance. As the EM is increased, the value for $\Delta\tau_{prop}[N \cdot m]$ and $\Delta Power_{prop}[W]$ represent the change in torque and power relative to $0\%\ EM_{thr}$ respectively. τ_{EM} doesn't directly correspond to $\Delta\tau_{prop}$ which may be due to the ICE contributing inconsistent torque as the RPM varies, but the trend is similar. With changes in RPM of less than 100 RPM, the change in torque supplied from the ICE is not expected to incur a drastic impact.

Exploring the torque distribution of the Dash Mode test results in more detail yields some interesting observations. In Figure 5.14 it can be seen that the output torque of the system rises with each throttle increase of the EM. In fact, it can be seen that the ICE torque input to the system stays constant in general, except at the 30% point. Here, the ICE torque is higher at $1.4Nm$ with no change to the ICE throttle position, further proving the inconsistent behaviour of the ICE. However, it can be seen as the EM throttle is increased, the EM torque input increases linearly. This observation is critical as it proves that the EM is the source contributing to the torque increases to the system.

Considering the ICE output torque as constant, the $\frac{\Delta Power_{prop}}{Power_{bat}}\ [\%]$ indicates that the EM is able to contribute to the system at higher efficiency at higher throttle values. Further, in Table 5.12, the amount of torque supplied by the EM in the Dash mode test is compared to the amount of torque supplied by the EM in the EM Only test. Illustrated in Figure 5.15, it can be seen that for an equivalent throttle setting, the amount of torque produced by the EM is different, indicating that the EM has different behaviour

		Dash Mode		EM Only Mode	
ICE_{thr}	EM_{thr}	$\Delta\tau_{prop}$	τ_{EM}	τ_{prop}	τ_{EM}
40%	10%	0.000	0.050	0.064	0.000
	20%	0.075	0.193	0.231	0.074
	30%	0.248	0.358	0.412	0.192
	40%	0.477	0.513	0.570	0.324
	50%	0.570	0.588	0.745	0.501

Table 5.12: Comparison of EM Only and Dash Mode test results.

between these two operating modes. This behaviour is anticipated since the RPM of the system is not equivalent for these throttle settings but should be analyzed in more detail in future work.

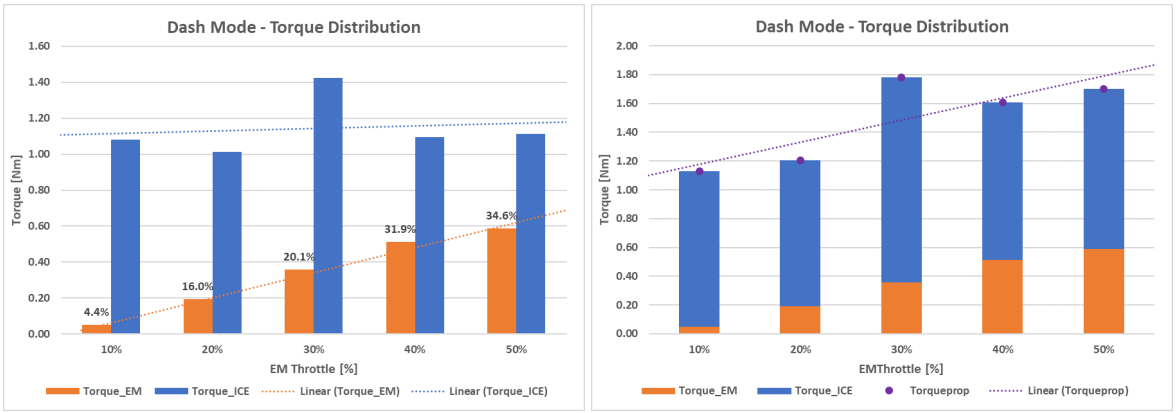

Figure 5.14: Results of torque distribution in the Dash Mode testing on the parallel HEPS test bench.

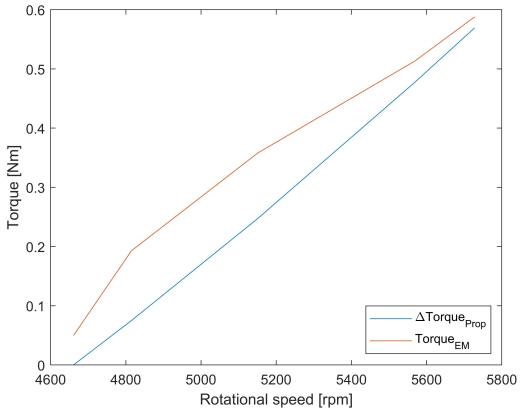

Figure 5.15: Results of torque from EM versus change in propeller torque in the Dash Mode testing on the parallel HEPS test bench.

5.3.4 Regenerative Mode

The regenerative braking mode (Regen Mode) of the HEPS is a critical aspect of testing in order to characterize the performance of the EM acting as a generator. As the generator withdraws power from the ICE to recharge the on-board batteries, not all of the torque supplied by the ICE is transmitted to the propeller. In this test, the ICE is held at a constant throttle of 60% and the EM is swept from 0% to

-90%, where the negative throttle is represented as regenerative braking. To minimize bias between test points, the test was repeated three times.

As can be observed in Figure 5.16, the Regen Mode was successfully able to draw power from the ICE to recharge the batteries. The mechanical coupling system developed in this system is proven to be functional in all of the operating modes. It can successfully split the system torque in both Dash Mode (where torque from EM is complimentary to the system) and in Regen Mode (where the torque from the EM is opposing the system.) Sweeping to -90%, the RPM of the system steadily decreased before dropping aggressively at -70%. This behaviour is expected as the EM is 'braking' and opposing the torque output of the ICE. With the exception of the -70% throttle position, the standard deviation of the system is low throughout the operation range leading to high predictability for system RPM as a function of applied brake. The observation of large standard deviation at -70% throttle is less of an indication of Regen Mode performance, and more an observation of the unstable behaviour of two-stroke combustion engines, especially at low RPM.

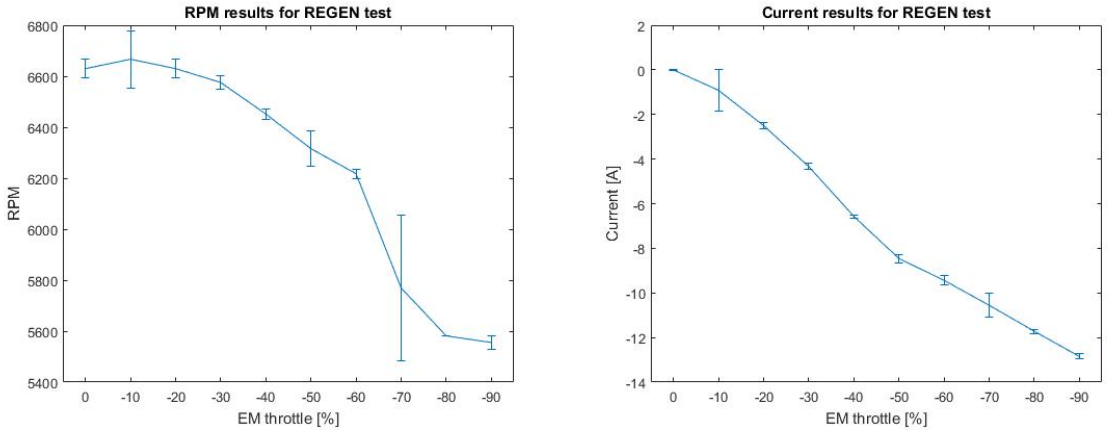

Figure 5.16: Results collected in the Regenerative Brake (Regen) testing on the parallel HEPS test bench.

Further, when observing the current flow of the EM during Regen Mode, it can be seen that the standard deviation is low. This behaviour is expected of the EM because of the ability of the BLDC speed controller to consistently make small adjustments to maintain a consistent current. In fact, throughout the sweep of the EM the trend-line of the EM current as a function of throttle sweep is linear. The maximum value recorded for current drawn from the system was $-12.85A$ or $930.84W$ at $5555.6RPM$. At braking powers above this point, it was found that the ICE was no longer able to sustain the brake and stalled.

At -10% throttle, the slight increase in RPM recorded by the system is not representative of the expected system behaviour as the EM is applying a braking torque to the ICE. As mentioned before, this behaviour is likely attributed to the ICE having variance of RPM between tests. In more detailed analysis of the Regen Mode testing, the reduction in torque to the propeller $\Delta\tau_{prop}[N \cdot m]$ follows the same trend as the EM_{thr} is decreased. As shown in Table 5.14 below, the $\Delta\tau_{prop}$ doesn't match with τ_{EM} suggesting that the torque opposing the ICE not only decreases output torque, but also reduces RPM and the overall output of the ICE.

Comparing the results of the Regen Mode to the Dash Mode of the parallel HEPS yields an interest-

ICE_{thr}	EM_{thr}	RPM	τ_{prop}	$Power_{prop}$	$Current$	$Voltage$	$Power_{bat}$
60%	0%	6629.83	2.271	1576.98	0.00	24.18	-0.09
	-10%	6666.67	2.297	1603.26	-0.92	24.19	-22.15
	-20%	6629.83	2.271	1576.98	-2.50	24.25	-60.63
	-30%	6575.39	2.235	1542.90	-4.34	24.32	-105.45
	-40%	6451.61	2.152	1453.85	-6.57	24.40	-160.29
	-50%	6315.79	2.063	1364.44	-8.46	24.48	-207.09
	-60%	6217.62	1.999	1302.15	-9.44	24.55	-231.60
	-70%	5769.23	1.724	1041.68	-10.55	24.61	-259.73
	-80%	5581.40	1.615	943.82	-11.72	24.67	-289.13
	-90%	5555.56	1.600	930.84	-12.85	24.75	-317.96

Table 5.13: Regen Mode results on parallel HEPS test bench.

ICE_{thr}	EM_{thr}	$\Delta\tau_{prop}$	τ_{EM}	$\Delta Power_{prop}$	$Power_{bat}$
60%	-10%	0.025	-0.060	26.28	-0.09
	-20%	0.000	-0.113	0.00	-22.15
	-30%	-0.037	-0.170	-34.07	-60.63
	-40%	-0.120	-0.240	-123.13	-105.45
	-50%	-0.208	-0.299	-212.53	-160.29
	-60%	-0.272	-0.330	-274.83	-207.09
	-70%	-0.547	-0.365	-535.30	-231.60
	-80%	-0.657	-0.401	-633.15	-259.73
	-90%	-0.671	-0.437	-646.13	-317.96

Table 5.14: Detailed results of the Regen Test

ing observation. As can be seen in Figure 5.17 the Dash Mode outputs significantly more torque than the absolute value of regenerative brake for equivalent throttle settings. [76] During the setup of the experimental test bench, the 'brake' parameters of the VESC could be configured for maximum current draw during regenerative braking. The VESC was configured for $I_{regen,max} = -15A$ as per the manufacturer recommendations, but since the system only produced $-12.85A$ at -90% throttle, the author believes that this value could be increased to the maximum rating of $-30A$. In future work, it is recommended to repeat the regenerative braking test multiple times with increasing $I_{regen,max}$ values to determine the maximum braking power. However, it should be noted that the author believes the AXI motor can sustain regenerative brake currents up to $-30A$ continuously, but this may lead to damage to the ESC and power electronics in the HEPS, and therefore was not attempted in this research.

5.4 Enhanced Solution - Controller Testing Results

In order to optimize the performance of the parallel hybrid-electric propulsion system, a supervisory controller was developed. This controller takes into account information from the component level testing of the various components of the HEPS, as well as manufacturer data, and commands the two propulsion systems in the most efficient combination. The purpose of the controller testing is to create a common-mission and evaluate the system performance in the three primary operating modes:

1. **EM Controller**
2. **ICE Controller**
3. **Hybrid Controller**

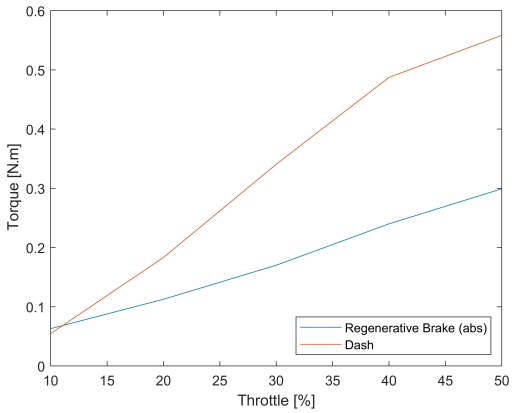

Figure 5.17: Comparison of torque output as a function of throttle % between Regen Mode and Dash Mode on the parallel HEPS test bench. [76]

To mitigate bias, the controller testing will allow experiments to be replicated multiple times to explore the system performance for consistency. This will allow observation of how the HEPS responds to torque requests for each operating mode. Several step functions were established as test points that will allow observation of the system's dynamic response to the changing inputs.

5.4.1 EM Controller Testing

For this exercise, the mission profile consists of three different torque requests, as depicted in Figure 5.18. These torque requests are consistent with torque ranges that are within the operating envelope found in the EM Only mode operations, and conducted 3 times to average performance.

Based on the look-up tables that the EM Controller references, the supervisory controller commands the ESC throttle setting to supply the desired torque output with the propeller used in the testing. As can be observed in Figure 5.18, the EM Controller is capable of matching the requested torque output closely, and consistently holds RPM throughout each phase of the mission profile. Further, it can be seen that the EM Controller has a rapid response to the step-inputs, and effectively adjusts system parameters to match new torque requests as generated. However, it can be observed that there is a slight error in torque output in the first phase of the mission, as well as torque fluctuations in the third phase. These results suggest that the EM Controller could be improved by collecting and comparing the test data collected in this exercise to update and improve the look-up tables. Therefore, the torque-throttle curve deployed in the EM Controller is considered successful in open-loop control.

5.4.2 ICE Controller Testing

The mission profile selected for the ICE Controller testing is identical to the mission profile for the hybrid controller testing. This is done intentionally so that the performance of the system can be compared where the supervisory controller separates the power distribution. The range of torque requests was selected as it falls within the range of the BSFC map above the intersection between the IOL and the 19x10" propeller where the system could benefit from having a portion of the torque supplied by the EM.

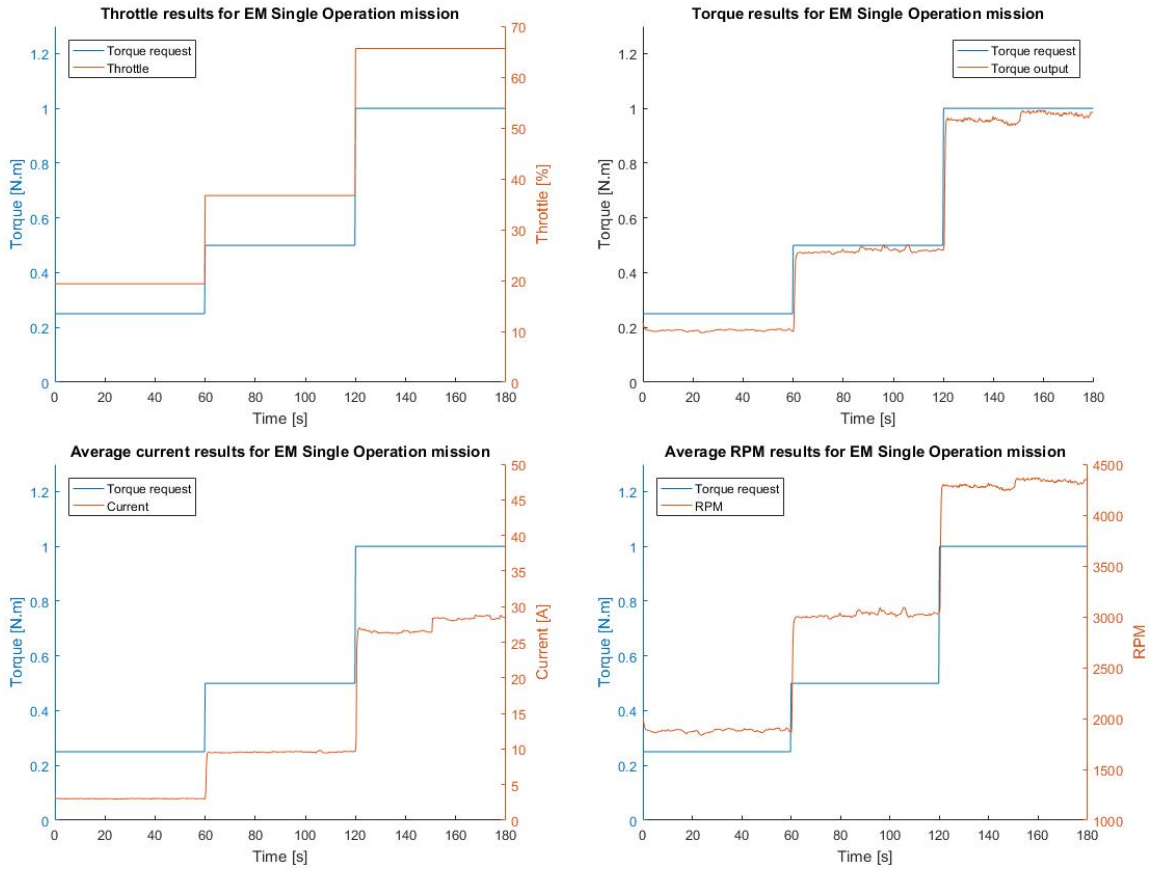

Figure 5.18: Results collected in the EM Controller testing on the parallel HEPS test bench with torque requests.

The ICE Controller interprets the torque requests successfully, as can be seen in Figure 5.19 below as the throttle setting is constant throughout each mission segment. However, it can be noted in Figure 5.19 that the resultant torque supplied by the system has complications. In the first segment, the torque output error is low and closely matches the request, despite fluctuations in the system. Later in the second and third segments, the torque request and resulting output begin to diverge, and do not closely match. However, the author notes that the system is consistently responding to the step inputs into the system and shows change in torque even if the value is not accurate.

Observing the RPM of the system during the ICE Controller testing, it is clear to see that instability and large amount of noise exists in the RPM of the ICE. In each segment the ICE is constantly fluctuating speed, varying up to 100 RPM in the first two segments, and up to $250RPM$ in the third segment. Further, at the beginning of the third segment when the system receives the step-input, the RPM of the system is observed falling rapidly over $400RPM$ from $6600 - 6200RPM$, before settling back to 6500 RPM. This behaviour is difficult for the system to handle, and yields unstable performance of the system, it may be beneficial to command smaller increments. With the observed variance in output torque, the author recommends additional testing of the ICE Controller, as well as updates to the engine maps to decrease output torque error. The author also recommends many repetitions of each experiment to collect system performance averages before implementing changes to the controller.

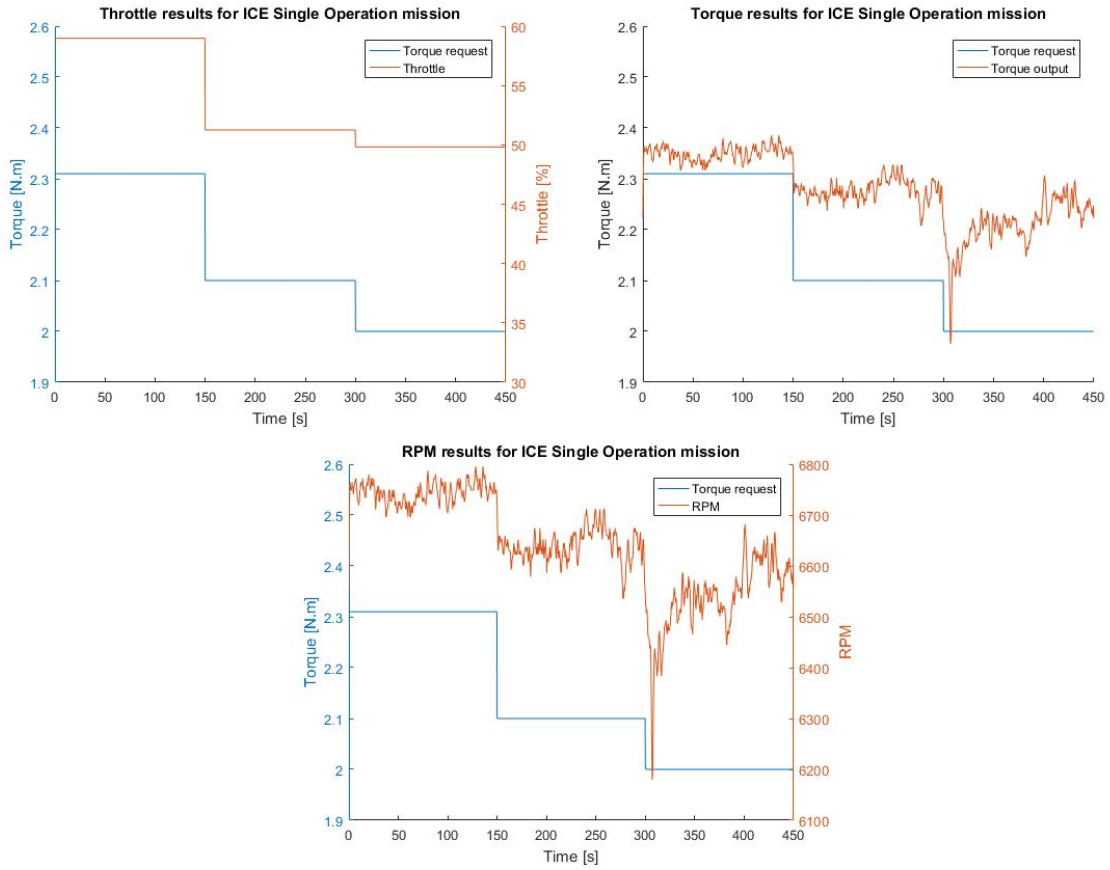

Figure 5.19: Results collected in the ICE Controller testing on the parallel HEPS test bench.

Segment	$\dot{m}_{fuel}[g/min]$	$m_{fuel}[g]$
1	24.50	61.15
2	24.62	61.45
3	22.62	56.46
Total	23.91 (average)	179.06

Table 5.15: Fuel consumption results from ICE Controller Testing on parallel HEPS test bench.

5.4.3 Hybrid Controller Testing

The most critical testing of this research is in the evaluation of the Hybrid Controller. In this experiment, the mission profile is the same as in the ICE Controller testing, but this controller allows the torque to be supplied by both the EM and ICE with Dash Mode. In each segment of the mission, the controller finds the optimal combination of ICE and EM throttle settings to supply the required torque that corresponds to the least amount of fuel burn. As can be seen in Figure 5.20, at each segment of the mission the EM throttle is varied, whereas the ICE throttle is kept constant at approximately 48%. This result indicates the Hybrid Controller is functioning, and is successful in determining the most efficient operating point for each propulsion system.

However, throughout this test there is an anomaly observed in the system RPM. At approximately the 50 second mark of the first segment, the system RPM spikes unexpectedly from $6000 - 6600RPM$. This increase of RPM is not the result of a commanded input to the system, but rather an anomaly in the output of the ICE. With the drastic change in system RPM, the Hybrid Controller recalculates the optimal

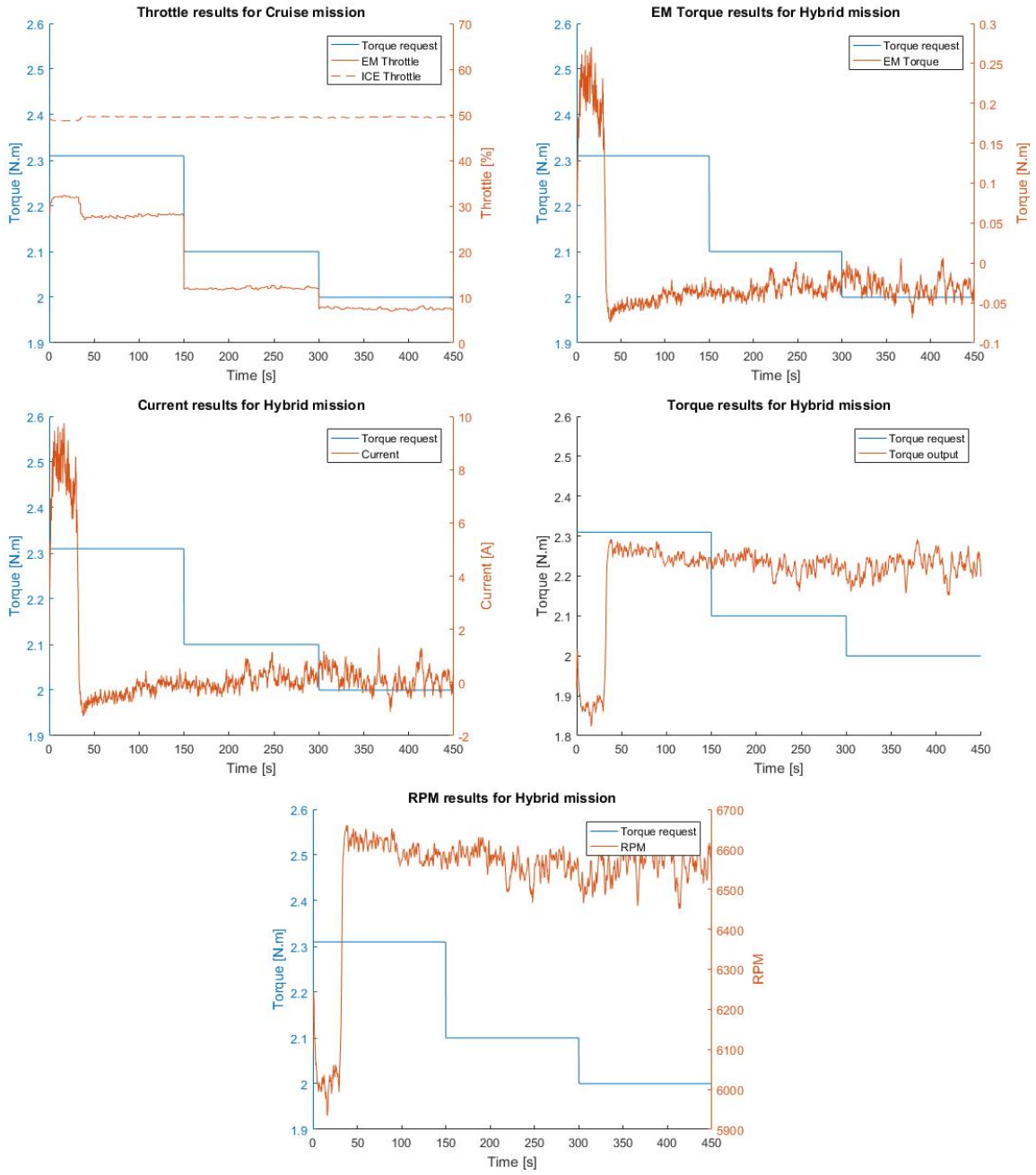

Figure 5.20: Results collected in the Hybrid Controller testing on the parallel HEPS test bench.

throttle positions, and adjusts the EM throttle from $32 - 28\%$, and the ICE throttle from $48 - 49\%$.

Observing the output current of the EM at the same 50 second position of the test, it can be seen that the EM current drops to nearly 0A. The author interprets this result as the EM is no longer able to effectively supply torque to the system as the rotational speed is too high. For the remainder of the mission, the EM draws very low current. As a result, since the ICE throttle remains at the most efficient throttle position of 49%, the output torque of the system remains constant. It can be seen that the RPM of the system is a very noisy signal with fluctuations of $100RPM$, but is not influenced by the changing torque requests. The fuel consumption of the Hybrid Controller in this mission are shown in Table 5.16. The results collected in this experimentation yield a 3% reduction in fuel consumption for the

Segment	$\dot{m}_{fuel}[g/min]$	$m_{fuel}[g]$
1	23.24	58.01
2	23.35	58.19
3	23.26	58.07
Total	23.38 (average)	174.27

Table 5.16: Fuel consumption results from Hybrid Controller Testing on parallel HEPS test bench.

Hybrid Controller compared against the ICE Controller. However, it should be noted that these results were collected with an inconsistent output torque, so the comparison is not conclusive. The author recommends additional testing of both the ICE and Hybrid Controllers on the parallel HEPS test bench in order to fully characterize the performance of the system.

5.5 Verification and Validation

An important aspect of the research project is to verify the accuracy of the MATLAB framework models developed in this research. In collaboration with a master's student from Instituto Superior Técnico in Lisbon, Portugal, studies were conducted between the theoretical results of the MATLAB framework and the experimental results collected on the parallel HEPS test bench. [76] In this thesis work, Pfurtscheller analyzes the predictive capability of the MATLAB framework to replicate results in the various test bench operating modes. A surrogate model is created to predict the behaviour of the DA-35 ICE performance. As can be seen in Figure 5.21, there are aspects of the framework which accurately predict test bench performance, and other aspects which do not. For both the ICE and EM throttle estimation as a function of RPM, the framework over-predicts. However, in the current of EM as a function of RPM, the framework predicts performance with low error. In the fuel flow rate estimation of the ICE Only mode, there is large error between $5400 - 5800RPM$, but decreases for higher speeds between $6000 - 6500RPM$. However, it was noted in the ICE Only mode test results section of this report that the ICE was consuming more fuel than anticipated compared to manufacturer data, which the MATLAB framework model is based on.

In Figure 5.22 the theoretical results for Dash Mode and Regen Mode are compared against results collected in the experimental bench testing. Here, it can be seen that the Dash Mode performance accurately predicts system performance, but there is some non-linear behaviour of the torque and current draw of the EM that is not accounted for in the MATLAB model. The Regen Mode test results shown in Figure 5.22 show strong correlation between the experimental and theoretical results. It is clear that the model is able to accurately predict performance of models involving the EM, but has difficulties with some of the complex modelling of performance of the ICE.

The MATLAB framework will continue to be updated and improved with findings such as these in order to improve the accuracy of the simulated results. Based on the findings of this study, the MATLAB framework is considered to be sufficiently accurate to draw useful conclusions from more advanced mission profiles. Although the results in these simulations may not exactly reflect the results of a UAV HEPS, and there is capacity for improvement in future work, the trends and trade-studies still yield useful conclusions for design engineers.

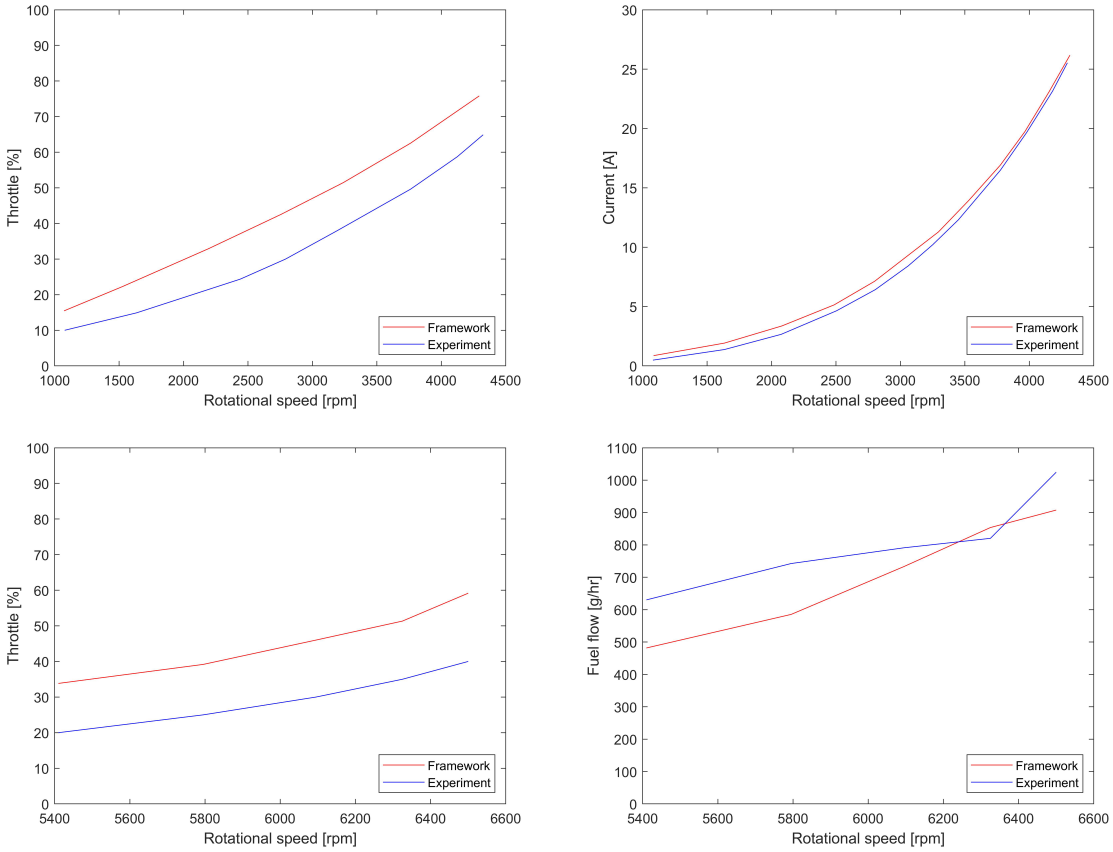

Figure 5.21: Results collected in the comparison between MATLAB framework theoretical result and experimental results collected on the parallel HEPS test bench. Throttle and current results as a function of RPM for the EM Only mode (top) and throttle and fuel-flow results for the ICE Only mode. (bottom) [76]

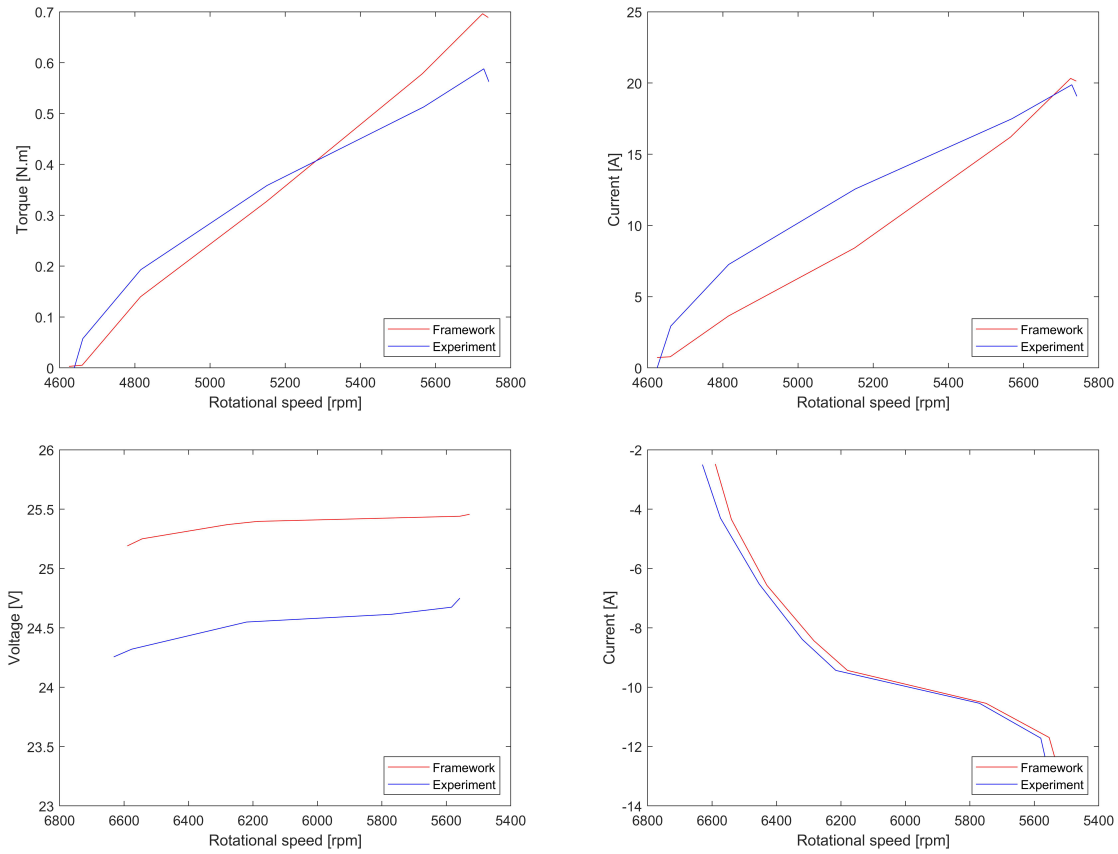

Figure 5.22: Results collected in the comparison between MATLAB framework theoretical result and experimental results collected on the parallel HEPS test bench. Torque and current draw of the EM results for Dash Mode, (top) and voltage and current draw of the EM results for the Regenerative brake mode. (bottom) [76]

Chapter 6

Conclusions

6.1 Achievements

Energy efficient propulsion technologies are an exciting aspect of research being conducted in various areas of the aviation industry. In this research, the benefits of a hybrid-electric propulsion system on a small-scale UAV are thoroughly explored through the design of an aircraft simulation framework and evaluation in an experimental apparatus. In the background research and analysis of the state of the art, HEPS were identified for their potential advantages and effectiveness for UAVs.

The initial stages of the project focused on the creation of the aircraft simulation framework in MATLAB to compare UAV propulsion architectures against one another. This research was able to successfully build an architecture that feeds manufacture data, experimental data as well as first-order models into the framework to create parametric models to predict propulsion system performance. In addition, the architecture allows for the definition of aircraft parameters and can simulate detailed mission profiles to explore performance in practical scenarios. Further, the MATLAB framework allows for trade studies to be explored as parameters of interest are swept to observe their influence on system performance. The estimated performance of the HEPS architectures was explored in more detail for 4 mission profiles: Interceptor Mission, Pipeline Inspection Mission, Communications Relay Mission and LIDAR Data Collection Mission. These missions provided a wide range of operating points for the propulsion systems to be evaluated in, and by sweeping parameters of the model trade-offs could be observed.

In the Pipeline Inspection mission, the exact payload capacities of each aircraft configuration could be observed in the fuel burn versus $C_{L,cruise}$ parameter sweep exercise. It was observed that the parallel HEPS configuration has an average of $3.52kg$ lower payload capacity for the $35kg$ aircraft (17.6%), but has a fuel consumption reduction of up to 26.1% compared to the gasoline aircraft configuration. In the LIDAR Data collection mission, the electric configuration could be suitable for collection ranges below $100km$ but suffers low LIDAR collection times. However, at $100km$ LIDAR collection range, the series HEPS has an endurance of $16hr$ and the parallel configuration has an endurance of $19hr$. In the Interceptor mission, at $32kg$ TOW, the parallel HEPS configuration has an endurance/TOW of $1.3[hr/kg]$ compared to $1.15[hr/kg]$ for the gasoline aircraft. This result yields a 13% increase in endurance from

$36.8hr$ for gasoline to $41.6hr$ for the parallel HEPS. Finally, in the Communications Relay mission, the gasoline configuration is recommended for all TOW above $28kg$ as it has the highest loiter endurance.

Although parallel and series hybrid-electric propulsion systems offer benefits over more conventional gasoline and electric configurations, the operating points and objectives of the mission have a large influence on which propulsion type is best suited. Results found in the parameter sweep analysis for each mission type will assist design engineers in making informed decisions in the design of UAV propulsion systems.

The results from this portion of the research required validation against experimental results, and so a test bench was developed. Each of the components were successfully integrated on the test bench, and were mechanically capable of transmitting and sharing power between propulsion systems. The test bench was designed to be modular to enable test operators to quickly assemble the system, and exchange components as necessary. Further, the power electronics and instrumentation was designed for the system to provide safe operation and accurate measurements. The parallel HEPS test bench developed in this research was able to successfully operate in the 4 operating modes: EM Only, ICE Only, Dash mode and Regen Mode. The system is able to run on electric power or ICE power interchangeably without making any modifications to the transmission as the one-way bearing assembly engages for whichever power source is rotating at the highest speed. The most impressive of these sets of tests is the Dash mode testing where the output torque of the propeller is supplied from both the EM and ICE. Working in tandem, it was proved that the EM was drawing $19.9A$ of current which corresponds to an estimated $0.57Nm$ additional torque to the propeller. Finally, the regenerative braking mode was proven to be operational, capable of recharging the battery systems at $13A$. All of these operating modes attest to the flexibility and convenience of having a hybrid-electric propulsion system.

All of the sensors used in the hybrid test bench mount directly to a custom PCB that interfaces with the NI cDAQ-9188. This allows the test operators to interact with and observe the data collected from the sensor arrays of the test bench, including RPM, voltage, current, and throttle positions. This research also included the GUI in LabView which allows test operators to observe the system performance, collect data, and make input requests to various states. The supervisory controller implemented in LabView allows the test operator to send manual commands, or run a script of torque commands for the test bench to execute. In the EM Controller and the ICE Controller the system will automatically configure the throttle settings for the input torque commands, and the Hybrid Controller sets each throttle value to optimize the efficiency of the system for minimal fuel consumption. This Hybrid Controller executes a rule-based control strategy based on the ideal operating line concept. This controller allowed the test operators to observe the system's open-loop response to a step function. The results collected in the experimental testing of the HEPS were compared against the models developed in the MATLAB framework. It was shown that although the models were not perfectly able to predict system performance, they were sufficiently accurate to draw useful conclusions from complex mission profile and parameter sweeps.

6.2 Future Work

The analysis and experiments conducted in this research will enable future research on hybrid-electric propulsion systems for UAVs at UVIC CfAR and other research institutions interested in the topic. The author believes that the aircraft simulation framework can provide insightful analysis of the trade-offs and comparisons between propulsion architectures. The experimental setup of the parallel HEPS test bench opens the door for many future experiments to adapt and improve the design. The test bench could also be easily adapted into other HEPS architectures such as series. The director of UVIC CfAR has expressed interest in pursuing additional research with HEPS for UAVs, and thus recommendations for future work by the author fall into three categories:

- Bench Test Improvements
- Advanced Controller Design
- Aircraft Integration

Bench Test Improvements

In the component level and system level testing of the parallel HEPS test bench, there were several observations made by the author for possible improvements. The first observation is of the friction between components in the hybrid transmission. Since the test bench was required to be modular, there are several bearing blocks that support the drive shafts and are used for alignment. The bearing blocks were selected based on their cost and availability, as well as the flexibility they provide to the system for misalignment compensation. Although these bearing blocks are well suited for a prototype test-bench environment, and provide precision alignment, they add losses to the system in the form of friction. Test operators removed bearing seals to exchange high-life grease with lower resistance oil, but these bearings could be replaced with higher-speed rated bearings that would contain lower friction losses. Further, the off-the-shelf bearing blocks could be replaced with custom bearing blocks that could be machined with high alignment tolerances. The bearing support assemblies that are mounted on the optical table must be spaced in one-inch increments to match the bolt patterns. If a custom bearing block assembly was being machined, the drive shafts and bearings could be compacted into a much smaller transmission, further decreasing misalignment and friction losses.

The addition of an electromagnetic clutch into the parallel HEPS test bench could add additional functionality to the system. The clutch could be used in a few different ways, but the author recommends that it be implemented with the one-way bearing assembly. When the clutch is closed, it would be directly coupled to the ICE and would be capable of starting the engine which is a desirable feature for the system. In addition, the closed clutch and EM could be used to restart the engine in the case of a stall during flight. The clutch could then open and allow the one-way bearing to operate in the same way it does on the present test bench.

In the results of the Dash Mode testing of the parallel HEPS test bench, it was found that the EM was unable to provide additional torque above $5700RPM$ suggesting that the 1:1 timing between the

EM and ICE could be adapted to better suit the operating range of the EM. The ideal performance of the Dash Mode would be to have the EM operate at $3979RPM$ where it was found to be most efficient in the EM Only testing and a different gear ratio could help achieve that. If the HEPS aircraft had sufficient mass budget for a gearing system, implementing a continuously variable transmission (CVT) could be an interesting option to maximize propulsion efficiency.

There were factors that may have contributed to data collection errors on the test bench that could also be improved in future work. The first consideration would be to keep the environmental operating conditions as consistent as possible with a sheltered test bench area. The changing temperature and outside wind speed may influence the performance of the HEPS system, and can introduce error in the measurements of the system sensors. In fact, the sensors selected for measuring the performance of the HEPS were selected due to their low cost and commercial availability. It is recommended that an additional in-line radial torque sensor be implemented onto the test bench as it would provide real torque readings of the output shaft rather than relying on RPM readings to extrapolate values. If possible, a torque sensor in-line radially or implemented as a strain measurement on the mount of the EM or ICE would provide further clarity on the torque distribution between the two propulsion sources.

The most important recommendation by the author to improve the ability to characterize the test bench HEPS performance is with the implementation of an electronic fuel injection system (EFI). Although an EFI system is expensive and more complicated, it is a far more precise means to inject fuel into the engine. An EFI can maintain a very precise range of air-fuel mixture ratio and dynamically adjust to increase fuel efficiency and reliability. Coupled with an in-line flow meter, it would be possible for the parallel HEPS to precisely measure and deliver fuel to the engine to maximize efficiency and consistency between tests.

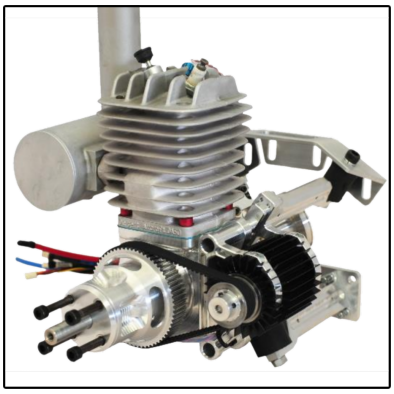

Figure 6.1: Power4Flight B50i fuel injected $50cc$ 2-stroke engine. [77]

Advanced Controller Design

The controller implemented in this research work was able to achieve open loop control of the HEPS for the 3 operating modes of EM Controller, ICE Controller and Hybrid Controller. As seen in the results section of this report, there is room for improvement in several areas of controller design. The first step of increasing the fidelity of the HEPS controller would be to conduct additional tests for each of the

various controller modes. Based on the noisy and sometimes unpredictable behaviour of the ICE, it can become difficult to properly model and control the system. However, if the recommended improvements are made to the HEPS test bench, the system could become more reliable and consistent.

A major objective of the advanced controller design would be to 'close the loop' and implement sensor feedback into the system. A proportional-integral-derivative (PID) closed-loop controller would be able to collect data from various sensors and make adjustments to the system to maintain performance, rather than just recommend optimal power combination like the supervisory controller. As could be seen in the Hybrid Controller results of this research, when an RPM deviation occurs in the system, a PID controller would be able to take corrective action to maintain the desired output power of the system. The test bench environment, and the controller architecture implemented in LabView created in this research provides the perfect environment to design, test and tune the gains of a PID controller.

Recommendations from the literature suggest that there are efficiency gains to be had by implementing controllers that are more advanced than rule-based controllers. More advanced controller types such as a fuzzy-logic controllers and CMAC controllers are substantially more complex than the controller implemented in this research, but show promise for efficiency improvements. [62] Harmon, Frank and Joshi published on the development of their CMAC controller which could use 6.3% less fuel compared to a baseline rule-based controller. [12]

To maximize the capabilities of the controller design, an important step of future work would be to characterize the regenerative braking of the system. The VESC controller has many setup parameters that influence the performance of the ESC in braking mode, and should be explored in more detail to fully understand the limits of regenerative braking on the HEPS. The author recommends careful examination of the regenerative braking performance on the HEPS, and small increments between experimental test points to prevent damage of the power electronics.

Finally, the author recommends more advanced and complex mission profiles be explored on the parallel HEPS test bench. As shown in the results of the aircraft simulation framework section, the parallel HEPS performs differently for a variety of mission profiles. With the LabView and controller of the test bench it would be a straight-forward process to command the test bench to follow these complex mission profiles, and open the door for any additional mission profiles the testing engineers develop. In fact, since the QT1 aircraft has been flown by UVIC CfAR for fully electric flight, an actual flight test mission profile could be simulated on the test bench for a direct case study.

Aircraft integration

The end goal of the hybrid-electric propulsion system research is to integrate into an airframe and perform flight tests. The HEPS system on a UAV would be tested in a real world scenario, and test data could be collected. Future work recommended by the author would include the detailed design and optimization of the HEPS for implementing into an aircraft. There are several major differences between the HEPS designed for the test bench that would not be present in the design for airframe integration.

On the parallel HEPS test bench, the amount of vibration produced by the small two-stroke engine were difficult to deal with, and caused damage to several components throughout the various test cam-

paigns. Although measures were taken to reduce this impact, future work could be dedicated to further reduce the system vibrations by different mounting methods or vibration dampers in the aircraft. Another option to reduce vibration is to explore opposed-cylinder engines, such as the RCV DF70 Twin Cylinder or the Power4Flight B150i UAV EFI shown in Figure 6.2 which use the opposing cylinder strokes to reduce the primary vibration of the system.

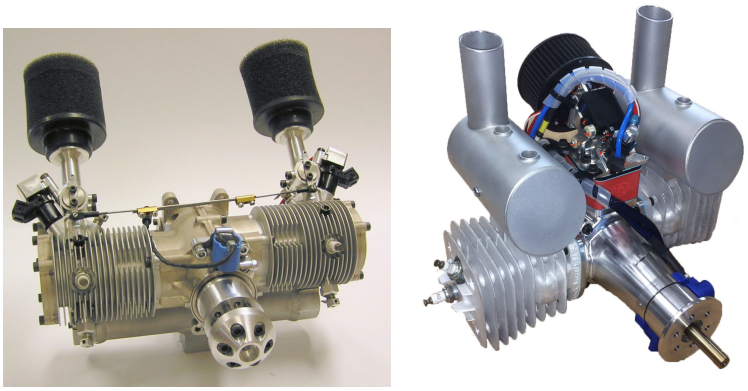

Figure 6.2: Twin-opposed engine configuration options to reduce onboard vibrations. [78] [79]

The next recommendation is to make the HEPS more compact for fitting into the aircraft. As shown earlier in the report, initial concepts were developed by the author for feasibility of fitting into the QT1 aircraft. Removing the extra mounting features and space for quickly accessing components should allow the parallel HEPS to reduce in size, mass and complexity. In the critical design of the HEPS for aircraft integration it is important to analyze the mass of each component of the system, and explore trade studies to optimally size each one. These decisions would need to be done in conjunction with the detailed mission profile analysis with the MATLAB framework. The ability to observe these trends and analyze the tradeoffs between different propulsion systems attests to the power and novelty of this framework.

The successful flight campaign of a HEPS on a small UAV would be the ultimate validation tier for this research project, and could impact the way that future aircraft are designed and built.

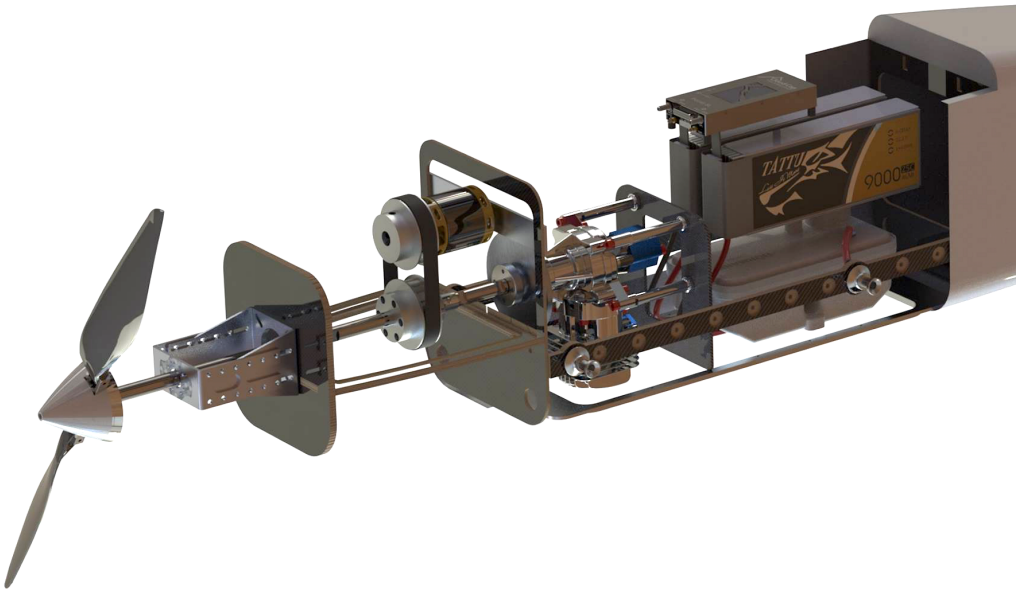

Figure 6.3: Detailed view of parallel HEPS conceptual design into QT1 UAV fuselage.

Bibliography

[1] E. Ewers, L. Fish, M. Horowitz, A. Sander, and P. Scharre. Drone proliferation policy choices for the trump administration, 2017. URL https://css.ethz.ch/en/services/digital-library/publications/publication.html/5d363b74-2de6-415b-b4c2-c40c0754691a.

[2] C. Pornet and A. Isikveren. Conceptual design of hybrid-electric transport aircraft. *Progress in Aerospace Sciences*, 79:114–135, Nov. 2015. ISSN 03760421. doi: 10.1016/j.paerosci.2015.09.002. URL https://linkinghub.elsevier.com/retrieve/pii/S0376042115300130.

[3] D. Lister, J. Penner, and D. Griggs. Summary for policymakers: Aviation and the global atmosphere - A special report of IPCC Working Groups I and III: Published for the Intergovernmental Panel Climate Change. *IPCC Working Groups*. URL https://www.academia.edu/476424/Aviation_and_the_Global_Atmosphere_A_Special_Report_of_IPCC_Working_Groups_I_and_III.

[4] J. Hupe, B. Ferrier, T. Thrasher, C. Mustapha, N. Dickson, T. Tanaka, P. Novelli, and S. Brand. Icao environmental report 2013: Destination green-aviation and climate change. Technical report, ICAO Environmental Branch, Montreal, Canada, 2013.

[5] M. N. Georgiou. Labour Cost and World Market Share: An Empirical Analysis with Panel Data (1999–2008). *SSRN Electronic Journal*, 2010. ISSN 1556-5068. doi: 10.2139/ssrn.1695441. URL http://www.ssrn.com/abstract=1695441.

[6] Flightradar24. Live Flight Tracker - Real-Time Flight Tracker Map. URL https://www.flightradar24.com/%22%3EFlightradar24.com.

[7] Europäische Kommission, editor. *Flightpath 2050: Europe's vision for aviation ; maintaining global leadership and serving society's needs ; report of the High-Level Group on Aviation Research*. Policy / European Commission. Publ. Off. of the Europ. Union, Luxembourg, 2011. ISBN 9789279197246. OCLC: 930887434.

[8] T. Rotramel. Optimization of hybrid-electric propulsion systems for small remotely-piloted aircraft. Master's thesis, Air Force Institute of Technology, Mar. 2011.

[9] Chan-Chiao Lin, Huei Peng, J. Grizzle, and Jun-Mo Kang. Power management strategy for a parallel hybrid electric truck. *IEEE Transactions on Control Systems Technology*, 11(6):839–849, Nov. 2003. ISSN 1063-6536. doi: 10.1109/TCST.2003.815606. URL http://ieeexplore.ieee.org/document/1255660/.

[10] C. R. Akli, X. Roboam, B. Sareni, and A. Jeunesse. Energy management and sizing of a hybrid locomotive. In *2007 European Conference on Power Electronics and Applications*, pages 1–10, Sept. 2007. doi: 10.1109/EPE.2007.4417333.

[11] B. Manouchehrinia. *Modeling, Optimization and Environmental Assessment of Electrified Marine Vessels*. PhD Thesis, University of Victoria, 2018.

[12] F. Harmon, A. Frank, and S. Joshi. Application of a CMAC neural network to the control of a parallel hybrid-electric propulsion system for a small unmanned aerial vehicle. In *Proceedings. 2005 IEEE International Joint Conference on Neural Networks, 2005.*, volume 2, pages 355–360, Montreal, Que., Canada, 2005. IEEE. ISBN 9780780390485. doi: 10.1109/IJCNN.2005.1555856. URL http://ieeexplore.ieee.org/document/1555856/.

[13] J. Hung and L. Gonzalez. On parallel hybrid-electric propulsion system for unmanned aerial vehicles. *Progress in Aerospace Sciences*, 51:1–17, May 2012. ISSN 03760421. doi: 10.1016/j.paerosci.2011.12.001. URL https://linkinghub.elsevier.com/retrieve/pii/S0376042112000097.

[14] C. J. Brace, M. Deacon, N. D. Vaughan, R. W. Horrocks, and C. R. Burrows. An operating point optimizer for the design and calibration of an integrated diesel/continuously variable transmission powertrain. *Proceedings of the Institution of Mechanical Engineers, Part D: Journal of Automobile Engineering*, 213(3):215–226, Mar. 1999. ISSN 0954-4070, 2041-2991. doi: 10.1243/0954407991526810. URL http://journals.sagepub.com/doi/10.1243/0954407991526810.

[15] M. Harmats and D. Weihs. Hybrid-Propulsion High-Altitude Long-Endurance Remotely Piloted Vehicle. *Journal of Aircraft*, 36(2):321–331, Mar. 1999. ISSN 0021-8669, 1533-3868. doi: 10.2514/2.2443. URL https://arc.aiaa.org/doi/10.2514/2.2443.

[16] J. Ausserer and F. Harmon. Integration, Validation, and Testing of a Hybrid-Electric Propulsion System for a Small Remotely Piloted Aircraft. In *10th International Energy Conversion Engineering Conference*, Atlanta, Georgia, July 2012. American Institute of Aeronautics and Astronautics. ISBN 9781624101908. doi: 10.2514/6.2012-4239. URL http://arc.aiaa.org/doi/10.2514/6.2012-4239.

[17] R. Glassock, J. Y. Hung, L. F. Gonzalez, and R. A. Walker. Design, modelling and measurement of a hybrid powerplant for unmanned aerial systems. *Australian Journal of Mechanical Engineering*, 6 (2):69–78, Jan. 2008. ISSN 1448-4846, 2204-2253. doi: 10.1080/14484846.2008.11464559. URL https://www.tandfonline.com/doi/full/10.1080/14484846.2008.11464559.

[18] J. Koster, C. Humbargar, E. Serani, A. Velazco, D. Hillery, and L. Makepeace. Hybrid Electric Integrated Optimized System (HELIOS) - Design of a Hybrid Propulsion System for Aircraft. In *49th AIAA Aerospace Sciences Meeting including the New Horizons Forum and Aerospace Exposition*, Orlando, Florida, Jan. 2011. American Institute of Aeronautics and Astronautics.

ISBN 9781600869501. doi: 10.2514/6.2011-1011. URL http://arc.aiaa.org/doi/10.2514/6.2011-1011.

[19] Launchpoint Technologies. Hybrid UAV systems, 2017. URL http://www.launchpnt.com/portfolio/aerospace/propulsion-by-wire-technology.

[20] A. Isikveren and A. Yezeguelian. Methods to Improve UAV Performance Using Hybrid-Electric Architectures. In *Research Symposium RSY-323: Hybrid/Electric Aero Propulsion Systems for Military Applications*, Trondheim, Norway, Oct. 2019. SAFRAN.

[21] M. Avera and R. Singh. Scalability of Hybrid-Electric Propulsion for VTOL UAS. In *Research Symposium RSY-323: Hybrid/Electric Aero Propulsion Systems for Military Applications*, Trondheim, Norway, Oct. 2019. U.S. Army Combat Capabilities Development Command, Army Research Lab.

[22] B. Picard, M. Picard, J. Plante, and D. Rancourt. Enabling Sub-Megawatt Hybrid-Electric Propulsion through High Efficiency Recuperated Inside-out Ceramic Turbogenerator. In *Research Symposium RSY-323: Hybrid/Electric Aero Propulsion Systems for Military Applications*, Trondheim, Norway, Oct. 2019. Exonetik Turbo Inc., Université de Sherbrooke.

[23] F. G. Harmon, A. A. Frank, and J.-J. Chattot. Conceptual Design and Simulation of a Small Hybrid-Electric Unmanned Aerial Vehicle. *Journal of Aircraft*, 43(5):1490–1498, Sept. 2006. ISSN 0021-8669, 1533-3868. doi: 10.2514/1.15816. URL https://arc.aiaa.org/doi/10.2514/1.15816.

[24] Rolls Royce. The E-Fan X Programme, . URL https://www.rolls-royce.com/media/our-stories/insights/2018/paul-stein-talks-about-e-fan-x.aspx,2019.

[25] Boeing. Boeing: How sweet the future of aviation. URL http://www.boeing.com/features/innovation-quarterly/aug2017/feature-technical-sugar.page.

[26] Airbus. Airbus and SAS Scandinavian Airlines sign hybrid and electric aircraft research agreement, . URL https://www.airbus.com/newsroom/press-releases/en/2019/05/airbus-and-sas-scandinavian-airlines-sign-hybrid-and-electric-aircraft-research-agreement.html.

[27] Bauhaus Luftfahrt e.V. - Project Centreline Objectives. URL https://www.centreline.eu/project/objectives/.

[28] A. Lentsch. Diamond aircraft 1st flight multiengine hybrid electric aircraft, 2018. URL http://www.diamond-air.at/en/media-center/press-releases/news/article/diamond-aircraft-1st-flight-multi-engine-hybrid-electric-aircraft/.

[29] F. Gern, A. Ko, B. Grossman, R. Haftka, R. Kapania, W. Mason, and J. Schetz. Transport Weight Reduction Through MDO: The Strut-Braced Wing Transonic Transport. In *35th AIAA Fluid Dynamics Conference and Exhibit*, Toronto, Ontario, Canada, June 2005. American Institute of Aeronautics and Astronautics. ISBN 9781624100598. doi: 10.2514/6.2005-4667. URL http://arc.aiaa.org/doi/10.2514/6.2005-4667.

[30] J. Zamboni. A method for the conceptual design of hybrid electric aircraft. 2018. URL https://repository.tudelft.nl/islandora/object/uuid%3A7b7dc56b-6647-4cc9-98f6-2ed5d488c759.

[31] R. Jansen, C. Bowman, S. Clarke, D. Avanesian, P. Dempsey, and R. Dyson. Nasa Electrified Aircraft Propulsion Efforts. In *Research Symposium RSY-323: Hybrid/Electric Aero Propulsion Systems for Military Applications*, Trondheim, Norway, Oct. 2019. NASA Glenn Research Center.

[32] W. Johnson, C. Silva, and E. Solis. Concept Vehicles for Air Taxi Operations. In *AHS Aeromechanics Design for Transformative Vertical Lift*, San Francisco, California, Jan. 2018.

[33] J. Kaiser and H. Kuhn. Electric Flight Map. In *Research Symposium RSY-323: Hybrid/Electric Aero Propulsion Systems for Military Applications*, Trondheim, Norway, Oct. 2019. Bauhaus Luftfahrt e.V.

[34] Pipistrel eVTOL Concept - eVTOL Aircraft Overview by TransportUP, . URL https://transportup.com/pipistrel-evtol-concept/.

[35] Volocopter - VoloCity, . URL https://www.volocopter.com/en/product/.

[36] Airbus. City Airbus, . URL https://www.airbus.com/innovation/urban-air-mobility/vehicle-demonstrators/cityairbus.html.

[37] R. D. Falck, J. Chin, S. L. Schnulo, J. M. Burt, and J. S. Gray. Trajectory Optimization of Electric Aircraft Subject to Subsystem Thermal Constraints. In *18th AIAA/ISSMO Multidisciplinary Analysis and Optimization Conference*, Denver, Colorado, June 2017. American Institute of Aeronautics and Astronautics. ISBN 9781624105074. doi: 10.2514/6.2017-4002. URL https://arc.aiaa.org/doi/10.2514/6.2017-4002.

[38] F. M. Capristan and J. R. Welstead. An Energy-Based Low-Order Approach for Mission Analysis of Air Vehicles in LEAPS. In *2018 AIAA Aerospace Sciences Meeting*, Kissimmee, Florida, Jan. 2018. American Institute of Aeronautics and Astronautics. ISBN 9781624105241. doi: 10.2514/6.2018-1755. URL https://arc.aiaa.org/doi/10.2514/6.2018-1755.

[39] J. C. Gladin, D. Trawick, C. Perullo, J. C. Tai, and D. N. Mavris. Modeling and Design of a Partially Electric Distributed Aircraft Propulsion System with GT-HEAT. In *55th AIAA Aerospace Sciences Meeting*, Grapevine, Texas, Jan. 2017. American Institute of Aeronautics and Astronautics. ISBN 9781624104473. doi: 10.2514/6.2017-1924. URL http://arc.aiaa.org/doi/10.2514/6.2017-1924.

[40] M. Green, B. Schiltgen, and A. Gibson. Analysis of a Distributed Hybrid Propulsion System with Conventional Electric Machines. In *48th AIAA/ASME/SAE/ASEE Joint Propulsion Conference & Exhibit*, Atlanta, Georgia, July 2012. American Institute of Aeronautics and Astronautics. ISBN 9781600869358. doi: 10.2514/6.2012-3768. URL http://arc.aiaa.org/doi/abs/10.2514/6.2012-3768.

[41] C. Pornet, C. Gologan, P. C. Vratny, A. Seitz, O. Schmitz, A. T. Isikveren, and M. Hornung. Methodology for Sizing and Performance Assessment of Hybrid Energy Aircraft. *Journal of Aircraft*, 52(1):341–352, Jan. 2015. ISSN 0021-8669, 1533-3868. doi: 10.2514/1.C032716. URL http://arc.aiaa.org/doi/10.2514/1.C032716.

[42] G. E. Wroblewski and P. J. Ansell. Mission Analysis and Emissions for Conventional and Hybrid-Electric Commercial Transport Aircraft. In *2018 AIAA Aerospace Sciences Meeting*, Kissimmee, Florida, Jan. 2018. American Institute of Aeronautics and Astronautics. ISBN 9781624105241. doi: 10.2514/6.2018-2028. URL https://arc.aiaa.org/doi/10.2514/6.2018-2028.

[43] A. Frediani, B. Mohammadi, O. Pironneau, and V. Cipolla, editors. *Variational Analysis and Aerospace Engineering: Mathematical Challenges for the Aerospace of the Future*, volume 116 of *Springer Optimization and Its Applications*. Springer International Publishing, Cham, 2016. ISBN 9783319456799 9783319456805. doi: 10.1007/978-3-319-45680-5. URL http://link.springer.com/10.1007/978-3-319-45680-5.

[44] J. M. Vegh, E. Botero, M. Clarke, J. Smart, and J. Alonso. Current Capabilities and Challenges of NDARC and SUAVE for eVTOL Aircraft Design and Analysis. In *AIAA Propulsion and Energy 2019 Forum*, Indianapolis, IN, Aug. 2019. American Institute of Aeronautics and Astronautics. ISBN 9781624105906. doi: 10.2514/6.2019-4505. URL https://arc.aiaa.org/doi/10.2514/6.2019-4505.

[45] A. Joksimović, X. Carbonneau, C. Crabé, and E. Benichou. Generalised Methodology for Sizing of Air Vehicles with Hybrid-Electric Propulsion. In *Research Symposium RSY-323: Hybrid/Electric Aero Propulsion Systems for Military Applications*, Trondheim, Norway, Oct. 2019. Institut Supérieur de l'Aéronautique et de l'Espace (ISAE-SUPAERO), Université de Toulouse.

[46] L. Costello. State of the Art of Piloted Electric Airplanes, NASA's Centennial Challenge Data and Fundamental Design Implications. *Dissertations and Theses*, Oct. 2011. URL https://commons.erau.edu/edt/37.

[47] W. Johnson, C. Silva, and E. Solis. Concept Vehicles for VTOL Air Taxi Operations. In *AHS Technical Conference on Aeromechanics Design for Transformative Vertical Flight*, San Francisco, California, Jan. 2018. NASA Ames Research Center.

[48] I. Diaz-Guardamino, S. Salas, and M. Nusseler. Challenges Associated to High Power Hybrid Electric Propulsion in Aerospace. In *Research Symposium RSY-323: Hybrid/Electric Aero Propulsion Systems for Military Applications*, Trondheim, Norway, Oct. 2019. Airbus Corporate Technology Office.

[49] T. Noll, J. Brown, M. Perez-Davis, S. Ishmael, G. Tiffany, and M. Gaier. Investigation of the Helios Prototype Aircraft Mishap. Mishap Report Volume I, NASA, NASA Glenn, NASA Langley, NOAA, NASA Dryden, NASA Ames, Jan. 2004. URL https://www.nasa.gov/sites/default/files/64317main_helios.pdf.

[50] J. Thauvin, G. Barraud, X. Roboam, B. Sareni, M. Budinger, and D. Leray. Hybrid propulsion for regional aircraft: A comparative analysis based on energy efficiency. In *2016 International Conference on Electrical Systems for Aircraft, Railway, Ship Propulsion and Road Vehicles & International Transportation Electrification Conference (ESARS-ITEC)*, pages 1–6, Toulouse, France, Nov. 2016. IEEE. ISBN 9781509008148. doi: 10.1109/ESARS-ITEC.2016.7841392. URL http://ieeexplore.ieee.org/document/7841392/.

[51] J. Sliwinski, A. Gardi, M. Marino, and R. Sabatini. Hybrid-electric propulsion integration in unmanned aircraft. *Energy*, 140:1407–1416, Dec. 2017. ISSN 03605442. doi: 10.1016/j.energy.2017.05.183. URL https://linkinghub.elsevier.com/retrieve/pii/S0360544217309799.

[52] S. Kumar, S. D. Heister, X. Xu, J. R. Salvador, and G. P. Meisner. Thermoelectric Generators for Automotive Waste Heat Recovery Systems Part I: Numerical Modeling and Baseline Model Analysis. *Journal of Electronic Materials*, 42(4):665–674, Apr. 2013. ISSN 0361-5235, 1543-186X. doi: 10.1007/s11664-013-2471-9. URL http://link.springer.com/10.1007/s11664-013-2471-9.

[53] J. Fleming, W. Ng, and S. Ghamaty. Thermoelectric-Based Power System for Unmanned-Air-Vehicle/ Microair-Vehicle Applications. *Journal of Aircraft*, 41(3):674–676, May 2004. ISSN 0021-8669, 1533-3868. doi: 10.2514/1.11486. URL https://arc.aiaa.org/doi/10.2514/1.11486.

[54] J. Langley, M. Taylor, G. Wagner, and S. Morris. Thermoelectric Energy Harvesting from Small Aircraft Engines. pages 2009–01–3093, Nov. 2009. doi: 10.4271/2009-01-3093. URL https://www.sae.org/content/2009-01-3093/.

[55] J. Schömann. *Hybrid-electric propulsion systems for small unmanned aircraft*. Luftfahrt. Dr. Hut, München, 1. aufl edition, 2014. ISBN 9783843918473. OCLC: 898076514.

[56] I. H. Mengistu. Small internal combustion engine testing for a hybrid-electric remotely-piloted aircraft. 2012.

[57] D. Khiar, J. Lauber, T. Floquet, and T. Guerra. An observer design for the instantaneous torque estimation of an IC engine. In *2005 IEEE Vehicle Power and Propulsion Conference*, pages 391–395, Chicago, IL, USA, 2005. IEEE. ISBN 9780780392809. doi: 10.1109/VPPC.2005.1554587. URL http://ieeexplore.ieee.org/document/1554587/.

[58] C. Wilson. *Performance of a small internal combustion engine using n-heptane and iso-octane*. Master of Science Degree, Air Force Institute of Technology, 2010.

[59] Dejan. How Brushless Motor and ESC Work, Feb. 2019. URL https://howtomechatronics.com/how-it-works/how-brushless-motor-and-esc-work/.

[60] Renold. Renold Sprag Clutch. URL https://www.youtube.com/watch?v=Fsp3fm4KHs0.

[61] N. Jalil, N. Kheir, and M. Salman. A rule-based energy management strategy for a series hybrid vehicle. In *Proceedings of the 1997 American Control Conference (Cat. No.97CH36041)*, pages

689–693 vol.1, Albuquerque, NM, USA, 1997. IEEE. ISBN 9780780338326. doi: 10.1109/ACC.1997.611889. URL http://ieeexplore.ieee.org/document/611889/.

[62] Y. Xie, A. Savvaris, and A. Tsourdos. Fuzzy logic based equivalent consumption optimization of a hybrid electric propulsion system for unmanned aerial vehicles. *Aerospace Science and Technology*, 85:13–23, Feb. 2019. ISSN 12709638. doi: 10.1016/j.ast.2018.12.001. URL https://linkinghub.elsevier.com/retrieve/pii/S1270963818326397.

[63] L. Machado. *Design and Development of a Hybrid Electric Propulsion System for Unmanned Aerial Vehicles*. Master of Science Degree in Aerospace Engineering, Instituto Superior Técnico, Lisbon, Portugal, May 2019.

[64] O. Tremblay and L.-A. Dessaint. Experimental Validation of a Battery Dynamic Model for EV Applications. *World Electric Vehicle Journal*, 3(2):289–298, June 2009. ISSN 2032-6653. doi: 10.3390/wevj3020289. URL http://www.mdpi.com/2032-6653/3/2/289.

[65] S. Warwick, J. Matlock, and J. Richards. UAV Propulsion Preliminary Design and Optimisation Framework Documentation. Technical report, University of Victoria Center for Aerospace Research, BC, Sept. 2017.

[66] C. Perullo and D. Mavris. A review of hybrid-electric energy management and its inclusion in vehicle sizing. *Aircraft Engineering and Aerospace Technology*, 86(6):550–557, Sept. 2014. ISSN 0002-2667. doi: 10.1108/AEAT-04-2014-0041. URL https://www.emerald.com/insight/content/doi/10.1108/AEAT-04-2014-0041/full/html.

[67] S. Bagassi, G. Bertini, D. Francia, and F. Persiani. Design analysis for hybrid propulsion. *28th Congress of the International Council of the Aeronautical Sciences 2012, ICAS 2012*, 4:2804–2810, 01 2012.

[68] T. C. Corke. *Design of aircraft*. Prentice Hall, Upper Saddle River, N.J, 2003. ISBN 9780130892348.

[69] T. Choi, D. Soban, and D. Mavris. Creation of a Design Framework for All-Electric Aircraft Propulsion Architectures. In *3rd International Energy Conversion Engineering Conference*, San Francisco, California, Aug. 2005. American Institute of Aeronautics and Astronautics. ISBN 9781624100628. doi: 10.2514/6.2005-5549. URL http://arc.aiaa.org/doi/10.2514/6.2005-5549.

[70] K. Reynolds. Trajectory Optimization of a Battery-Powered Competition Aircraft. In *51st AIAA Aerospace Sciences Meeting including the New Horizons Forum and Aerospace Exposition*, Grapevine (Dallas/Ft. Worth Region), Texas, Jan. 2013. American Institute of Aeronautics and Astronautics. ISBN 9781624101816. doi: 10.2514/6.2013-1155. URL http://arc.aiaa.org/doi/10.2514/6.2013-1155.

[71] B. Lee, P. Park, C. Kim, S. Yang, and S. Ahn. Power managements of a hybrid electric propulsion system for UAVs. *Journal of Mechanical Science and Technology*, 26(8):2291–2299, Aug. 2012.

ISSN 1738-494X, 1976-3824. doi: 10.1007/s12206-012-0601-6. URL http://link.springer.com/10.1007/s12206-012-0601-6.

[72] R. Glassock, J. Y. Hung, L. F. González, and R. A. Walker. Multimodal hybrid powerplant for unmanned aerial systems(uas) robotics. 2008.

[73] Enertion. Focbox Motor Controller. URL https://www.enertionboards.com/FOCBOX-foc-motor-speed-controller.html.

[74] C. M. Greiser. Implementation of a rule-based open-loop control strategy for a hybrid-electric propulsions system on a small rpa. 2011.

[75] G. Thomas. Overview of Storage Development DOE Hydrogen Program. In *Hydrogen Program Review*, San Ramon, California, May 2000. Sandia National Laboratories, Livermore California.

[76] D. Pfurtscheller. *Development of a hybrid-electric propulsive system model for Unmanned Aerial Systems*. Master of Science Degree in Aerospace Engineering, Instituto Superior Técnico, Lisbon, Portugal, Oct. 2019.

[77] B50i Fuel Injected UAV Engine, . URL https://power4flight.com/uav-engine-products/uav-engine-systems/b50i-uav-efi-engine-system/.

[78] UAV Engines - Heavy Fuel 4-Stroke Drone Engines for UAS | RCV Engines. URL https://www.unmannedsystemstechnology.com/company/rcv-engines/.

[79] B150i UAV EFI Engine System, . URL https://power4flight.com/uav-engine-products/uav-engine-systems/b150i-uav-efi-engine-system/.

[80] R. Glassock. Design, Modelling and Measurement of Hybrid Powerplant for Unmanned Aerial Vehicles (UAVs). Master's thesis, Queensland University of Technology, Brisbane, Australia, Nov. 2012. URL https://eprints.qut.edu.au/61052/1/Richard_Glassock_Thesis.pdf.

[81] C. Pettit. Experimental Performance Characteristics of a Hybrid Aircraft Propulsion System. ENGR 446 - Final Report, University of Victoria, Sidney, BC, Nov. 2018.

Appendices

Appendix A

Bench Test Component Analysis

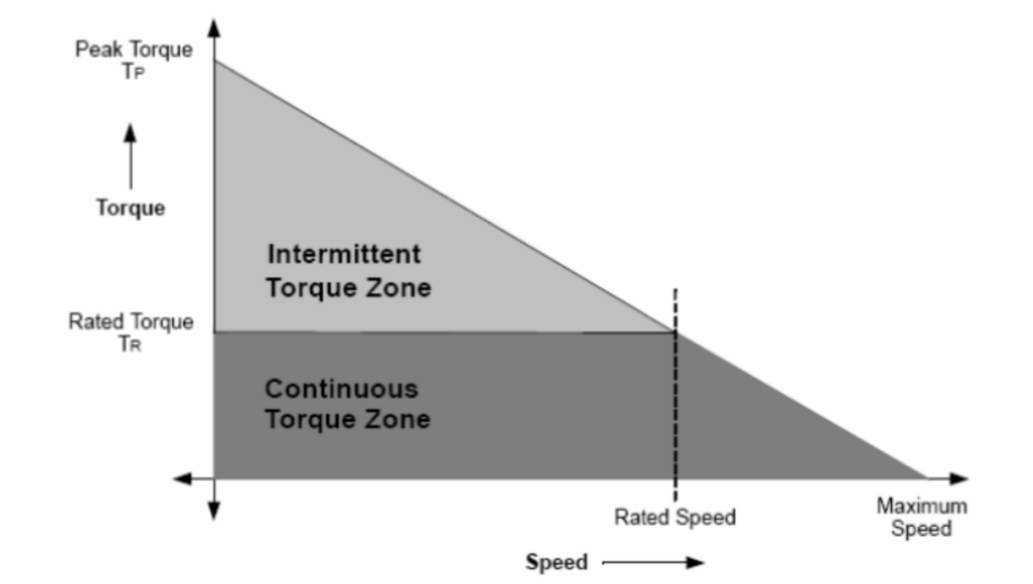

Figure A.1: Torque characteristics for direct-current electric motors. [80]

	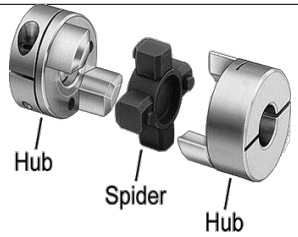	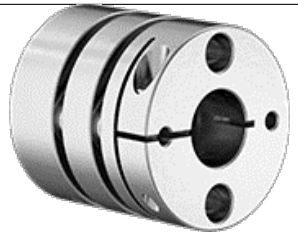	
Name	Clamping Hub and Durometer 98A Spider	Servomotor Precision Flex 1/2”	Servomotor Precision Flex1/2”-3/4”
McMasterCarr Part No.	9845T14, 9845T2	2764K511	2764K628
Cost (USD)	$58.17	$110.75	$163.21
Material	2024 Aluminum, Polyurethane Durometer 98A	2017 Aluminum, 304 Stainless Steel	2017 Aluminum, 304 Stainless Steel
Construction	Multipiece - Hub and Spider	One Piece	One Piece
OD	1”	1 47/64”	2 7/32”
Overall Length	1 13/32”	1 57/64”	2 23/64”
Maximum Speed $[RPM]$	8000	10000	10000
Maximum Torque $[Nm]$	16.94	10	25
Misalignment Capability			
Parallel	0.003”	0.009”	0.011”
Angular	$0.8°$	$1°$	$1°$
Axial	-	0.024”	0.031”
For Motion Type	Parallel, Angular, Axial	Parallel, Angular, Axial	Parallel, Angular, Axial
Test Bench Status	Failed	Failed	Passed

Table A.1: Specifications of Flexible Shaft Couplers used in parallel HEPS test bench.

Figure A.2: Two types of mechanical couplers used in the HEPS that clamp between shafts. Rubber 'spider' coupler failed, as well as a flexible coupler with metal-leaf springs. Prevailing solution was flexible metal-leaf spring coupler with larger torque rating, as well as increased mounting stiffness to ICE.

Attempt	Design	Result
1	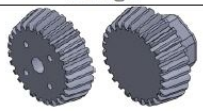 1:1 PLA gear train	Bevel gears transmit power from original 12V starter. Easy gear train to model and print, but 12V starter could not overcome system friction to turn over ICE. Suggest changing gear ratio to improve torque.
2	 2:1 PLA gear train	Smaller ratio to reduce starter torque; engine turned over but many gear teeth shattered due to size reduction. Suggest stronger print material or tooth size increase.
3	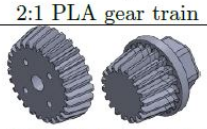 1.3:1 PLA gear train	Smaller ratio to reduce starter torque; designed and prototyped but not tested due to result of Attempt 2.
4	 2.6:1 PLA gear train	Smaller ratio to reduce starter torque; designed and prototyped but not tested due to result of Attempt 2.
5	 Stacked spur bevel alu. gear train	Replaced bevel gear design with stacked aluminum spur gears of receding pitch circle. Requires water jet cutting and metal gear seat for and shaft mounting. Difficult to fabricate and found not feasible due to space limitations. Suggest different fabrication technique.
6	 2:1 Carbon gear train	Returned to Attempt 2 design and researched options to print in hi-strength carbon fibre. Options were costly and complex; not worth pursuing. Suggest new starter design approach.
7	 [11] Ripcord starter	Inline ripcord starter provides startup torque for ICE. Recoil starters can be commercially bought but typically are not installed inline. This method is currently being investigated.

Figure A.3: Summary parallel HEPS starting mechanism attempts. [81]

Appendix B

Propeller Test Data

Trendlines for data collected on propeller test data for Thrust $T_{prop}[N]$ and Torque $\tau_{prop}[Nm]$.

18x10" $T_{prop} = \left(1.68 \cdot 10^{-6}\right) x^2 + \left(7.65 \cdot 10^{-5}\right) x - \left(5.31 \cdot 10^{-1}\right) \qquad R^2 = 0.9904$ (B.1)

18x10" $\tau_{prop} = \left(4.47 \cdot 10^{-8}\right) x^2 + \left(1.97 \cdot 10^{-6}\right) x + \left(1.38 \cdot 10^{-4}\right) \qquad R^2 = 1$ (B.2)

19x10" $T_{prop} = \left(2.13 \cdot 10^{-6}\right) x^2 - \left(1.02 \cdot 10^{-3}\right) x - \left(1.02 \cdot 10^{-3}\right) \qquad R^2 = 0.9989$ (B.3)

19x10" $\tau_{prop} = \left(5.32 \cdot 10^{-8}\right) x^2 - \left(4.86 \cdot 10^{-6}\right) x + \left(5.90 \cdot 10^{-3}\right) \qquad R^2 = 0.1$ (B.4)

22x10" $T_{prop} = \left(3.33 \cdot 10^{-6}\right) x^2 - \left(6.69 \cdot 10^{-4}\right) x - \left(6.74 \cdot 10^{-2}\right) \qquad R^2 = 0.9999$ (B.5)

22x10" $\tau_{prop} = \left(9.69 \cdot 10^{-8}\right) x^2 - \left(7.15 \cdot 10^{-6}\right) x + \left(6.03 \cdot 10^{-3}\right) \qquad R^2 = 1$ (B.6)

Throttle	Current $[A]$	Voltage $[V]$	τ_{prop}	Thrust $[N]$	RPM	$P_{in}[W]$	$P_{out}[W]$	$\eta[\%]$
0	0.04	25.16	0.000	0.00	0.0	0.9	0.0	0.0%
10	0.30	25.15	0.030	0.76	787.8	7.5	2.5	33.4%
15	0.56	25.14	0.058	1.53	1111.5	14.0	6.7	47.9%
20	0.91	25.12	0.090	2.52	1395.2	23.0	13.1	57.2%
25	1.45	25.10	0.132	3.93	1697.8	36.3	23.4	64.5%
30	2.20	25.06	0.184	5.80	2009.1	55.1	38.7	70.2%
35	3.20	25.02	0.245	7.96	2321.6	80.1	59.6	74.4%
40	4.47	24.96	0.314	10.51	2626.2	111.6	86.4	77.4%
45	6.02	24.88	0.389	13.83	2923.0	149.8	119.1	79.5%
50	7.84	24.79	0.468	16.33	3208.5	194.3	157.2	80.9%
55	9.96	24.69	0.551	26.81	3484.4	245.9	200.9	81.7%
60	12.27	24.57	0.633	22.82	3745.5	301.3	248.4	82.4%
65	14.96	24.42	0.723	25.85	3998.3	365.5	302.8	82.9%
70	17.88	24.26	0.811	29.03	4238.5	433.6	360.0	83.0%
75	21.26	24.06	0.906	32.72	4475.2	511.5	424.4	83.0%
80	24.87	23.84	0.997	36.39	4698.6	592.9	490.3	82.7%
85	28.83	23.60	1.087	40.03	4910.8	680.3	559.2	82.2%
90	32.87	23.33	1.173	43.50	5099.6	766.7	626.5	81.7%
95	36.86	23.02	1.249	46.59	5263.7	848.6	688.6	81.1%
100	39.30	22.74	1.293	48.52	5353.0	893.7	724.9	81.1%

Table B.1: 18x10” Propeller test results with AXI 4130/20.

Throttle	Current $[A]$	Voltage $[V]$	τ_{prop}	Thrust $[N]$	RPM	$P_{in}[W]$	$P_{out}[W]$	$\eta[\%]$
0	0.03	25.16	0.000	0	0	0.7	0.0	0.0%
10	0.29	25.15	0.033	0.66	753.67	7.4	2.6	35.1%
15	0.56	25.14	0.063	1.32	1062.2	14.2	7.0	49.3%
20	0.96	25.12	0.101	2.30	1352.4	24.2	14.3	59.0%
25	1.57	25.09	0.150	3.76	1666.9	39.5	26.2	66.3%
30	2.41	25.06	0.208	5.71	1981.8	60.3	43.2	71.7%
35	3.52	25.01	0.276	8.10	2295.3	88.0	66.4	75.5%
40	4.90	24.94	0.351	11.11	2595.5	122.3	95.5	78.0%
45	6.60	24.87	0.433	14.06	2884.8	164.0	130.9	79.8%
50	8.62	24.77	0.522	19.91	3163	213.4	172.7	80.9%
60	13.57	24.55	0.707	25.23	3686.7	333.1	273.0	81.9%
65	16.52	24.38	0.804	28.18	3925.5	402.6	330.7	82.1%
70	19.71	24.18	0.900	31.54	4151.9	476.7	391.5	82.1%
75	23.14	23.97	0.995	35.07	4361.4	554.7	454.4	81.9%
80	27.30	23.72	1.100	39.11	4581.7	647.5	527.6	81.5%
85	31.54	23.43	1.195	42.85	4773.5	739.1	597.4	80.8%
90	35.85	23.12	1.283	46.31	4943.1	828.8	664.1	80.1%
95	40.17	22.80	1.364	49.55	5090.1	915.8	727.0	79.4%
100	42.74	22.50	1.408	51.41	5169.5	961.7	761.9	79.2%

Table B.2: 19x10” Propeller results with AXI 4130/20

Throttle	Current $[A]$	Voltage $[V]$	τ_{prop}	Thrust $[N]$	RPM	$P_{in}[W]$	$P_{out}[W]$	$\eta[\%]$
0	0.02	25.02	0.001	0.00	0.0	0.6	0.0	0.0
10	0.51	25.00	0.068	1.60	764.7	12.6	5.5	43.2
15	0.98	24.98	0.121	3.24	1139.2	24.5	14.5	59.1
20	1.75	24.95	0.193	5.64	1433.3	43.5	29.0	66.7
25	2.83	24.91	0.280	8.54	1719.2	70.5	50.4	71.5
30	4.29	24.85	0.379	11.80	1993.7	106.6	79.1	74.2
35	6.06	24.77	0.483	15.27	2254.2	150.2	114.0	75.9
40	8.18	24.68	0.592	19.00	2501.5	202.0	155.1	76.8
45	10.76	24.57	0.710	23.10	2728.3	264.3	202.9	76.8
55	16.96	24.33	0.954	31.27	3165.6	412.7	316.2	76.6
60	20.58	24.16	1.078	35.39	3372.6	497.2	380.9	76.6
65	24.65	23.98	1.208	39.82	3556.9	591.0	449.8	76.1
70	28.86	23.78	1.334	44.03	3739.1	686.2	522.3	76.1
75	33.37	23.56	1.455	48.05	3899.8	786.2	594.2	75.6
80	38.43	23.33	1.575	51.93	4056.6	896.7	669.2	74.6
85	43.71	23.09	1.687	55.64	4200.5	1009.5	741.9	73.5
90	49.58	22.84	1.798	59.42	4336.1	1132.3	816.3	72.1

Table B.3: 22x10” Propeller results with AXI 4130/20

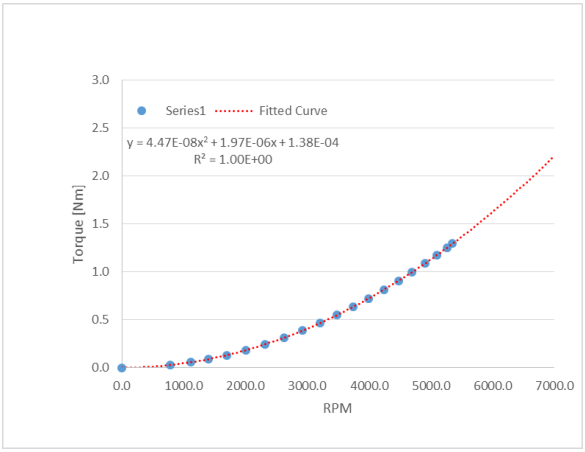

(a) 18x10” Propeller Torque vs RPM curve.

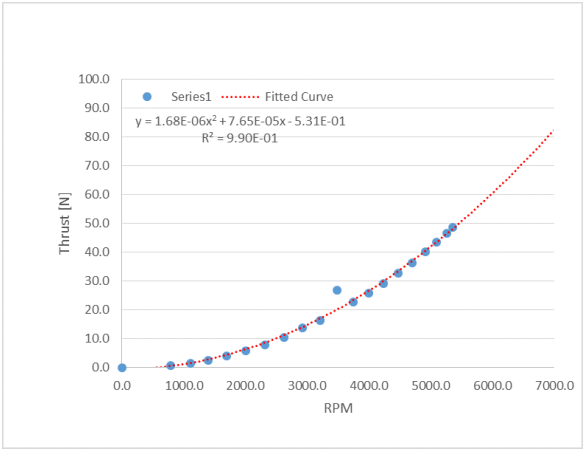

(b) 18x10” Propeller Thrust vs RPM curve.

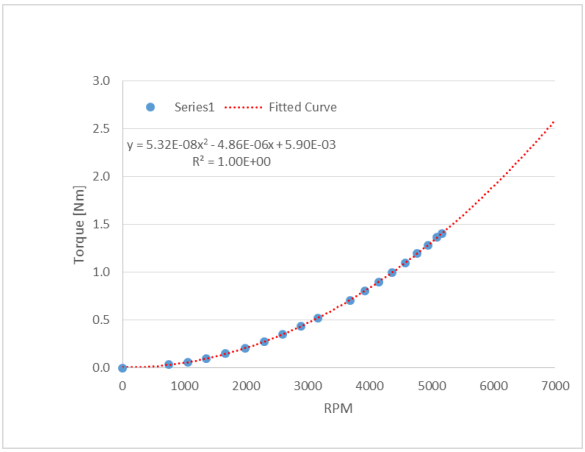

(c) 19x10” Propeller Torque vs RPM curve.

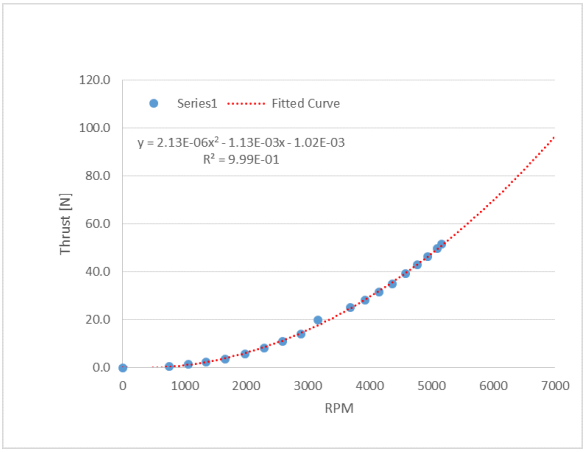

(d) 19x10” Propeller Thrust vs RPM curve.

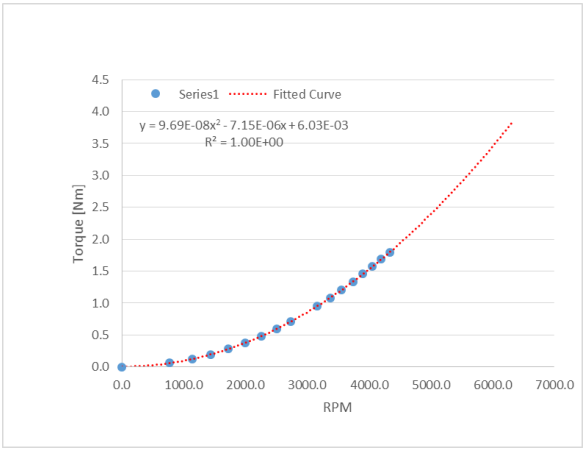

(e) 22x10” Propeller Torque vs RPM curve.

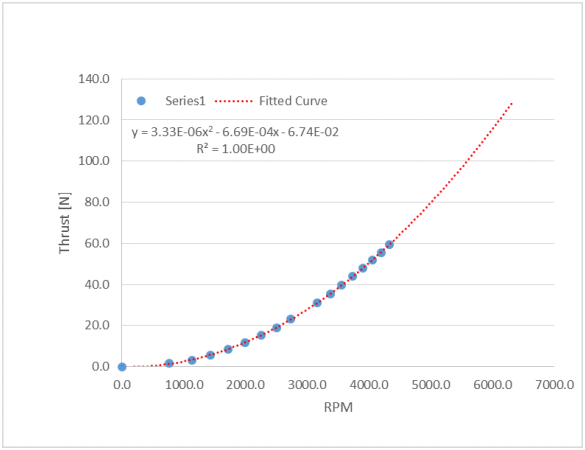

(f) 22x10” Propeller Thrust vs RPM curve.

Figure B.1: Torque and Thrust curves for 18x10”, 19x10” and 22x10” propeller testing.